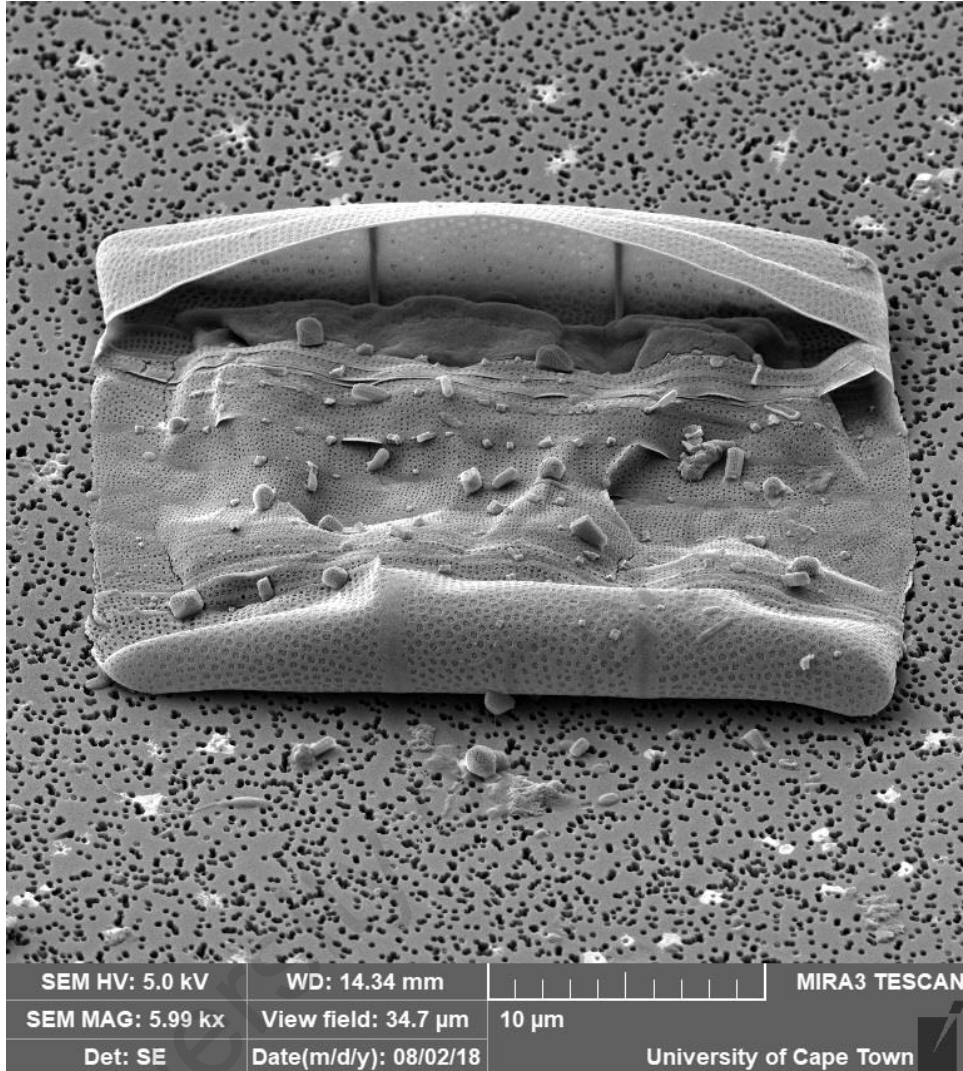


# Diel and seasonal dynamics of *Anaulus australis* at Muizenberg Beach, South Africa



By Casha de Vos

Dissertation presented for the degree of Master of Science in the Department  
of Biological Sciences, University of Cape Town

February 2024

Supervisors: Dr Maggie M. Reddy, Associate Professor Coleen L. Moloney,  
Dr Emma Rocke and Dr Nicole R. Dames

The copyright of this thesis vests in the author. No quotation from it or information derived from it is to be published without full acknowledgement of the source. The thesis is to be used for private study or non-commercial research purposes only.

Published by the University of Cape Town (UCT) in terms of the non-exclusive license granted to UCT by the author.

## Plagiarism declaration

I know the meaning of plagiarism and declare that all the work in the dissertation, save for that which is properly acknowledged, is my own.

Signed by candidate

---

Casha de Vos

Signed by: 445714e2-a152-4f4d-a7a5-06862494155b

## Abstract

This study aimed to expand the geographical range of study the surf zone diatom *Anaulus australis* in South Africa, focusing on temporal and spatial variations at Muizenberg Beach in False Bay on the south-west coast. The diel cycle of *A. australis* was studied through hourly samples over 13 hours, by analysing water column and sediment samples at three stations. Phytoplankton cell and chlorophyll-*a* concentrations, along with nutrient levels, were assessed. Forecast tidal heights and in-situ wind speed and direction data were incorporated into the analysis. At Muizenberg Beach, the diel cycle persisted even when patches were not visible, with cell concentrations peaking in the morning (mean  $\pm$  SD:  $4.64 \pm 6.19 \times 10^4$  cells.mL<sup>-1</sup>) and declining by late afternoon, reaching zero cells.mL<sup>-1</sup> by 17:00 at some stations. A large resident benthic population of *A. australis* cells was noted (mean  $\pm$  SD:  $160.40 \pm 164.51 \times 10^4$  cells.mL<sup>-1</sup> of sediment) in comparison to the well-studied Sundays River Beach on the South Coast of South Africa. *A. australis* concentrations in surface waters decreased further offshore and increased with onshore wind direction and tidal heights, while sediment populations increased towards the station behind the breaker. Wind speed and direction and tidal heights were identified as potential influencers of diatom abundance, but causal links could not be established. In addition to this diel timescale study, a long-term timeseries dataset was collected to establish seasonal patterns in surf zone diatom patches. Photographs of the Muizenberg surf zone at 12-minute intervals were taken for two years (2019-2021) and analysed using machine learning image analysis techniques. Data on the presence of *A. australis* patch events were generated and a strong seasonal signal was found, with increased prevalence in patch frequency in the winter months (May, June, July), possibly due to increased turbulence. A maximum number of 15 days with patch events were recorded in May 2021. Environmental data were incorporated, and tidal heights were identified as a likely influential factor on patch event frequency. The increased understanding of these diatoms' diel periodicity and seasonal cycles will not only advance our understanding of these organisms but also contribute to broader knowledge of coastal ecosystem dynamics, with potential implications for conservation and management efforts in these critical environments.

## Acknowledgements

I would like to extend my heartfelt gratitude to several people who played instrumental roles in the completion of my Master's dissertation. Their support, encouragement, and expertise have been invaluable.

Firstly, I would like to express my deepest appreciation to my supervising team, Maggie, Coleen, Emma, and Nicole. Their unwavering enthusiasm and interest in my work, coupled with endless patience, made my research journey an enriching experience and there was not a day that I did not learn something from them. Special thanks to Coleen for leaving your well-earned retirement bubble to provide assistance in this last year and for creating an incredibly fun and supportive learning environment in this lab. The collaborative efforts of this exceptional supervising team significantly contributed to the success of my dissertation, and these are memories and learnings I will keep with me throughout my career. A great acknowledgment goes to Maggie, who dove headfirst into guiding me. Your ability to balance patience and motivation was crucial in overcoming challenges, and your support played a pivotal role in bringing my work to completion this year. I am excited to see your work grow from strength to strength.

Thank you to my family who's love and understanding sustained me throughout this academic endeavour. Your unwavering support and belief in my abilities fuelled my determination to succeed. Philip, your steadfast presence, and support during all the late nights, fuelled by coffee and, towards the end, copious amounts of wine, provided the moral support I didn't know I needed. Thank you for reminding me of my strengths and the good things in life when I needed it most, I couldn't have navigated this without your encouragement. Of all the people in my life, you have been most excited for this day, and I look forward to celebrating with you!

A huge thank you to Marthinus Bosman for generously sharing your expertise in machine learning and for always being a generously supportive friend. Your help was invaluable, not only in saving me countless hours of time, but uplifting the quality of my work, and I am grateful to have had the opportunity to learn from you. May your innovative spirit and laughter in the face of challenges continue to inspire and lead you to new adventures in the future!

Finally, to the lab team, wherever you may be, thank you for being pillars of support. May your journeys involve ample coffee, sound statistics, lively debates, and the same camaraderie that lifted me during challenging times. May there be an Oudekraal sampling trip in our future!

To everyone mentioned and countless others who contributed to my academic journey, your impact will be forever cherished. Thank you for being an integral part of completing this work.

## Contents

Plagiarism declaration.....	1
Abstract.....	2
Acknowledgements.....	3
Contents.....	4
List of Figures and Tables.....	6
Chapter 1: Literature Review .....	10
Sandy beach surf zone ecosystems.....	10
Surf zone diatoms .....	10
Diel cycle .....	11
Surf zone diatoms in South Africa.....	12
Morphology.....	15
Buoyancy.....	16
Physical forcing .....	17
Light.....	19
Nutrients .....	19
Study Site: Muizenberg Beach .....	21
Aims .....	21
Chapter 2: Diel Cycle of <i>Anaulus australis</i> at Muizenberg Beach .....	22
Abstract.....	22
Introduction .....	23
Methods.....	26
Sampling.....	26
Laboratory analysis .....	27
Other environmental data .....	31
Statistical analyses .....	31
Results.....	32
Cell Concentrations in the Surface Water.....	32
Cell Concentrations in the Sediment .....	35
Environmental Variables.....	37
Characteristics of <i>Anaulus australis</i> Cells.....	42
Discussion.....	46
Chapter 3: Time series view of <i>Anaulus australis</i> patch events at Muizenberg Beach (2019-2021) ...	51
Abstract.....	51
Introduction .....	52
Aims for Muizenberg Beach, South Africa .....	54

Methods.....	55
Photographic data – Model input data set up.....	55
Photographic data – Model training.....	58
Environmental data.....	58
Analysis .....	59
Results.....	60
Discussion.....	64
Chapter 4: Conclusion.....	66
References .....	68
Appendix .....	73

## List of Figures and Tables

### Figures

- Figure 1: Facebook post by City of Cape Town on the occurrence of a species of *Anualus australis* at Melkbosstrand on the West Coast of South Africa (City of Cape Town, 2016). ..... 13
- Figure 2: Figure of South African Beaches where surf zone diatom populations have been noted, modified after Campbell & Bate (1991) and redrawn using Google Earth. .... 14
- Figure 3: Diagram of the proposed diel cycle of the surf zone diatom *A. australis*..... 14
- Figure 4: Muizenberg Beach on a) the sampling day, 16 August 2019 at 12:02, representing typical conditions for the sampling day, and b) the day after sampling, 17 August 2019 at 10:52, showing a patch that was first noted at 07:30 and disappeared by 12:00..... 26
- Figure 5: Map of False Bay region in South Africa, with the red pinpoint indicating the location of Muizenberg Beach, relative to Cape Town. A schematic diagram of the sampling strategy is also included on the right..... 26
- Figure 6: Mean ( $\pm$  standard error) (n=20) cell concentrations of *A. australis* at different times of the day at Muizenberg Beach on 16 August 2019 for a) Station 1, b) Station 2, and c) Station 3. Blue lines show concentrations (cells.mL<sup>-1</sup>) from surface waters. Orange lines show concentrations (cells.mL<sup>-1</sup> of sediment) from sediment samples. .... 32
- Figure 7: Mean ( $\pm$  standard error) (n=2) bulk chlorophyll-*a* concentrations (orange,  $\mu\text{g.L}^{-1}$ ) and cell concentrations of *A. australis* (blue) and other phytoplankton species (black) at different times of the day at Muizenberg Beach on 16 August 2019. Results for surface waters are given as a) Station 1, b) Station 2, and c) Station 3, and results for sediments as d) Station 1, e) Station 2, and f) Station 3..... 34
- Figure 8: Bulk chlorophyll-*a* concentrations ( $\mu\text{g.L}^{-1}$  of water or sediment) at different cell concentrations of a) *A. australis* in surface waters (cells.mL<sup>-1</sup>), b) other species in surface waters (cells.mL<sup>-1</sup>), c) *A. australis* in sediments (cells.mL<sup>-1</sup> of sediment), d) other species in sediments (cells.mL<sup>-1</sup> of sediment) at Muizenberg Beach on 16 August 2019. .... 36
- Figure 9: Mean ( $\pm$  standard error) cell concentrations of *A. australis* (cells.mL<sup>-1</sup>) at the three sampled stations and tidal heights at different times of the day at Muizenberg Beach on 16 August 2019 for a) surface waters and b) sediments. Blue = station 1, red = station 2, orange = station 3, black = tidal height. .... 36
- Figure 10: Wind vector plot showing wind speed and direction at different times of the day on 16 August 2019, measured at Cape Town International Airport..... 37
- Figure 11 : Log cell concentrations of *A. australis* (cells.mL<sup>-1</sup>) in surface waters at Muizenberg Beach on 16 August 2019, plotted against nutrient concentrations ( $\mu\text{g.L}^{-1}$ ) for a) nitrite (NO<sub>2</sub>), b)

nitrate (NO<sub>3</sub>), c) silicate (SiO<sub>4</sub>), d) phosphate (PO<sub>3</sub>) and e) ammonium (NH<sub>4</sub>). (Different colour dots represent different stations: Station 1 = red; station 2 = green; station 3 = blue) ..... 39

Figure 12: Changes during the day of mean ( $\pm$  Standard Error) cell volume (blue,  $\mu\text{m}^3$ ) and proportions of dividing (orange) and paired (black) cells of *Anaulus australis* at Muizenberg Beach on 16 August 2019. a) Station 2 surface samples, b) station 3 surface samples, c) station 2 sediment samples, d) station 3 sediment samples ..... 43

Figure 13: Boxplots showing the estimated volumes ( $\mu\text{m}^3$ ) of individual *Anaulus australis* cells from stations 2 and 3 at Muizenberg Beach on 16 August 2019. a) Cells in the surface waters and sediments, b) cells that are dividing or not dividing, and c) comparisons of Volume ( $\mu\text{m}^3$ ) of the surface and sediment (right) and dividing and non-dividing cells (left) of *A. australis* cells across Station 2 & 3..... 44

Figure 14: Relationships between chlorophyll-*a* concentrations ( $\mu\text{g}\cdot\text{mL}^{-1}$ ) and *Anaulus australis* biovolumes ( $\mu\text{m}^3\cdot\text{mL}^{-1}$ ) at Muizenberg Beach on 16 August 2019. a) surface waters, b) sediment. .... 45

Figure 15: Original input images (a) resized to crop out buildings and sky and reduce resolution (b).56

Figure 16: Examples of images classified as a score of 1 (a) indicating presence of a mild patch, and a score of 2 (b) indicating an intense patch..... 57

Figure 17: Examples of photographs classified according to the Beaufort scale with a score of 1 (a), 2 (b), 3 (c) and 4 (d)..... 57

Figure 18: The standardised summed number of days where patches were observed over the study period, with tidal heights in meters overlayed on the secondary y-axis (orange line). ..... 60

Figure 20 :Patch events (1 = mild patch, 2 = intense patch, 0 = no patch) recorded for wind speeds where the wind direction is onshore direction (South-East, or South-South-East) for more than 2 hours ..... 61

Figure 19: The standardised summed number of days where patches were observed over the study period, with the average monthly sea state score overlayed on the secondary y-axis (orange line). ..... 61

Figure 21: Number of patches recorded standardised against the number of photographs taken and plotted against the hour of the day over the study period, with blue indicating the portion of mild patches and orange for intense patches..... 63

## Tables

Table 1: Generalised linear model results tables for surface (a) and sediment (b) <i>A. australis</i> cell concentrations as response variables and surface (c) and sediment (d) chlorophyll- <i>a</i> concentrations response variables. ....	41
Table 2: Generalised linear model results tables for <i>A. australis</i> presences-absence as response variable and tidal height (m), wind speed (m.s-1), wind direction (degrees from north), sea state score, and no. of hours of wind in an SSE direction as explanatory variables.....	63

## Appended Figures

Figure A 1: Standard curves used to determine nutrient concentrations for a) phosphate, b) nitrite, c) nitrate + nitrite, d) silicate and e) ammonium.....	73
Figure A 2: Model validation plots ANOVA and Post-hoc Tukey test for comparison between stations for surface <i>A. australis</i> cell concentrations (square root transformed data) .....	74
Figure A 3: Residual plots with <i>A. australis</i> cell concentrations as a response variable in the surface water (a, b, c) and the sediment (d, e, f) .....	76
Figure A 4: Residual plots with Chlorophyll- <i>a</i> concentrations as a response variable in the surface water (a, b, c) and the sediment (d, e, f) .....	77
Figure A 5: Proportion of dividing cells (black, %), alongside total cell concentrations of <i>A. australis</i> (blue, cells.mL-1) plotted over time of day for Station 2 & 3 .....	78
Figure A 6: Scatterplot of total cell concentrations of <i>A. australis</i> (cell/ml) at the surface (a) and sediment (b) against tidal heights (m). .....	78
Figure A 7: Nutrient concentrations ( $\mu\text{g.L}^{-1}$ ) of nitrite (NO <sub>2</sub> ), nitrate (NO <sub>3</sub> ), silicate (SiO <sub>4</sub> ), phosphate (PO <sub>3</sub> ) and ammonium (NH <sub>4</sub> ) for each station, plotted alongside cell concentrations of <i>A. australis</i> (cells.mL-1) in hourly timescales. ....	80
Figure A 8: Generalised linear model validation plots with patch presence-absence as a response variable.....	83

## Appended Tables

Table A 1: Table A1: Results of the ANOVA and Tukey tests comparing <i>A. australis</i> cell concentrations between stations in the surface and sediment. ....	75
Table A 2: Descriptive statistics for nutrients including Mean (mean), standard deviation (St. Dev), variance (Var) and sample size (n) of for surface water samples of nutrient concentrations at three stations (Station 1-3) for all time points sampled.....	81

Table A 3: Descriptive statistics for nutrients including Mean (mean), standard deviation (St. Dev), variance (Var) and sample size (n) of for surface water samples of nutrient concentrations of the combined samples across all three stations. .... 81

Table A 4: Mean (mean), standard deviation (St. Dev), variance (Var) and sample size (n) of for surface and sediment (depth) samples of *A. australis* at three stations (Station) for all time points sampled..... 82

## Chapter 1: Literature Review

### Sandy beach surf zone ecosystems

Our world's coasts are dominated by the presence of sandy beach and dune habitats, where these ecosystems are functional in providing habitat for many species, carrying out biogeochemical cycling, and supporting cultural, socio-economic, and recreational activities (Schlacher et al., 2014). These ecosystems are unique as they act as a link between marine and terrestrial ecosystems and are unstable habitats where morphology is constantly changing with shifts in tides, winds, waves, and currents on variable timescales (Schlacher et al., 2014).

Sandy beach ecosystems have in the past been regarded as more oligotrophic habitats, with studies in the most recent decades indicating that surf zones, although spatially confined, are often highly productive (Kahn & Cahoon, 2012). Energy flow in these ecosystems primarily consist of inputs from primary production by resident phytoplankton in the surf zone water column and sediment, as well as imported macrophytes and phytoplankton (Schlacher et al., 2014; McLachlan & Defeo, 2018). There is also an input from terrestrial sources in many forms, most notably from river runoff, stormwater runoff and groundwater inputs (Talbot, Bate & Campbell, 1990).

In some sandy beaches, large populations of phytoplankton species, referred to as surf zone diatoms, play an especially important role as a source of primary production. These diatoms contribute to nutrient cycling and are often found to be critical food sources for various intertidal organisms, including meiofauna (Netto & Meneghel, 2014), planktonic larvae (Cahoon et al., 2017) and small pelagic fish species (McGregor & Strydom, 2020).

### Surf zone diatoms

In some sandy beach surf zones, populations of surf zone diatoms are often present in such abundance that they cause the water to become dark rusty brown in colour in clear "patches" (Bate & McLachlan, 1987). These patches are the result of an accumulation of cells in the surface waters and are dominated by a single, or in some cases two, species of diatoms (McLachlan & Lewin, 1981; Bate & McLachlan, 1987; Talbot, Bate & Campbell, 1990; Campbell, 1996; Odebrecht et al., 2014). Since surf zone diatoms are specialised to remain in the surf zone area, they rarely occur outside these sandy beach ecosystems (Odebrecht et al., 2014).

Globally, there are 11 distinct species of surf zone diatoms, belonging to four genera: *Anaulus*, *Attheya*, *Aulacodiscus* and *Asterionellopsis* (da Silva Maria et al., 2016). Surf zone diatoms have been recorded in several Southern Hemisphere countries including Brazil, New Zealand, Australia, and South Africa, as well as the North-Western and Gulf Coasts of the United States in the Northern

Hemisphere (Campbell, 1996; Odebrecht et al., 2014). To date, surf zone diatoms have been recorded at 90 beaches globally (da Silva Maria et al., 2016).

The oldest records of “brown water” patches date to 1896 from the Banana Beach, Zaire in the Congo, with a few reports published on the occurrence of this phenomenon prior to the 1970s, from both New Zealand and the United States of America (Campbell, 1996). However, in the 1970s research on these patches was characterized by studies from the Washington Coast, where focus was placed on the study of the surf zone diatom species *Attheya armatus*. Studies from Washington, USA, from the 1970's were highly influential in determining much of the narrative surrounding other species of surf zone diatoms, like *A. australis* and *Asterionellopsis glacialis*.

Lewin & Norris (1970) first noted that surf zone diatom populations of Copalis Beach, West Coast of the Olympic Peninsula, Washington Coast, USA, bore a striking resemblance in species composition to that of the North Island, West Coast of New Zealand. This study also noted that accumulations tended to be dominated by one or two species of diatoms (later also established by McLachlan & Lewin (1981) and Campbell (1996)), and that these species remain semi-permanently present in the surf regardless of conditions (later also established by Lewin, Hruby & Mackas (1975)).

### Diel cycle

A key characteristic of all surf zone diatoms is the phenomenon of diel periodicity in the occurrence of patches in the surf zone. Several studies note the appearance of patches in the morning, which then dissipate entirely within a few hours. Studies also note that this diel cycle is also present when patches are not visible, where cell concentrations peak in the morning, only to disappear (in some cases entirely) from the surf zone by the late afternoon (Lewin & Hruby, 1973; Lewin & Rao, 1975; Sloff, McLachlan & Bate, 1984; Talbot & Bate, 1988a; Talbot, Bate & Campbell, 1990; de Vos, 2018).

Studies along the Washington Coast first established the presence of a diel cycle in two surf zone diatoms, *C. armatum* and *Asterionellopsis socialis* and recorded their formation of accumulations, whilst McLachlan & Lewin, (1981) first noted such a cycle for *A. australis* in South Africa. During these and further studies, some investigation was made into the mechanisms behind the appearance (floatation and accumulation) and disappearance (sinking or redistribution) of these diatoms in the water column. Similar to previous work on the diatom species *Ditylum brightwellii* (Eppley et al., 1967), it was noted that *C. armatum* appears in the water column during the early morning before sunrise and thus floatation or the rising of the cells to the surface cannot be light induced (Lewin & Hruby, 1973), but rather factors such as tides and cell characteristics (cell density and surface area, chain length, cell division and mucus layer) were considered to play a role in the floatation mechanism. It was also noted that *C. armatum* was not present in the sediment (Lewin, 1978), and thus the

disappearance of cells was attributed to a redistribution of the cells in the water column (Lewin & Hruby, 1973).

Talbot & Bate (1987a) first found evidence of *A. australis* cells being captured in the sediment of the surf zone and later Talbot & Bate (1988a) found higher concentrations of cells ( $10^9$  cells per running meter of beach, where cells were eluted from Sediment samples) in the sediment at Sundays River Beach, South Africa. Talbot & Bate (1988b) found that surf zone diatoms were not being removed from the water column due to offshore transport, and were not blooming due to cell division, and proposed that they must be sedimented within the inner surf zone. Thus, *A. australis* cells must be largely epipsammic, meaning these diatoms live primarily in the sediment (Talbot & Bate, 1988b). Talbot, Bate & Campbell (1990) suggest that adaptation to an epipsammic niche would allow diatoms to access a first helping of nutrients available through the seeping of groundwater into surf zone beaches.

Based on studies from Sundays River Beach, the proposed hypothesis for the pattern of the diel cycle for surf zone diatoms can be summarised as follows: cells are suspended from the sediment in the early morning (mechanism of floatation unknown) and accumulate in the surface water during the day where photosynthesis takes place. A large proportion of cells are also noted to be dividing during this phase (Talbot & Bate, 1986). Cells sink from the surface waters during the afternoons, often within less than two hours from when they first appear (Talbot & Bate, 1987b), and can lie dormant in the sediment until favourable conditions return. Figure 3 depicts this process visually.

### Surf zone diatoms in South Africa

Four species of surf zone diatoms have been recorded in South Africa: *Asterionellopsis glacialis*, *Anaulus australis*, *Aulacodiscus johnsonii* and *Aulacodiscus petersii* (Odebrecht et al., 2014). Of these species, *Anaulus australis* is most prevalent in South Africa and has been particularly well studied (Talbot & Bate, 1986, 1987a,b, 1988a,b,c, 1989; Campbell & Bate, 1987, 1988, 1991, 1996, 1997, 1998; Campbell, du Preez & Bate, 1988; du Preez, Campbell & Bate, 1989, 1990; Bate, Campbell & Rust, 1990; Talbot, Bate & Campbell, 1990; Campbell, 1996; du Preez & Campbell, 1996b,a; Odebrecht et al., 2014).

In South Africa these diatoms have been recorded on several beaches on the South Coast, where major accumulations or patches are noted to occur at Muizenberg, Macassar, Vleesbaai and Sundays River Beach, with occasions of accumulations noted at Struisbaai, De Hoop, Van Stadens, Wilderness, Cintsas, Buffalo Bay, Glentana, Sedgefield and Oyster Bay (Figure 2; Campbell & Bate, 1991). However, in recent years reports of the occurrence of visible patches of surf zone diatoms have also been noted on the West Coast, most notably at Melkbosstrand (Figure 1) where surf zone diatoms species were previously recorded primarily in the sediment on the West Coast (Bate, Campbell & Rust, 1990).

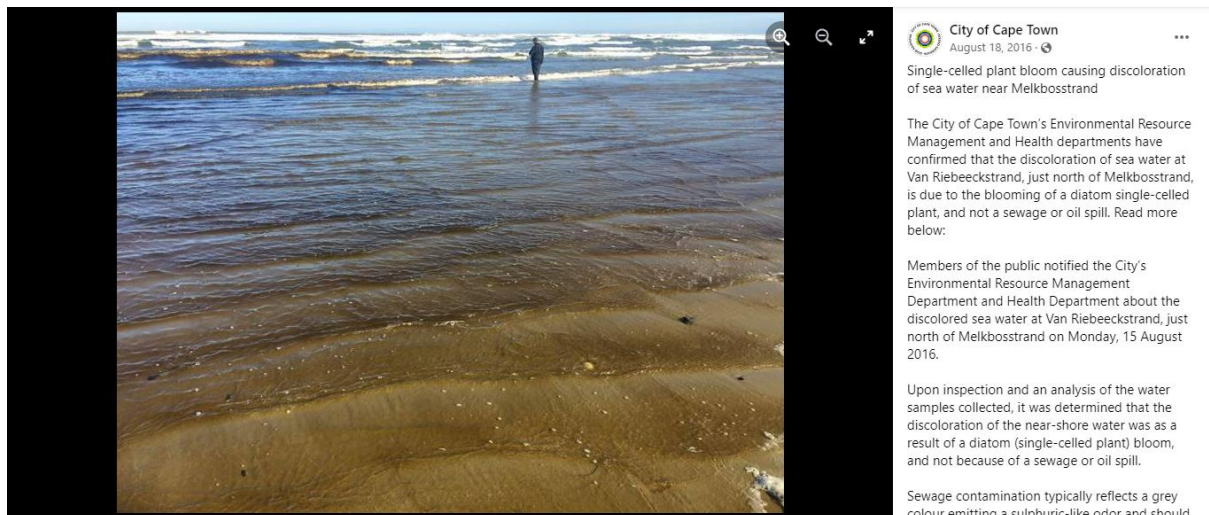


Figure 1: Facebook post by City of Cape Town on the occurrence of a patch of *Anaulus australis* at Melkbosstrand on the West Coast of South Africa (City of Cape Town, 2016).

McLachlan & Lewin (1981) presented the first study of surf zone diatoms on the coast of South Africa, from Sundays River Beach on the South Coast. This paper was highly influential in defining the diel cycle of surf zone diatoms in South Africa and drew a lot of information from past work on the Washington Coast. A key comparison was that the South African surf zone diatom populations generally consisted of a single diatom species, *Anaulus australis*, where the presence of secondary species like *Asterionellopsis glacialis* is noted on occasion, although they are generally less dominant (Talbot & Bate, 1988c).

Talbot & Bate (1986) proposed that, due to division only accounting for 20% of the population increase during patch events, these dark brown patches of *A. australis* cells are not in fact a result of cell division and unlike other species of surf zone diatoms, they are not algal blooms, but rather accumulations of cells due to hydrological forces. They are thus referred to as “patches” or “accumulations”. Talbot & Bate (1988b) similarly concluded that the rapid 30-fold increase in population size in the early morning could not be due to cell division due to cells only dividing once a day.

The link between this phenomenon of patch formation and cell morphology and physiology (cell division, mucus production, pairing of cells) has been the subject of much study (Lewin & Rao, 1975; Sloff, McLachlan & Bate, 1984; Talbot & Bate, 1986, 1988a).



Figure 2: South African Beaches where surf zone diatom populations have been noted, modified after Campbell & Bate (1991) and redrawn using Google Earth.

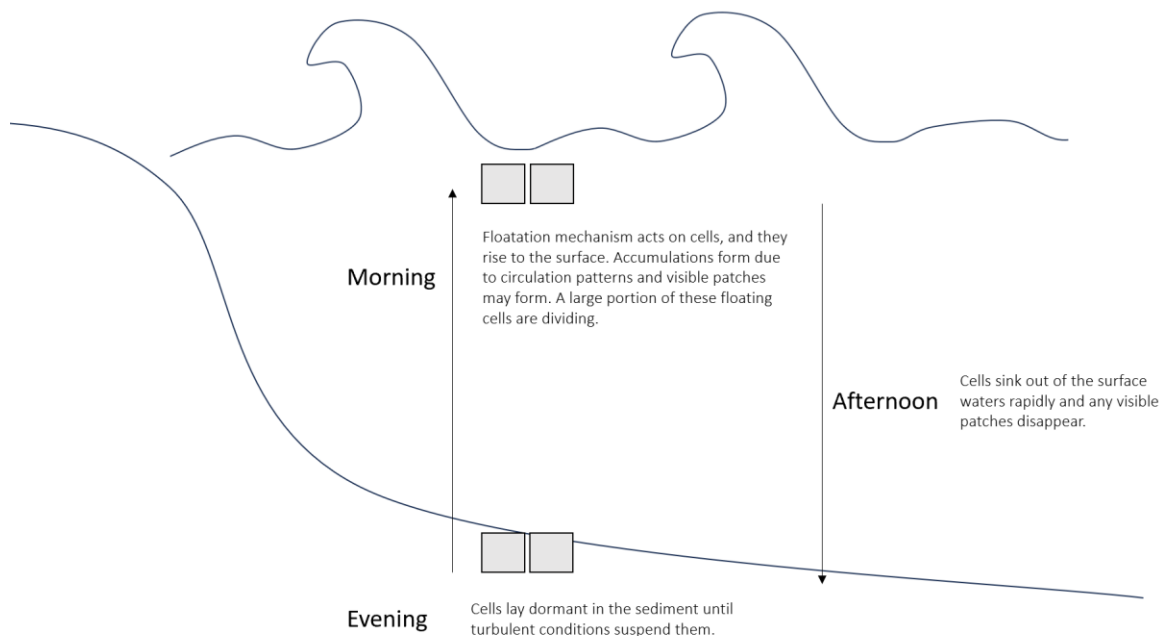


Figure 3: Diagram of the proposed diel cycle of the surf zone diatom *A. australis*

## Morphology

*Anaulus australis* is a pillow shaped single celled diatom, that often occurs in pairs. Cells are characteristically 11 – 22  $\mu\text{m}$  broad, 15 – 58  $\mu\text{m}$  long, with a transapical axis diameter between 5 – 9  $\mu\text{m}$  (Drebes & Schulz, 1989).

The diel cycle described for surf zone diatoms on the Washington Coast was also noted for certain cell characteristics such as (1) cell division, where cells divided almost exclusively during the day, (2) chain formation of the cells, where cells formed longer chains during the morning and shorter chains in the afternoon, (3) and the formation of a mucus layer on the cells' surfaces in the late afternoon (Lewin & Rao, 1975). Talbot & Bate (1986) noted, in addition to the diel cycle being a key characteristic of these diatoms, cell division frequency, cell dimensions and frustule condition also exhibited diel patterns in *A. australis* at Sundays River Beach.

Several species of surf zone diatoms like *A. socialis* and *C. armatum* (Lewin & Mackas, 1972) as well as *A. glacialis* have been noted to produce a mucus coating that covers the frustule of the cell. Some studies noted the prevalence of particles clinging to the cell wall of *A. australis* under electron microscopy analysis, suggesting the presence of such a mucus coating in this species (Talbot & Bate, 1988a). The mucilage coating is a distinctive feature of some surf zone diatoms and initial studies suggested that this coating appears more frequently on cells in the afternoons (Talbot, Bate & Campbell, 1990). However, more recent research utilising more modern microscopy and specific sampling strategy focussed on mucus of several species, suggests that if such mucus layer is present for *A. australis*, it is very thin and only noted on a few cells as a secretion of polysaccharides, and the role of this feature in controlling buoyancy of cells is questionable and still under investigation (du Preez & Campbell, 1996a).

Cells complete division and cease to divide in the dark (du Preez & Bate, 1992) with peak cell division most often noted in the early morning (Talbot & Bate, 1986). Cell division does not occur in the sediment (Talbot & Bate, 1987a, 1988a). Talbot & Bate (1987a) and de Vos (2018) noted that division is higher in patches than non-patch areas, raising the question whether the floatation mechanism of these cells could perhaps be linked to cell division. No cell division was noted beyond the breaker zone (Talbot & Bate, 1987a).

*Anaulus australis* cells have a resting phase (du Preez & Bate, 1992). It is proposed that during calm conditions, *A. australis* cells are removed from the water column and lay dormant in low light conditions on or in the sediment (possibly behind the breaker zone) (Talbot & Bate, 1988b). From this resting phase, a key component of the life cycle of these diatom species is the ability to resurface and to remain buoyant, yet the mechanism of this process is not very well understood.

## Buoyancy

Lewin & Schaefer, (1983) proposed two reasons why diatoms float: 1) floatation allows diatoms to remain in the surf zone via surface wave forcing, and 2) floatation allows diatoms to be exposed to high irradiance close to full sunlight at the surface, maximising photosynthesis (although this was later found to be an unlikely explanation due to the photoinhibition of cells at surface light irradiance (du Preez, Campbell & Bate, 1990)). The mechanism of this floatation or buoyancy is still unclear for many species of surf zone diatoms, however, some hypotheses have been proposed and are discussed in this section.

Previous research by Lewin & Hruby (1973) noted that *C. armatum* has a diel periodicity in its buoyancy and proposed that this phenomenon could not be attributed to light induction – since cells rise to the surface of the water column well before sunrise. They suggested cells may be excreting heavy ions to incur changes in their buoyancy during select times of the day, although no evidence of this has been presented to date. Lewin & Rao (1975) noted that cells of *C. armatum* elongate prior to appearing in the surface waters, but since cells are noted to be negatively buoyant at any time of day and physiological state, buoyancy cannot be due to a physiological effect in this species.

For many diatom species, including *A. australis*, the dominant hypothesis behind the floatation mechanism for surf zone diatoms has been that these cells are able to attach to air bubbles introduced to the surf zone by passing waves (Sloff, McLachlan & Bate, 1984). However, other than the suggestion by Sloff, Maclachlan & Bate (1984), very little evidence has been presented in support of this hypothesis, with no experimental studies to confirm it. Additionally, *A. australis* does not form foam like many other species of surf zone diatoms, such as *C. armatum* (Lewin & Hruby, 1973), thus negating the hypothesis that these cells attach to bubbles as a mechanism of floatation.

McLachlan & Lewin (1981) were the first to note the diel periodicity in buoyancy of *A. australis* and suggested that the loss of floatation protected the diatoms from grazers at night, whilst floatation during the day would utilise currents to remain in the surf zone (Winter, 1983) as well as allow for optimal light exposure for photosynthesis. For *A. australis*, it has been proposed that density changes during cell division controls mobility in the surf zone (Talbot & Bate, 1986, 1988a). Talbot & Bate (1986) proposed that instead of the bubble attachment hypothesis, cells may be floating due to the decrease in density during cell division. This may be supported by the fact that in most cases, no dividing cells are found in the sediment, and cells are thought to be resident both inshore and behind the breaker (Talbot & Bate, 1988b,a).

Whilst the mechanism of floatation remains unknown, the reasons why cells sink back down to the sediment are also somewhat speculative. The predominant hypothesis states that cells attach or

gather sediment particles on their surface towards the late afternoon, hence allowing them to sink out of the water column (Talbot & Bate, 1988a). Unlike many other species of surf zone diatoms, there is little or no mucus layer present for *A. australis*, negating the idea that they attach to sediment when sinking out of the surface water (Campbell, 1996; du Preez, 2017). Talbot & Bate (1988a) in turn proposed that redistribution of cells in the water column causes cells to advect out of the surf zone, hence the disappearance. Thus, the prevailing hypothesis is in summary that biotic factors induce floatation of single cells, and forcing factors induce accumulation.

### Physical forcing

Sandy beach semi-closed ecosystems are described as being beaches with an intermediate to dissipative wave energy state, a longshore bar-trough (Campbell & Bate, 1988; Odebrecht et al., 2014), entrained bodies of water which retain and concentrate cells (Odebrecht et al., 2014), a minimum beach length of 4 km (Campbell & Bate, 1997; Odebrecht et al., 2014), the presence of rip current circulation i.e. sufficient surf zone width (Campbell & Bate, 1997), and finally, a sufficient input of nutrients (Campbell & Bate, 1997; Odebrecht et al., 2014).

Campbell & Bate (1997) investigated beaches in South Africa and noted that South Coast beaches are most suitable for surf zone diatom habitation since many of the above characteristics are featured along this coastline. In contrast, the East Coast has no occurrence of patches as few beaches have rip current circulation and beaches have narrow surf zones with aquifers contributing low nutrient concentrations to the surf zone. The West Coast also has little to no visible patches occurring in previous studies, possibly due to fewer rip currents and no coastal dunes with aquifers (Campbell & Bate, 1991).

Cells accumulate between rip and onshore flow, utilising the counterbalance of waves and surface currents to remain inshore despite flushing by rip currents, and the breakers form a barrier with little outflow of cells past this point (Talbot & Bate, 1987a, 1988b).

Further investigation is needed to understand the link between diatom population abundance and tides. Lewin & Hruby (1973) proposed that floating cells are deposited on the beach during the receding tide, resulting in higher cell counts or patches during the next high tide. Sloff, McLachlan & Bate (1984) found that patches are linked to onshore winds and not to tidal heights, in contrast to Talbot & Bate (1987a), who found patches occur overwhelmingly at low tide adjacent to rip currents and that patches at high tide move with the alongshore current.

More so than tides, the link between wave height and diatom population abundance seems clearer, with several studies expressing the likelihood of patches increasing with an increase in wave height

(Talbot & Bate, 1988c, 1989; Talbot, Bate & Campbell, 1990; Campbell & Bate, 1996). Talbot & Bate (1988a, 1989) found wave height to be positively correlated with cell populations of *A. australis* and *A. glacialis* at Sundays River Beach. However, it is again difficult to discern whether this is a direct effect, or whether wave height in turn induces changes in beach morphodynamics.

Patch occurrence decreases with a decrease in wave energy (Talbot & Bate, 1989), thus linking patches to turbulence (du Preez & Bate, 1992; du Preez & Campbell, 1996b). It is thought that low energy states lower the number of waves, i.e. if cells are attaching to bubbles as per the prevailing floatation hypothesis there will be less means to float, and allow for cells to settle out into the sediment, where high energy states resuspend sedimented cells and also creates an environment where other coastal diatom species cannot occur due to the harsh conditions (Talbot & Bate, 1988d; Campbell & Bate, 1997).

Temperature (Talbot, Bate & Campbell, 1990), salinity (Campbell & Bate, 1987; Talbot & Bate, 1989) and pH (Talbot & Bate, 1989) show little variation and have been found to be insignificant in influencing the occurrence of patches at other sites, including Sunday River Beach, South Coast of South Africa (Odebrecht et al., 2014). It been found that patch development coincides with onshore winds (Talbot, Bate & Campbell, 1990) and, conversely, that offshore winds remove cells from the surf zone (Talbot & Bate, 1989).

Thus, our current understanding is that the physical features that induce the formation of patch accumulations are increased wave height, turbulence, and wind (Odebrecht et al., 2014). Where buoyancy is responsible for the diel periodicity of these diatoms (vertical migration), physical forcing is responsible for the formation of these patches/accumulations (horizontal migration) (Talbot & Bate, 1988a, 1989).

Due to the link between patch occurrence and several meteorological and physical features of surf zones, one would expect some seasonality in the formation of patches. *Anaulus australis* patches in Ilheus, Brazil have been found to be linked to South-South-Easterly wind directions and river outflows, where patches increase during cold fronts and turbulent periods of strong winds (Tedesco et al., 2017). Similarly, a seasonal effect has been noted for *A. glacialis* (discussed in Chapter 3) (Talbot, Bate & Campbell, 1990). However, to date, no such seasonal effects have been noted for *A. australis* in South Africa (Talbot & Bate, 1986; Odebrecht et al., 2014).

## Light

To date limited research has been done on the light usage of surf zone diatoms, although the photophysiology has been well described for *A. australis* (Campbell, du Preez & Bate, 1988; du Preez, Campbell & Bate, 1990; du Preez & Campbell, 1996b).

Since *A. australis* can float to the surface water layers, these surf zones form a unique light environment where cells are tumbled into the water column by waves and rise back up once the wave has passed. This results in a variable light environment – from full sunlight exposure to low light conditions (du Preez & Campbell, 1996b), created by attenuation by waves (bubbles), disturbed sand and phytoplankton accumulations (shading) (du Preez & Campbell, 1996b). Du Preez & Bate (1992) found *A. australis* to be more photo efficient at lower light conditions, and Lewin & Mackas (1972) found similar results for *C. armatum*, where these cells were able to dominate in abundance during high cell densities when shading effects occur.

Du Preez and Campbell (1996) found that surface light conditions i.e. high irradiance, induces photoinhibition in *A. australis* cells, indicating that there must be an alternative reason for floatation – or perhaps that turbulence causes enough light attenuation and that being at the surface for a short period of time allows for more light absorption. In addition, du Preez and Campbell (1996) noted that when cells are exposed to full sunlight conditions, with high cell density, photoinhibition is delayed substantially. Du Preez and Campbell (1996) proposed that the prevailing reason for floatation must be to keep the cells within the surf zone and are thus not necessarily dependent on light exposure. Photoinhibition is not permanent and photosynthetic ability is typically restored within 14 hours (du Preez & Bate, 1992). However, more recent research by da Silva Maria et al. (2016) stated that *A. glacialis* is considered a benthic diatom, adapted to utilize a high cell density to create a shaded environment to protect cells from light stress. Similar strategies have been proposed for *A. australis*, where shading may be a strategy to delay photoinhibition (du Preez & Bate, 1992). *Anaulus australis* cells can survive in the dark for up to 75 days (du Preez & Bate, 1992), thus allowing them to lay dormant in the sediment during periods of calm conditions and resurface to photosynthesize once turbulent conditions emerge.

## Nutrients

Surf zones are generally not nutrient limited (Sloff, McLachlan & Bate, 1984), though the extent to which nutrient availability influences the occurrence of surf zone diatoms populations is not well understood. Whilst nutrient concentrations in surf zone ecosystems are generally sufficient to support diatom populations, nutrient variability across the coastline may contribute to determining the

distribution of populations, and variability on longer timescales may have more seasonal effects on populations. However, causative effects are difficult to establish.

Lewin (1978) noted that nitrate concentrations at Copalis Beach, Washington, USA, were depleted offshore during the winter months, and these nitrate lows corresponded to a decrease in the presence of surf zone diatoms in inshore environments. In addition, Lewin (1978) reported that nutrient uptake rates in surf zone diatoms were generally low, and that nutrient limitation may play a role in shaping surf zone diatom communities. It is further noted that surf zone diatoms occur in sandy beach ecosystems with high nutrient loading – often occurring in areas where there is the presence of a river, rainfall, or nutrient loaded groundwater outflow into the surf zone (Odebrecht et al., 2014).

McLachlan & Lewin (1981), drew key comparisons of the higher nitrogen component concentrations found at both Muizenberg (South-West Coast) and Maitland River Beach (South Coast) when compared to other study sites. At Sundays River Beach, on the South Coast of South Africa, it is indicated that *A. australis* requires a considerable requirement of nutrients (Bate & McLachlan, 1987). McLachlan & Lewin (1981) found a difference in nutrient concentrations between the inside and outside of patches – inside the patches, ammonium concentrations are higher, nitrite concentrations are similar and nitrate concentrations are lower than samples taken outside patches (McLachlan & Lewin, 1981). Campbell & Bate (1998) also noted a correlation between rate of groundwater discharge variability and the diatom populations at Sundays River Beach. Groundwater nutrient inputs are thought to be a key in determining the presence of surf zone diatoms in beaches in South Africa and Muizenberg Beach receives substantial nutrient inputs from river outflow as well as groundwater sources (Campbell & Bate, 1991).

One nutrient that should be noted as critical for the survival of large diatom populations, is that of silicate. Muizenberg Beach is thought to have a substantial input of nutrients, including silicate, from groundwater inputs (Campbell & Bate, 1991). Silicate is generally not a limiting nutrient for surf zone diatoms, but Talbot & Bate (1986) suggest that the paucity of dividing at night in *A. australis* diatoms is due to an inability to store enough energy for silicic acid uptake and division. Talbot & Bate (1986) suggested *A. australis* may overcome this by dividing at night and retarding valve formation until peak photosynthetic activity during the day.

Campbell & Bate (1996) proposed that surf zone diatoms at Muizenberg Beach absorb excess nutrients from anthropogenic sources, thereby reducing the nutrient loading to the surf zone ecosystem. The absorption of nutrients by diatoms also plays an important role in buffering the ecosystem against nutrient loading and shielding the rest of the ecosystem (Bate & McLachlan, 1987; Campbell & Bate,

1996). Carbon supply from *A. australis* to the microbial loop is thought to play a role in the nutrient cycling of surf zone diatom dominated sandy beaches (Odebrecht et al., 2014).

### Study Site: Muizenberg Beach

Muizenberg Beach, on the coastline of False Bay, South Africa has a high prevalence of patches of *A. australis*, although few dedicated studies have taken place here. Grindley & Taylor (1970) first reported the presence of the surf zone diatom *Anaulus australis* at Muizenberg Beach in the 1960s, but the occurrence of these patches gained public interest in the 1980s (Campbell & Bate, 1996). It is also suspected that there has been an increase in the occurrence of *A. australis* patches at Muizenberg Beach (Campbell & Bate, 1996). Muizenberg Beach is a popular surfing site and a tourist attraction, and the presence of these dark brown water patches is often cause for concern amongst beach users who question the water quality as these patches are often mistaken for sewage pollution.

### Aims

This study aimed to establish further understanding of the diel cycle of *Anaulus australis* at Muizenberg beach, which, thus far, is underrepresented in the literature. Several variables were measured on daily time scales alongside cell concentrations with the aim of drawing comparisons between this site and other locations where surf zone diatoms have been investigated on these time scales.

This study also aims to use a two-year data set consisting of photographs taken at 12-minute intervals to investigate the seasonality of surf zone diatom patches and linkages to environmental variables. Prior to this, long term data sets of this time scale and resolution were limited, and these results should yield insights into the seasonality and influence of various factors on this phenomenon.

## Chapter 2: Diel Cycle of *Anaulus australis* at Muizenberg Beach

### Abstract

In South Africa, the surf zone diatom species *Anaulus australis* has been well studied on the South Coast at Sundays River Beach, Algoa Bay. The aim of this study was to extend the geographical range of study of *A. australis* in South Africa, with the goal of understanding how environmental conditions and cell concentrations change across time and space in the Muizenberg surf zone on the South-West Coast. A transect of three stations across the width of the surf zone was sampled, with samples taken from both the surface and sediment at hourly intervals from 06:30 to 18:30 on a single day. Samples were collected and analysed for nutrients, cell characteristics, cell concentrations, and chlorophyll-*a* concentrations. In situ wind and forecast tidal height data were obtained for the same period from the South African Weather Service and the South African Navy, respectively. Similar to other surf zone diatoms and studies at Sundays River Beach, the *A. australis* population in surface water at Muizenberg Beach (mean  $\pm$  SD:  $4.64 \times 10^4 \pm 6.19 \times 10^4$  cells.mL<sup>-1</sup>) exhibited a strong diel cycle, with peak concentration in the late morning and a rapid decrease in concentration towards the evening. Sediment cell concentrations also exhibited a diel cycle, with a large number of cells being retained within the sediment throughout the day (mean  $\pm$  SD:  $160.40 \times 10^4 \pm 164.51 \times 10^4$  cells.mL<sup>-1</sup> of sediment), indicating a large reservoir population is present in the sediment. A strong positive relationship was found in the surface water between chlorophyll-*a* and cell concentrations of *A. australis* suggesting that *A. australis* composes the dominant phytoplanktonic biomass in the surface water. In the surface water, cell concentrations decreased with distance from shore, tidal height, and a shift towards Northerly winds. In the sediment, *A. australis* cell concentrations also decreased with distance from the shore while cell concentrations of other phytoplankton species increased. Cell volume was significantly larger for single (non-paired) and dividing *A. australis* cells compared to paired cells, and cells found in the surface water were also significantly larger in volume than those found in the sediment, however, no conclusions on the role of cell volume in the floatation mechanism of these cells can be drawn from this data. Muizenberg Beach exhibits higher concentrations of nitrate ( $1.29 \pm 1.41$   $\mu$ mol.L<sup>-1</sup>), nitrite ( $0.13 \pm 0.03$   $\mu$ mol.L<sup>-1</sup>), and ammonium ( $15.39 \pm 11.89$   $\mu$ mol.L<sup>-1</sup>) compared to Sundays River Beach. The nutrient-rich environment in Muizenberg Beach, influenced by coastal upwelling and various factors including stormwater runoff and sewage wastewater inputs, contributes to these elevated nutrient concentrations. A negative correlation between *A. australis* concentrations and ammonium, while nitrate and nitrite show positive relationships, may suggest a preferential uptake of ammonium by *A. australis*. However, uptake rate measurements and further research would be needed to establish causal relationships.

## Introduction

Globally there are 11 species of surf zone diatoms, belonging to four genera: *Anaulus*, *Attheya*, *Aulacodiscus* and *Asterionellopsis* (da Silva Maria et al., 2016). These species are phylogenetically distinct but occur almost exclusively in surf zones. Surf zone diatoms have a common feature in forming intense, dark brown patches that are often mistaken for pollution in the surf zones of sandy beaches (Odebrecht et al., 2014). The patches are often semi-permanent features and are not blooms as they are not a result of cell division, but rather the result of accumulations via physical forcing within the surf zone circulation (Talbot & Bate, 1986). These patches are usually dominated by one or, in some cases, two species of diatoms (McLachlan & Lewin, 1981; Talbot & Bate, 1988a; Talbot, Bate & Campbell, 1990; Campbell & Bate, 1991).

Surf zone diatom patches are believed to be formed through the combination of two transport mechanisms: the horizontal circulation of the surf zone water masses, and the vertical migration of the cells in the water column. Surf zone diatoms require a dissipative beach state, with a wide surf zone, strong wave action, formation of rip current circulation, and significant beach length to form these accumulations (McLachlan & Defeo, 2018). These features are important in maintaining the horizontal aspect of the movement of the surf zone diatoms and will be discussed further in Chapter 3. Another key aspect in the biology of surf zone diatoms and the formation of patches is their diel vertical migration through the water column. Several species of surf zone diatoms, including *Attheya armata*, *Anaulus australis*, *Asterionellopsis socialis* and *Asterionellopsis glacialis*, have been found to exhibit diel periodicity in their vertical position in the surf zone. Cell characteristics, such as cell division, mucus formation, length of cell chains and cell sizes have also been shown to exhibit diel periodicity (Lewin & Rao, 1975; Talbot & Bate, 1986; da Silva Maria et al., 2016).

A diel cycle was first noted for *A. armata*, where cells rise to the surface in the early morning (well before sunrise) and disappear from the surf zone before sunset; cell concentrations were always orders of magnitude higher during the day ( $10^5$  cells.mL<sup>-1</sup>) than during the evening ( $10^3$  cells.mL<sup>-1</sup>) (Lewin & Hruby, 1973; Lewin & Rao, 1975). This phenomenon was later also established for *A. australis* and *A. socialis* and is suspected to be a common feature among surf zone diatoms (Talbot, Bate & Campbell, 1990). The diel periodicity of *A. australis* and *A. armata* have been well studied (Lewin & Rao, 1975; McLachlan & Lewin, 1981; Talbot, Bate & Campbell, 1990), although there is still some room for improving our understanding of the mechanisms behind the vertical migrations and the possible benefits such a cycle may hold for these species. Extensive studies have been conducted on surf zone diatom populations at Sundays River Beach, Algoa Bay, South Africa (Sloff, McLachlan &

Bate, 1984; Bate, Campbell & Rust, 1990; Talbot, Bate & Campbell, 1990; Campbell & Bate, 1991, 1998). *Anaulus australis* is the dominant surf zone diatom here. *Asterionellopsis glacialis* also has been recorded and, on a few occasions, has been recorded as the dominant species in patches (Talbot & Bate, 1988a; Talbot, Bate & Campbell, 1990). From studies at Sundays River Beach, a diel cycle has been proposed for *A. australis*; McLachlan & Lewin (1981) and Sloff, McLachlan & Bate (1984) were among the first to report this characteristic for South African surf zone diatom populations. *Anaulus australis* forms dense rust-brown patches in the inner surf zone during the late morning. Cells rise to the surface via a floatation mechanism and are kept in the inshore environment by remaining in the surface film. The floatation mechanism is thought to be via the attachment of cells to air bubbles; however, evidence for this phenomenon has not been tested experimentally for *A. australis*. Cells can accumulate in the surface film, and densities in the top few centimetres of the surface water can be orders of magnitude higher than those in the rest of the water column, as also noted for *A. armata* (Lewin & Rao, 1975; Sloff, McLachlan & Bate, 1984; Bate & McLachlan, 1987). As wave bores pass, these cells can be momentarily mixed into the water column, but the net transport of the cells in the surface film is in an onshore direction (du Preez & Campbell, 1996b). Patches are present next to rip currents, which cause net offshore transport of water, but the surface layer circulation remains in a net onshore direction as opposed to offshore rip-flow. Strong onshore winds are suspected to add to this effect (Talbot & Bate, 1989; Talbot, Bate & Campbell, 1990). During their phase in suspension, cells complete division, and have been reported to reach cell concentrations in the order of  $10^5$  cells.mL<sup>-1</sup> during peak cell concentrations at Sundays River Beach, South Africa (Sloff, McLachlan & Bate, 1984).

During the late afternoon, *A. australis* cells disappear almost entirely from the water column at Sundays River Beach in a short time frame, coinciding with the formation of a mucus layer around the cells. The cells are thought to lose their floatation mechanism by switching adherence from bubbles to sediment particles, allowing them to be deposited to the benthos. Thus, the bulk of the populations should switch from being present at the surface during the day to the sediment at night (McLachlan & Defeo, 2018). A portion of the population is also thought to be transported offshore via rip currents and longshore flows; this part of the population can repopulate the surf zone across weekly or monthly timescales (Talbot & Bate, 1987; Talbot, Bate & Campbell, 1990). In the sediment, *A. australis* enters a resting phase (du Preez & Bate, 1992) and is resuspended in favourable conditions thought to be linked to turbulent wave action (du Preez & Bate, 1992).

Several species of surf zone diatoms exhibit a strong diel cycle (e.g. *A. australis*, *Attheya armata* and *Asterionellopsis socialis*), but this phenomenon has been most extensively studied for *A. australis* on the South Coast of South Africa at Sundays River Beach (Talbot, Bate & Campbell, 1990). This study aims to investigate the diel cycle in cell concentrations of *Anaulus australis* at Muizenberg Beach in False Bay, Cape Town, on the South-West Coast of South Africa. The primary aim is to investigate patterns of cell movement over the duration of a single day. High resolution sampling is used to investigate the variability of cell concentrations across multiple stations in the surf zone, providing insight into the vertical movement of cells in the water column in snapshot locations across the shore. Along with the cell concentrations, patterns in cell characteristics and environmental variables also will be recorded, with the aim of assessing how cell concentrations change in relation to these factors. A key aspect for consideration will be how the findings compare with those from the well-studied Sundays River Beach surf zone system.

## Methods

### Sampling

Muizenberg Beach is a gently sloping, high energy, dissipative sandy beach located in False Bay, near Cape Town, South Africa. This chapter focuses on the diel cycle of *A. australis* on one day, 16 August 2019 (Figure 4).

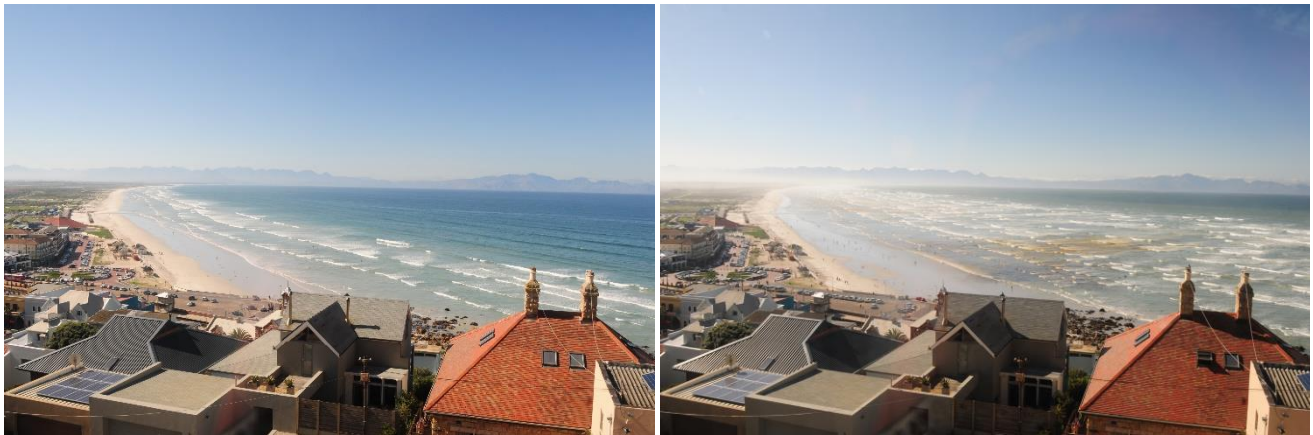


Figure 4: Muizenberg Beach on the sampling day, 16 August 2019 at 12:02 (left), representing typical conditions for the sampling day, and the day after sampling, 17 August 2019 at 10:52 (right), showing a patch that was first noted at 07:30 and disappeared by 12:00.

A transect with three stations across the width of the surf zone was sampled, with samples taken from both the surface water and the sediment (Figure 5). At Station 1 ( $34^{\circ}6'37.7''\text{S}$ ,  $18^{\circ}28'23.3''\text{E}$ ), the inshore samples were taken by wading into the water to reach a buoy marking the site ( $\pm 1$  m depth depending on tide), while Station 3 ( $34^{\circ}6'42.2''\text{S}$ ,  $18^{\circ}28'19.1''\text{E}$ ) samples were taken from approximately 330 m offshore, behind the breaker line. Station 2 ( $34^{\circ}6'37.2''\text{S}$ ,  $18^{\circ}28'18.0''\text{E}$ ) mid-shore samples were taken approximately 200 m from the high-water mark, between Station 1 and

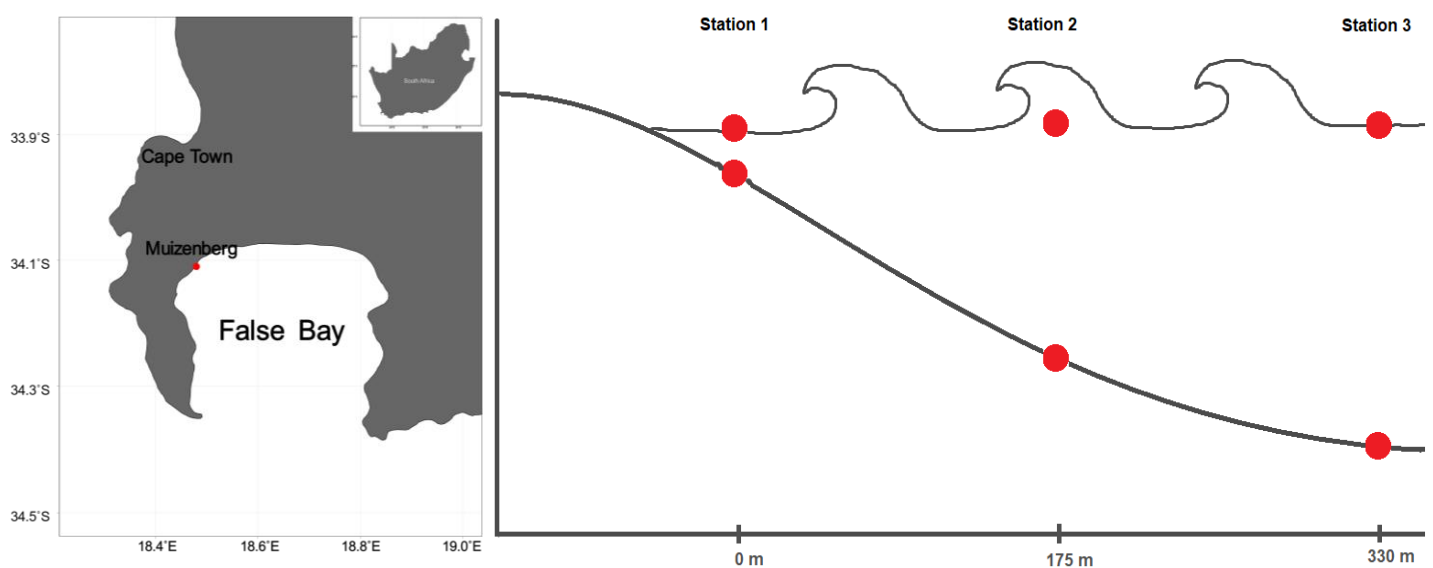


Figure 5: Map of False Bay region in South Africa, with the red pinpoint indicating the location of Muizenberg Beach, relative to Cape Town. A schematic diagram of the sampling strategy is also included on the right.

Station 3. At each station, a 25 L bucket of surface water and seven sediment samples were collected by divers and brought to shore. Sediment samples were collected by scooping the surface layer of sand (to an approximate depth of 5 cm) into a 250 mL plastic jar. Samples were collected at each station every hour from 06:30 to 18:30 on the 16th of August 2019. See Figure 5 for a visual schematic.

The surface water in the buckets was filtered through a 200 µm mesh funnel and samples were decanted. Three 50 mL Falcon tubes were rinsed thrice and filled with seawater for nutrient analyses. The Falcon tubes were frozen at -20°C until they were processed. In addition, a single 500 mL black bottle was half filled with seawater and preserved with 3 mL Lugol's solution to be used for phytoplankton counts by light microscope. Three 500 mL black bottles were also filled three quarters with seawater for chlorophyll-*a* measurements. They were kept in a -4°C freezer until a 250 mL subsample could be filtered onto a 0.3 µm GF/F filter on the day of sampling, after which the foil-wrapped filters were frozen at -80°C.

From the sediment jars brought to shore, one sample was taken for inverted light microscope phytoplankton counts by half filling a 500 mL black bottle with sediment and preserving with 3 mL Lugol's solution. For chlorophyll-*a* measurements, three Falcon tubes were filled from three different sediment jars. These tubes were frozen at -20°C. Sediment jars were shaken before decanting to ensure mixing.

## Laboratory analysis

### *Phytoplankton cell concentrations*

For surface samples, the Utermohl method was used to determine cell counts with an inverted light microscope (Utermohl 1958). Sample bottles were inverted 100 times, after which an aliquot of 0.5 - 2.5 mL was diluted to a final volume of 12.5 mL. This subsample was poured into a 10 mL settling chamber, with an inverted slide with a volume of 2.5 mL and allowed to settle for 1 hour. Samples were analysed using a Nikon Ti-E Inverted Microscope with Double Port FRET System. The chamber bottom was divided into a grid, and coordinates of 20 different random fields of view were generated using Microsoft Excel. Cells were counted in each field of view using 200x magnification, with notes taken on counts of paired cells, single cells, dividing cells and any other phytoplankton species visible. Phytoplankton samples from Station 1 were processed by another student for an honours project (Minkley, unpublished data) and during the analysis the cell division and cell size (volumes) were not noted; thus, these variables were only analysed for Station 2 & 3.

Dividing cells were classified according to Talbot and Bate (1986), who defined three easily observed characteristics of dividing cells: (i) polarization of the cell chromatophores, (ii) some evidence of

protoplast division, and (iii) the absence of a dividing valve. Stages of cell division were determined according to Talbot and Bate (1986) while using 400x magnification.

Cell length and width were measured for every *A. australis* cell in the first ten fields of view by using the NIS-Elements AR imaging software measuring tool. Width was defined as the distance between two frustules, and length was defined as the side of the frustule. Cell height or thickness (transapical axis) has been reported to be between 3 – 9  $\mu\text{m}$  (Kruger & Wilson, 1984), thus a constant value of 5.20  $\mu\text{m}$  was calculated using the geometric mean. The cell surface area and volume were calculated from these measurements using formulae for “pillow shaped cells” (Sun & Liu, 2003):

$$\text{Cell Volume } (\mu\text{m}^3) = \frac{\pi}{4} \times \text{Cell Length } (\mu\text{m}) \times \text{Cell Width } (\mu\text{m}) \times 5.20 \mu\text{m}$$

Cell counts of the surface samples obtained by microscopy were converted to cell concentrations using the following formula:

$$\text{cells. mL}^{-1} = \text{cells counted} \times \left( \frac{\text{area of chamber bottom } (\text{mm}^2)}{\text{area of field of view} (\text{mm}^2) \times \text{volume of subsample settled } (\text{mL})} \right)$$

where the area of the chamber bottom was 530.93  $\text{mm}^2$  and the area of a field of view was 0.0095  $\text{mm}^2$ .

Sediment samples were decanted into measuring cylinders and allowed to settle to obtain the volume of sediment. Each sample was then decanted into a glass beaker. Measured amounts (around 50 mL but depending on the sample) of filtered seawater were added, and the beaker was swirled for 30 seconds to suspend any phytoplankton. Large particles were allowed to settle for 5 seconds, and the supernatant was poured into another beaker. This process was repeated five times for each sample. The supernatant was then filtered through a 200  $\mu\text{m}$  sieve and the filtered water was poured through a 10  $\mu\text{m}$  sieve. The sieve was then turned upside down and rinsed into a glass beaker. The final volume of water added to the sample (rinsing volume) was measured and 10% of the sample volume of Lugol's solution was added as preservative. Samples were then settled and analysed using microscopy, as for the surface water samples.

Cell counts of the sediment samples obtained via microscopy were converted to cell concentrations (cells. $\text{mL}^{-1}$  of sediment) using the following formula:

$$\text{cells. mL}^{-1} = \text{cells counted} \times \left( \frac{\text{area of chamber bottom } (\text{mm}^2)}{\text{area of field of view} (\text{mm}^2) \times \text{volume of subsample } (\text{mL})} \right) \times \left( \frac{\text{Volume of rinsing water}}{\text{Volume of sediment sample}} \right)$$

where the area of the chamber bottom was 530.93 mm<sup>2</sup> and the area of a field of view was 0.0095 mm<sup>2</sup>. Biovolume (a proxy for biomass) of *A. australis* was calculated by multiplying the average *A. australis* cell volume by the average *A. australis* cell concentration for every phytoplankton sample.

#### *Nitrate and Silicate*

Two 5 mL subsamples were taken from a single Falcon tube for each summed nitrate and nitrate and silicate analysis. Concentrations of nitrate and silicate were determined using the Lachat Quikchem Flow Injection Analysis platform. A channel each for summed nitrate and nitrate, and silicate was auto analysed, with two replicates of each sample being measured. Egan (2008) and Diamond (1994), respectively, were used to determine final concentrations of nitrate and silicate using standard curves (Appendix, Figure A 1).

#### *Nitrite*

Two 5 mL replicate aliquots of each sample were placed in test tubes, 0.1 mL of sulphanilamide solution (0.0581 M) was added and each tube was vortexed and allowed to incubate for approximately 10 minutes. 0.5 mL of N-(1-naphthyl)-ethylenediamine dihydrochloride (NNED, 0.00386 M) was then added, and the tubes vortexed and allowed to incubate for 5 minutes. Standard concentrations of 0, 0.05, 0.1, 0.25, 0.5, and 0.75 µmol.L<sup>-1</sup> nitrite were prepared, with two replicates created as for the samples. A spectrophotometer set to 543 nm was used to read the absorbance of each test tube. The standard curve (Appendix, Figure A 1) was drawn from the known standard concentrations and their respective absorbance values, and this curve was used to determine the final concentrations of nitrite per sample. Nitrate concentrations were calculated by subtracting nitrite concentrations from the final summed nitrate and nitrite concentrations.

#### *Phosphate*

Two replicate 5 mL aliquots of each sample were placed in test tubes. 0.5 mL of mixed reagent (molybdate (0.0047 M); dilute sulphuric acid (1.21 M); ascorbic acid (0.061 M); potassium antimonyl tartrate (0.00028 M)) was added to each test tube, and each tube was vortexed and allowed to incubate for 5 minutes. Standard concentrations of 0, 0.1, 0.25, 0.5, 0.75, 1, 1.5, 2 and 3 µmol.L<sup>-1</sup> potassium phosphate were prepared, with two replicates created as for the samples. A spectrophotometer set to 885 nm was used to take duplicate readings of the absorbance of each test tube containing the standards and the samples. The standard curve was drawn (Appendix, Figure A 1) from the known standard concentrations and their respective absorbance values, and this curve was used to determine the final concentrations of phosphate per sample.

### *Ammonium*

Two 10 mL subsamples were taken from a single Falcon tube for ammonium analyses. The method of Holmes et al. (1999) was used to measure ammonium concentrations. Two replicates each of standard concentrations of 0, 0.1, 0.25, 0.5, 1, 1.5, 2, 3 and 6  $\mu\text{mol.L}^{-1}$  of ammonium chloride were prepared. 5 mL of o-Phthalaldehyde (OPA, 0.298 M) reagent was added to each sample and standard, which were incubated for 3 hours. A fluorometer with a UV module was used to measure the fluorescence of each sample and standard. A standard curve was drawn (Appendix, Figure A 1) from the linear equation of fluorescence versus ammonium concentration, and this equation was used to determine the concentration of ammonium in each sample. The matrix effect was calculated by adding 0.5 mL of 10  $\mu\text{M}$  ammonium stock to one replicate of a sample and one replicate of a standard concentration. The matrix effect accounts for variation in fluorescence caused by substances in the sample that are not present in the standards.

### *Chlorophyll-a*

Water samples for chlorophyll-*a* determination were filtered through a 0.3  $\mu\text{m}$  glass microfiber filter with a 25 mm diameter. This was done by fitting an Erlenmeyer flask to a vacuum pump, with a bung attached to a 25 mm frit sealing the mouth of the flask. A filter was sandwiched between the frit and a filter tower, and these were secured with a metal clamp. 250 mL of each sample was filtered, after which the filter was folded in half, covered in foil and frozen at  $-80^{\circ}\text{C}$ .

For processing, each filter was inserted into a test tube and 8 mL of acetone was added. The filters were stored at  $-20^{\circ}\text{C}$  for 24 hours. A test tube of acetone with no sample underwent the same procedure to act as a blank. A fluorometer, for which a standard curve had already been calibrated in 2019, was used to measure the fluorescence (RFU) of each sample. Three readings were taken for each sample and a blank reading was taken four times at regular intervals between samples. The final concentration of chlorophyll-*a* was determined by averaging the readings for each sample, subtracting the previous blank reading, multiplying this corrected value by the calibration factor and the 8 mL of added acetone divided by the volume of sample that was filtered.

$$[\text{Chl} - \text{a}] = (\text{Average sample RFU} - \text{Blank RFU}) \times \text{Calibration factor} \times \frac{8 \text{ mL acetone}}{\text{Sample volume}}$$

For the sediment samples, the 5 mL of sediment sample was placed into a Falcon tube, and 50 mL of acetone was added. These tubes were also stored at  $-20^{\circ}\text{C}$  for 24 hours. To take the fluorometer readings, the samples were shaken well, and the sediment allowed to settle once again. The supernatant was then poured into a cuvette to take the readings. Blank readings were also taken before and after the batches were measured.

## Other environmental data

Wind speed and direction were obtained from the South African Weather Services for measurements taken at the Cape Town International Airport at hourly timescales. Since the wind measurement data were of observations taken every hour, on the hour, measurements were adjusted to a midpoint between the hours to account for hourly seawater samples taken 30 minutes past the hour. For analysis, wind directions were indicated as numeric values as degrees from North ( $0^\circ$ ). Directions on this day ranged from  $170$  to  $190^\circ$ . Similarly, forecast tidal height data were received from the South African Navy Hydrographic Office and adjusted to a mid-point between hourly values (South African Navy, 2019).

## Statistical analyses

All statistical analyses were conducted in R version 2023.12.0.369 (Posit team, 2023). For comparing the *A. australis* cell concentrations between stations in the surface and sediment, an ANOVA with a post-hoc Tukey test was conducted. The data were square root transformed as the residuals were found not to be equal and not normally distributed. The tabled results of the ANOVA and Tukey tests and the model validation graphs of the residuals can be found in the Appendix (Appendix, Figure A 2, Table A 1).

### *General Linear Models:*

Several general linear models were fit to the data to determine influential variables for *A. australis* cell concentrations, chlorophyll-*a* concentrations, and cell volumes. All models were conducted using a stepwise approach to select models of lowest AIC values in R (Posit team, 2023).

A general linear model was fit to the square root transformed *A. australis* cell concentration data. This model was selected using a stepwise regression with the following predictors: time, station, other cells, nutrients ( $NO_2^-$ ,  $NO_3^-$ ,  $PO_3^{3-}$ ,  $SiO_4^{4-}$ ,  $NH_4^+$  for surface only), tidal height, wind direction and wind speed. Average cell volumes or surface areas, and proportions of dividing cells were not included in this model as these data were only collected for Station 2 and 3. Chlorophyll-*a* also was not included in this model as it is a proxy variable for cell concentrations. Residual plots are included in the Appendix (Appendix, Figure A 3).

A general linear model was fit to the untransformed data for chlorophyll-*a*. This model was selected using a stepwise regression with the following predictors: time, station, nutrients ( $NO_2^-$ ,  $NO_3^-$ ,  $PO_3^{3-}$ ,  $SiO_4^{4-}$ ,  $NH_4^+$  for surface only), tidal height, wind direction and wind speed. Average cell volumes or surface areas, and proportions of dividing cells were not included in this model as these data were only collected for Station 2 & 3. Other phytoplankton cell concentrations also were not included in this model. Residual plots are included in the Appendix (Appendix, Figure A 4).

## Results

On the day of sampling, no visible patches were present for the duration of sampling (Figure 4a). However, it should be noted that a patch event was recorded on the day after sampling (17 August 2019) in the early morning, until around midday (Figure 4b), which may explain differences in samples compared to other studies.

### Cell Concentrations in the Surface Water

Across all stations, surface cell concentrations of *A. australis* were low in the early morning, increasing to a peak in cell concentration in the late morning around 11:00 (Figure 6). Thereafter, cell concentrations generally declined, except for some secondary, small peaks in the late afternoon at Stations 1 and 3 (Figure 6a, c). Cell concentrations in the water declined to low concentrations in the late afternoon to early evening (Figure 6).

Cell concentrations differed significantly between stations ( $F = 10.63$ ,  $df_1 = 2$ ,  $df_2 = 33$ ,  $p < 0.001$ ), decreasing with distance from shore. Mean cell concentrations were significantly greater in Station 1

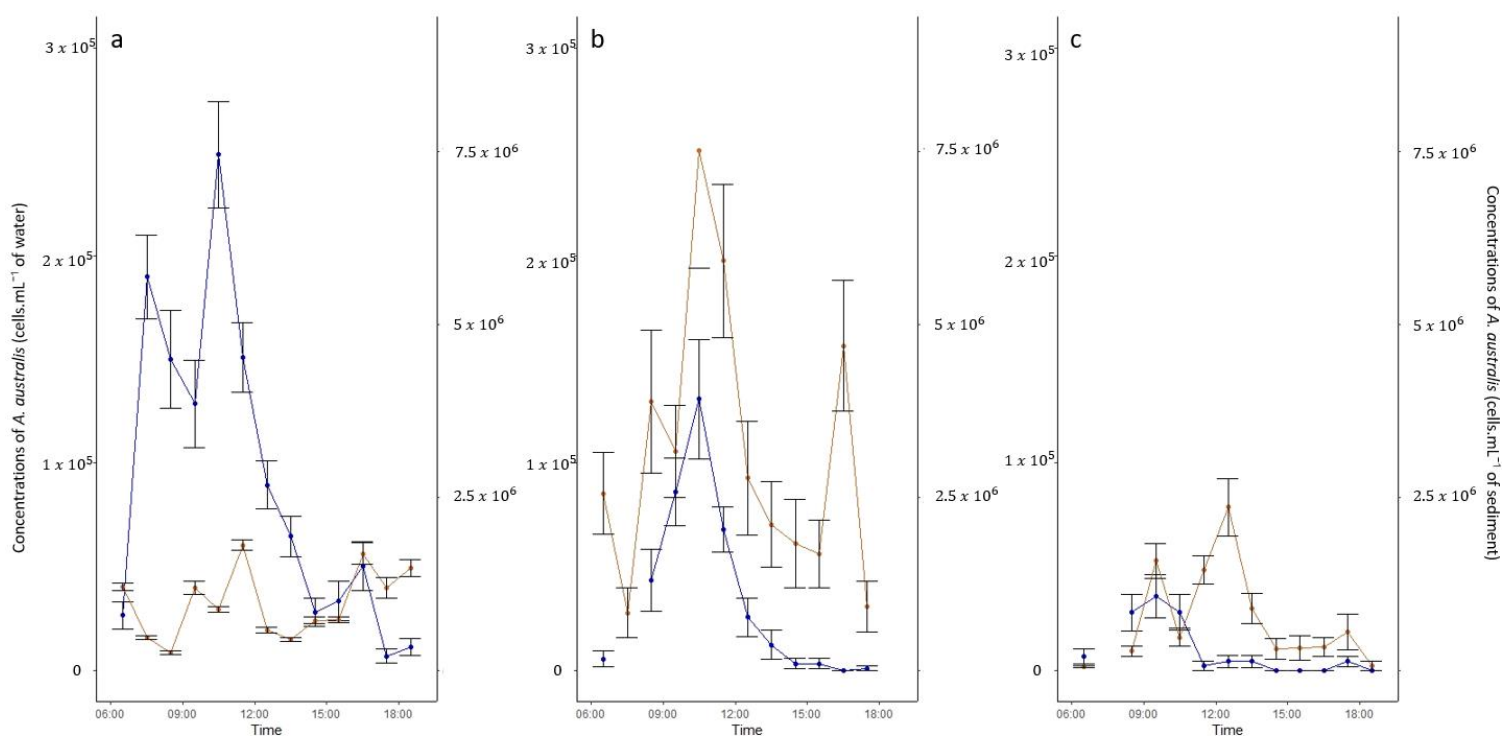


Figure 6: Mean ( $\pm$  standard error) ( $n=20$ ) cell concentrations of *A. australis* at different times of the day at Muizenberg Beach on 16 August 2019 for a) Station 1, b) Station 2, and c) Station 3. Blue lines show concentrations ( $\text{cells.mL}^{-1}$  of water) from surface waters. Orange lines show concentrations ( $\text{cells.mL}^{-1}$  of sediment) from sediment samples.

than Station 2 (Tukey HSD,  $p < 0.05$ ) and Station 3 (Tukey HSD,  $p < 0.001$ ). There was no difference in cell concentrations between Station 2 and 3 (Tukey HSD,  $p > 0.05$ ) (Appendix, Figure A 2, Table A 1).

Cell concentrations of the other species were always lower than the cell concentrations of *A. australis*, even though there was no brown patch visible on the day of sampling. In contrast to the pattern for *A. australis*, cell concentrations of other phytoplankton species increased from the inshore station to behind the breaker zone (Figure 7). Similar to the results for *A. australis*, cell concentrations of other species were larger at Station 1 than Station 2 ( $H = -3.03$ ,  $p < 0.05$ ) and Station 3 ( $H = -4.74$ ,  $p < 0.001$ ), but concentrations were similar at Station 2 and Station 3 ( $H = -1.58$ ,  $p > 0.05$ ) (Kruskal-Wallis,  $\chi^2 = 23.31$ ,  $df = 2$ ,  $p \ll 0.001$ ). Both phytoplankton groups followed a similar diel cycle of an early morning peak in the water column and a decrease in the afternoon. However, the other species of phytoplankton tended to fluctuate in concentration throughout the afternoon, with no decline to 0 cells.mL<sup>-1</sup>, as observed for *A. australis* (Figure 7).

Peaks in surface chlorophyll-*a* concentrations regularly corresponded to peaks in cell concentrations of *A. australis* (Figure 7). Other species also contributed to these chlorophyll measurements, therefore chlorophyll-*a* concentrations did not decline to zero in the late afternoons, as did the cell concentrations of *A. australis*. There was a strong positive relationship between chlorophyll-*a* concentrations in the surface water and the cell concentrations of *A. australis* (Figure 8a,  $r = 0.94$ ,  $df = 34$ ,  $p < 0.0001$ ). No such relationship was found between the concentrations of other cells and chlorophyll-*a* concentrations (Figure 8b,  $r = -0.17$ ,  $df = 34$ ,  $p > 0.05$ ).

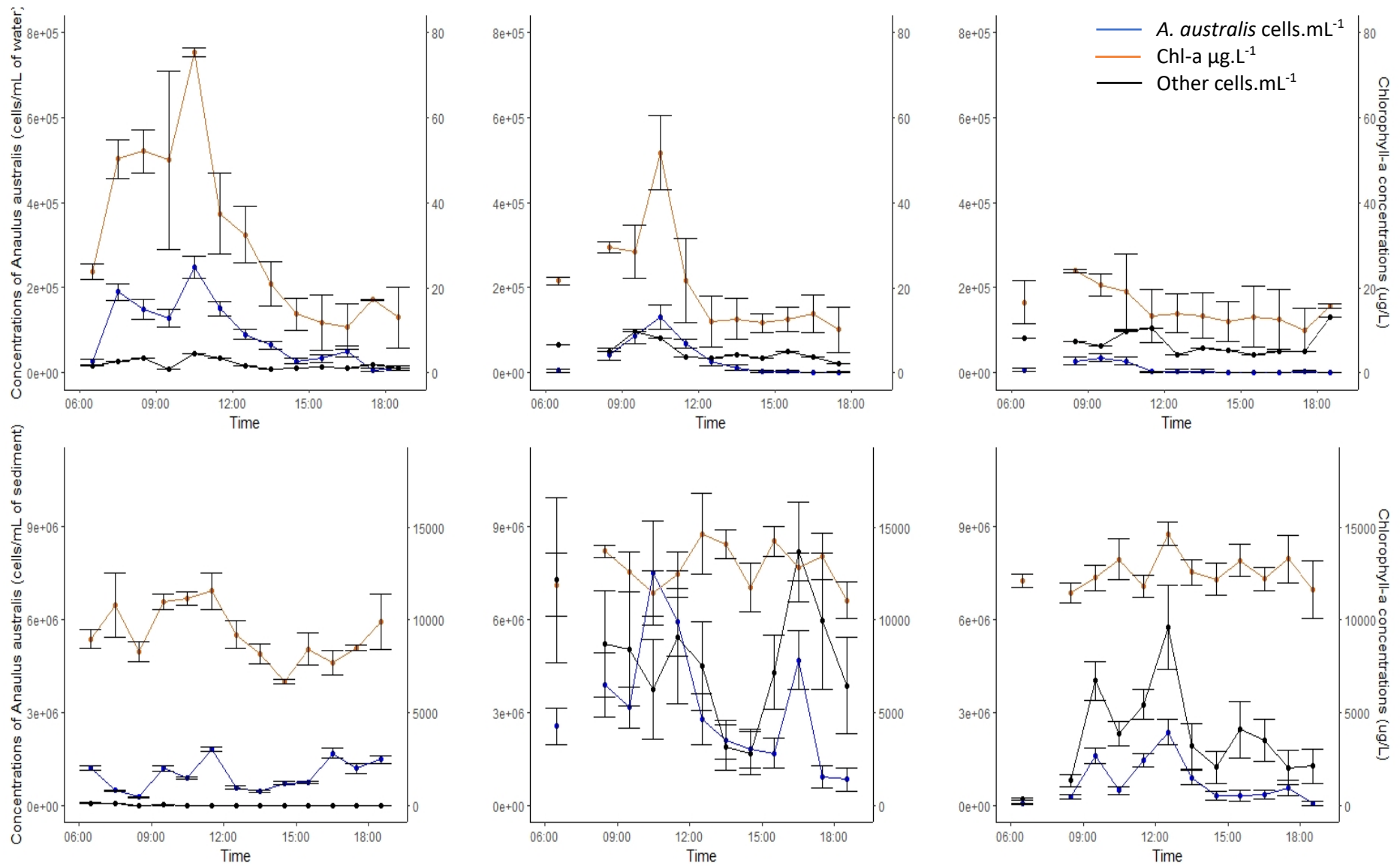


Figure 7: Mean ( $\pm$  standard error) ( $n=2$ ) bulk chlorophyll-a concentrations (orange,  $\mu\text{g.L}^{-1}$ ) and cell concentrations of *A. australis* (blue) and other phytoplankton species (black) at different times of the day at Muizenberg Beach on 16 August 2019. Results for surface waters are given as a) Station 1, b) Station 2, and c) Station 3, and results for sediments as d) Station 1, e) Station 2, and f) Station 3.

### Cell Concentrations in the Sediment

Cell concentrations of *A. australis* in the sediment generally reached a maximum in the late morning and declined thereafter, with a secondary peak in the late afternoon (Figure 6). The exception was at the inshore Station 1, where sediment cell concentrations fluctuate throughout the day, and increased in the afternoon. However, there was still a slight peak in the mid-morning and late afternoon.

Sediment cell concentrations differed significantly between stations ( $F = 16.54$ ,  $df_1 = 2$ ,  $df_2 = 34$ ,  $p < 0.001$ ). Mean cell concentrations differed between Station 1 and 2 (Tukey HSD,  $p < 0.001$ ) and Station 2 and 3 (Tukey HSD,  $p < 0.001$ ), with Station 2 having the highest mean sediment cell concentrations. There was no difference in sediment cell concentrations between Station 1 and 3 (Tukey HSD,  $p < 0.05$ ) (Appendix, Figure A 2, Table A 1).

*Anaulus australis* dominated the composition of cells found in the surf zone sediment at the inshore Station 1, where very few other phytoplankton species were present in the sediment (Figure 7). Across the other two stations, *A. australis* sediment cell concentrations much less those of the other species of phytoplankton combined. Sediment cell concentrations of the other phytoplankton species differed significantly between the three stations (Kruskal-Wallis  $\chi^2 = 28.45$ ,  $df = 2$ ,  $p < 0.001$ ), with differences between Station 1 and 2 ( $H = -5.25$ ,  $p < 0.001$ ), Station 1 and 3 ( $H = -3.35$ ,  $p < 0.001$ ), and between Station 2 and 3 ( $H = -1.86$ ,  $p < 0.05$ ). At Station 1, only a few cells of other species were noted in the sediment in the early morning, whereas Station 2 had the greatest sediment cell concentration. Peaks in other species cell concentrations in the sediment of Station 2 and 3 tracked the peaks of *A. australis* cell concentrations.

At Station 1 the chlorophyll-*a* concentration peaks corresponded within an hour to peaks in cell concentrations of *A. australis*, also following similar trends in declines after 11:30 and an increase in the late afternoon. Similarly, chlorophyll-*a* concentrations at Station 3 peaked in the morning, corresponding to peaks in cell concentrations of *A. australis*; however, chlorophyll-*a* concentrations fluctuated more regularly in the afternoon. In contrast, Station 2 chlorophyll did not match patterns in *A. australis* cell concentrations, and chlorophyll-*a* concentrations fluctuated throughout the day, following a trend closer to that of the cell concentration of other species of phytoplankton.

There was a positive relationship between chlorophyll-*a* concentrations in the sediment and the cell concentrations of other species (Figure 8d,  $r = 0.65$ ,  $df = 35$ ,  $p < 0.001$ ). No such relationship was found between the concentration of *A. australis* cells and chlorophyll-*a* concentration in the sediment (Figure 8c,  $r = 0.26$ ,  $df = 35$ ,  $p > 0.05$ ).

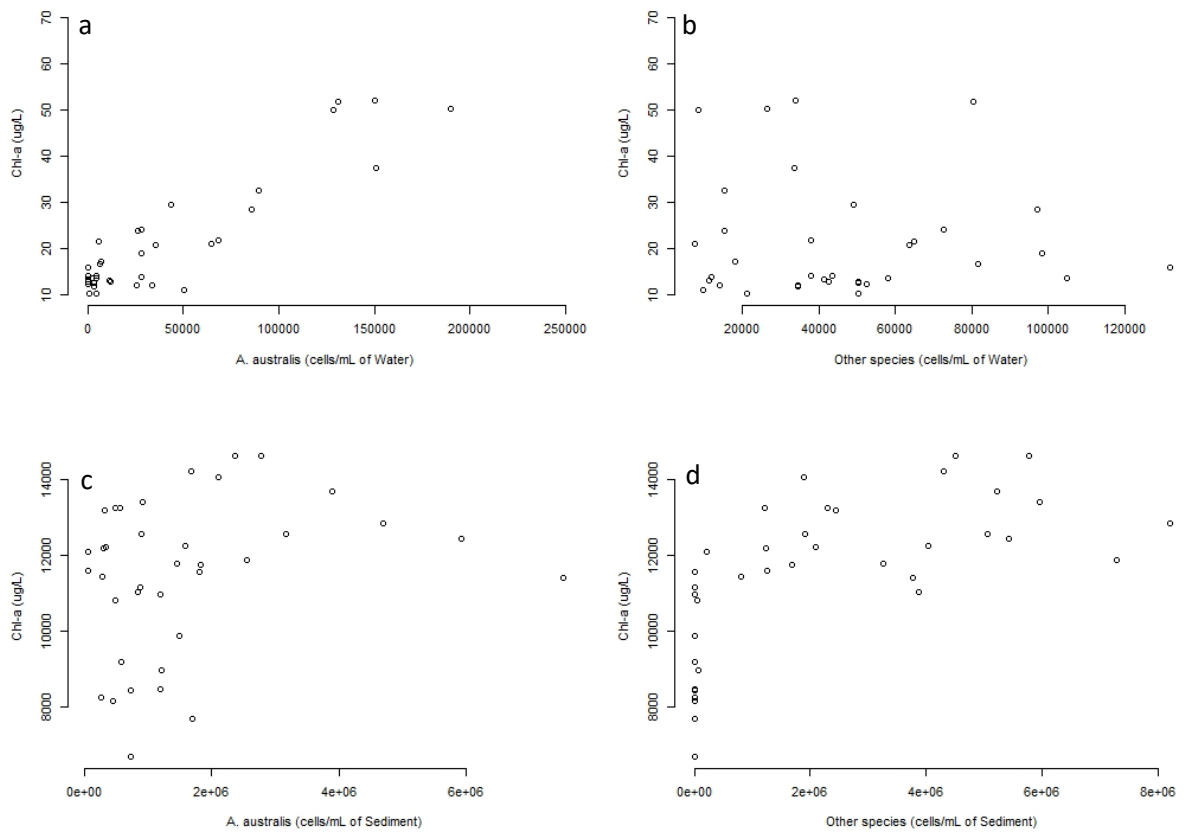


Figure 8: Bulk chlorophyll-a concentrations ( $\mu\text{g.L}^{-1}$  of water or sediment) at different cell concentrations of a) *A. australis* in surface waters ( $\text{cells.mL}^{-1}$ ), b) other species in surface waters ( $\text{cells.mL}^{-1}$ ), c) *A. australis* in sediments ( $\text{cells.mL}^{-1}$  of sediment), d) other species in sediments ( $\text{cells.mL}^{-1}$  of sediment) at Muizenberg Beach on 16 August 2019.

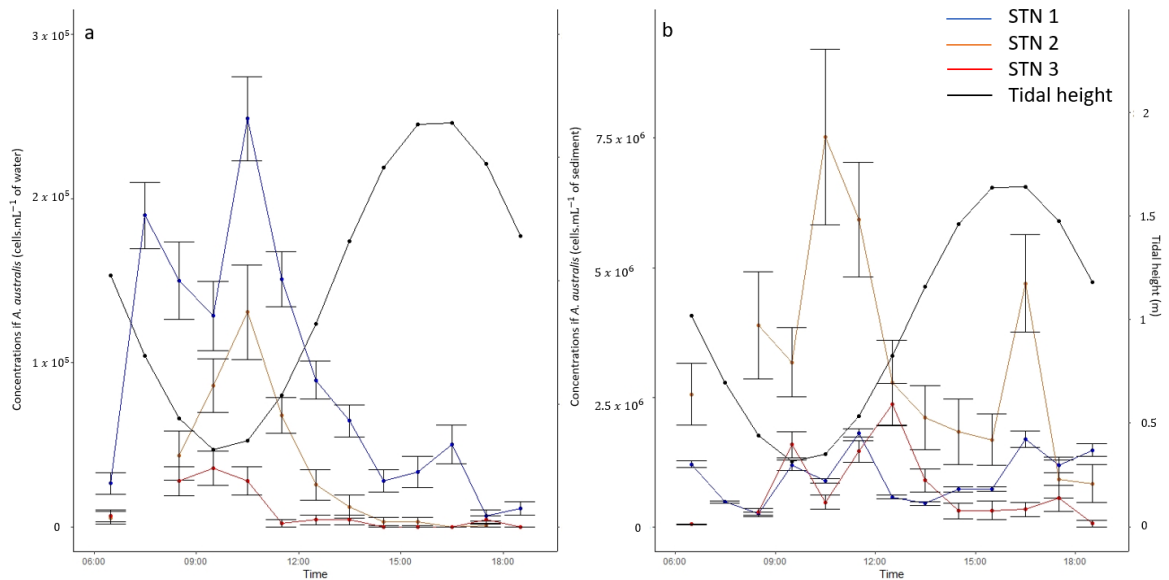


Figure 9: Mean ( $\pm$  standard error) cell concentrations of *A. australis* ( $\text{cells.mL}^{-1}$ ) at the three sampled stations and tidal heights at different times of the day at Muizenberg Beach on 16 August 2019 for a) surface waters and b) sediments. Blue = station 1, red = station 2, orange = station 3, black = tidal height.



### Nutrients

Nitrite concentrations were generally low ( $<0.2 \mu\text{mol.L}^{-1}$ ) and differed among the three stations ( $F = 4.097$ ,  $df_1 = 2$ ,  $df_2 = 33$   $p < 0.05$ ), being lower at Station 3 than Station 1 and 2 ( $p < 0.05$ ), which had similar mean concentrations ( $p > 0.05$ ). There was a significant positive relationship between nitrite concentrations and *A. australis* abundance in the surface waters ( $r = 0.48$ ,  $df = 34$ ,  $p < 0.01$ ) (Figure 11b).

Nitrate concentrations were also relatively low ( $< 7 \mu\text{mol.L}^{-1}$ ) and did not differ among stations (Kruskal-Wallis,  $\chi^2 = 2.06$ ,  $df = 2$ ,  $p > 0.05$ ). There was a significant positive relationship between nitrate concentrations and cell concentrations of *A. australis* across all stations ( $r = 0.34$ ,  $df = 34$ ,  $p < 0.05$ ) (Figure 11c).

For the phosphate concentrations, there was a significant difference among stations (Kruskal-Wallis,  $\chi^2 = 8.54$ ,  $df = 2$ ,  $p < 0.05$ ), where Station 3 had significantly lower phosphate concentrations than Station 1 and 2 ( $p < 0.05$ ), but the concentrations of Station 1 and 2 did not differ ( $p > 0.05$ ). Phosphate concentrations had a significant positive relationship with cell concentrations of *A. australis* ( $r = 0.36$ ,  $df = 34$ ,  $p < 0.05$ ) (Figure 11d).

There were no significant differences in silicate concentrations among stations ( $F = 3.90$ ,  $df_1 = 2$ ,  $df_2 = 33$ ,  $p = 0.056$ ). There was no relationship between silicate concentration and *A. australis* cell concentrations in the surface waters ( $r = -0.12$ ,  $df = 34$ ,  $p = 0.50$ ) (Figure 11e).

Ammonium concentrations did not differ significantly between Station 1 and 2 but these two stations had much lower ammonium concentrations than Station 3 (Kruskal-Wallis,  $\chi^2 = 4.54$ ,  $df = 2$ ,  $p = 0.1$ ). There was a significant negative relationship between the cell concentrations of *A. australis* in surface waters and ammonium concentrations ( $r = -0.62$ ,  $df = 34$ ,  $p\text{-value} < 0.001$ ) (Figure 11a).

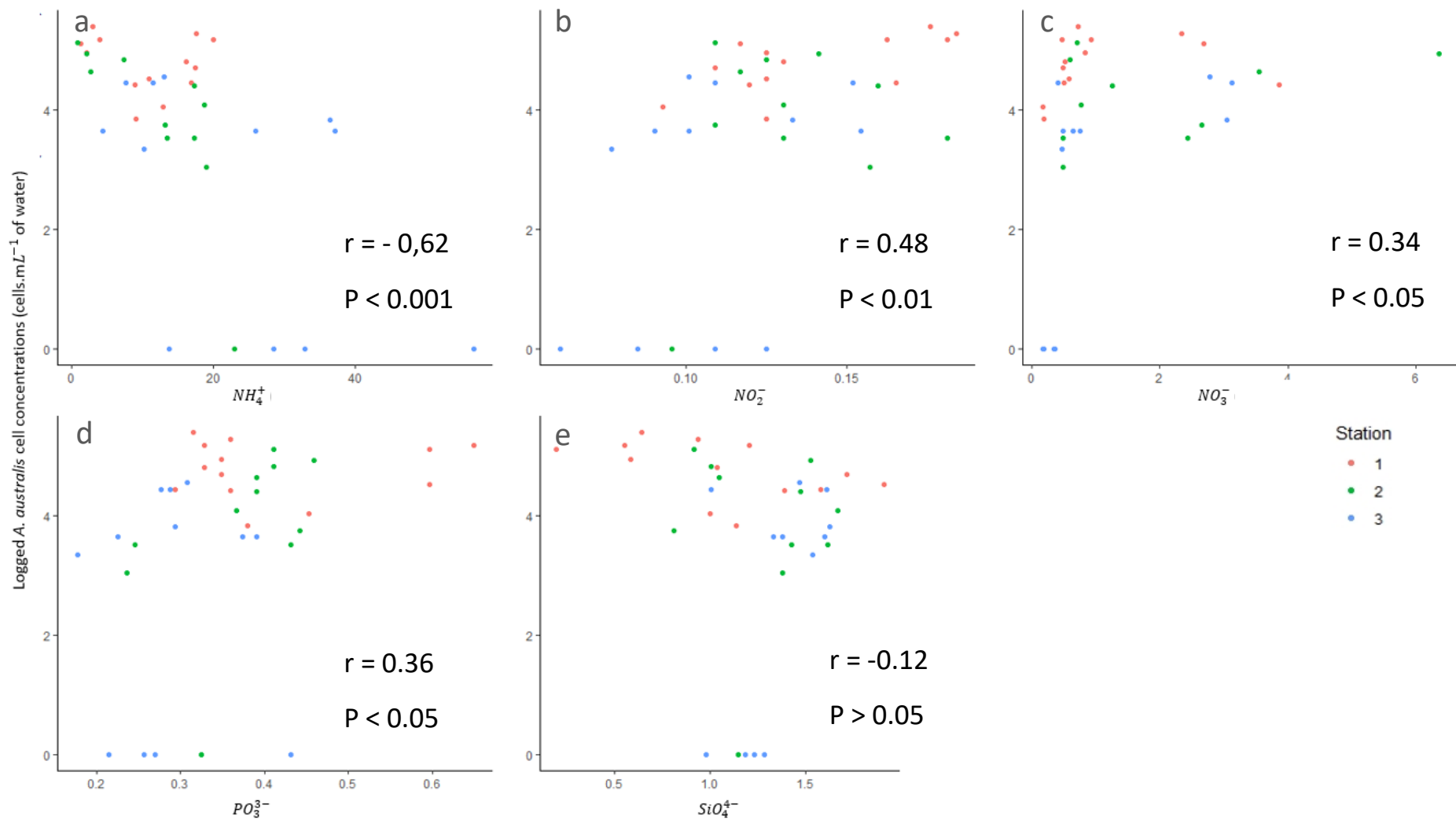


Figure 11 : Log cell concentrations of *A. australis* (cells.mL<sup>-1</sup> of water) in surface waters at Muizenberg Beach on 16 August 2019, plotted against nutrient concentrations (μg.L<sup>-1</sup>) for a) ammonium (NH<sub>4</sub><sup>+</sup>), b) nitrite (NO<sub>2</sub><sup>-</sup>), c) nitrate (NO<sub>3</sub><sup>-</sup>), d) phosphate (PO<sub>3</sub><sup>3-</sup>) and e) silicate (SiO<sub>4</sub><sup>4-</sup>). (Different colour dots represent different stations: Station 1 = red; station 2 = green; station 3 = blue)

*Models with Total Anaulus australis cells as the response variable*

In the surface waters, distance from shore (station), wind direction (a shift toward Northerly offshore winds) and tidal height had significant negative associations with cell concentrations of *A. australis* (Table 1a).

In the sediment, a decrease in *A. australis* cell concentrations was associated with an increase in distance from shore (station) and increases in cell concentration of other species of phytoplankton (Table 1b).

*Models with Chlorophyll-a as the response variable*

In the surface waters, an increase in the chlorophyll-*a* concentration was associated with increases in tidal height and cell concentrations of *A. australis* (Table 1c). An increase in chlorophyll-*a* concentration was also associated with a decrease in silicate concentrations and a more onshore, southerly wind direction (Table 1c).

In the sediment, an increase in chlorophyll-*a* concentrations was associated with an increase in distance from shore (stations) as well as an increase in tidal height (Table 1d).

Table 1: Generalised linear model results tables for surface (A) and sediment (B) *A. australis* cell concentrations as response variables and surface (C) and sediment (D) chlorophyll-a concentrations response variables.

A)	Estimate	Std. Error	t-value	P-values	B)	Estimate	Std. Error	t-value	P-values
Intercept	1180.89	321.55	3.67	9.31x10 <sup>-4</sup>	(Intercept)	1176.25	160.78	7.32	2.57 x10 <sup>-8</sup>
Station 2	-123.99	21.64	-5.73	2.97x10 <sup>-6</sup>	Station 2	-192.70	358.74	-0.54	5.95x10 <sup>-1</sup>
Station 3	-177.08	23.33	-7.59	1.83x10 <sup>-8</sup>	Station 3	-799.05	257.60	-3.10	4.00x10 <sup>-3</sup>
NO2	667.21	330.15	2.02	5.23x10 <sup>-2</sup>	Other	0.4491	0.16	2.86	7.41 x10 <sup>-8</sup>
Tidal Height	-155.46	20.11	-7.73	1.27x10 <sup>-8</sup>	Tidal Height	-246.73	126.69	-1.95	6.03 x10 <sup>-2</sup>
Wind Direction	-4.72	1.77	-2.67	1.22x10 <sup>-2</sup>					

C)	Coeff. Estimate	Std. Error	t-value	P-values	D)	Coeff. Estimate	Std. Error	t-value	P-values
(Intercept)	72.85	27.01	2.70	1.15x10 <sup>-2</sup>	(Intercept)	9830.2	530.70	18.52	<2x10 <sup>-16</sup>
Cell concentration	1.92x10 <sup>-4</sup>	1.80 x10 <sup>-5</sup>	10.93	<1.00x10 <sup>-6</sup>	Station 2	3601.5	485.6	7.42	1.61 x10 <sup>-8</sup>
Other	4.40x10 <sup>-5</sup>	2.70x10 <sup>-5</sup>	1.59	1.23x10 <sup>-1</sup>	Station 3	3311.3	485.6	6.82	8.86 x10 <sup>-8</sup>
SiO4	-7.75	2.26	-3.44	1.81x10 <sup>-3</sup>	Tidal Height	-593.2	419.2	-1.42	0.17
Tidal Height	5.61	3.19	1.76	8.92x10 <sup>-2</sup>					
Wind Direction	-2.22	0.66	-3.36	2.21x10 <sup>-3</sup>					
Wind Speed	-0.23	0.14	-1.58	1.24x10 <sup>-1</sup>					

### Characteristics of *Anaulus australis* Cells

There was a strong diel signal in cell volume at Station 2 and 3 (Figure 12), which increased until midday before decreasing again. The proportion of dividing cells showed a similar pattern, which was negatively correlated with the proportion of paired cells. Thus, cells increased in volume through the morning, and at the same time the proportions of dividing and single cells also increased.

Across samples of Station 2 and 3, cells of *A. australis* in the surface water were significantly greater than cells in the sediment (Figure 13a) (T-test,  $t = 15.98$ ,  $df = 368.6$ ,  $p < 0.001$ ). This could be caused by whether the cells were single or paired, because the volumes of single *A. australis* cells were significantly larger than those of paired cells (T-test,  $t = -5.55$ ,  $df = 103.05$ ,  $p < 0.001$ ) (Figure 13d). However, the proportions of single and paired cells did not differ significantly between the surface and sediment (Pearson's Chi-squared,  $\chi^2 = 62.76$ ,  $df = 61$ ,  $p > 0.05$ ) (Figure 13c).

Dividing cells of *A. australis* were also significantly larger in volume than non-dividing cells (Figure 13b) (T-test,  $t = 8.60$ ,  $df = 108.54$ ,  $p < 0.001$ ), and this likely influenced the differences in cell size between surface waters and sediment; the proportion of dividing cells was significantly larger in the surface than the sediment (Figure 10d) (Pearson Chi-Squared,  $X^2 = 22.94$ ,  $df = 21$ ,  $p = 0.35$ )

The total biovolume of *A. australis* in the surface waters was positively correlated with the chlorophyll-*a* concentrations ( $r = 0.87$ ,  $df = 12$ ,  $p < 0.001$ ) (Figure 14a), but there was no such correlation found in the sediment ( $r = 0.12$ ,  $df = 22$ ,  $P > 0.5$ ) (Figure 14b).

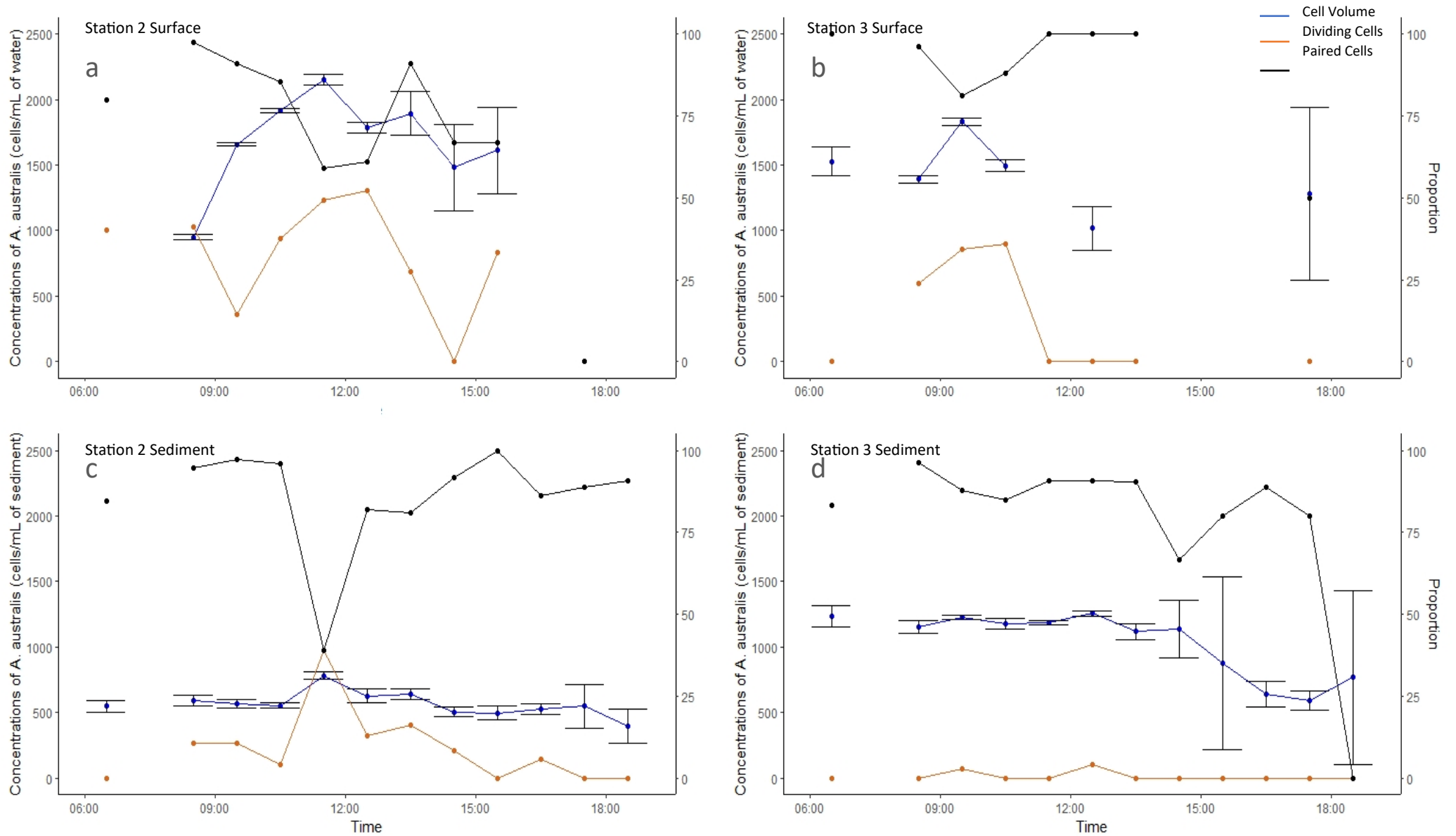


Figure 12: Changes during the day of mean ( $\pm$  Standard Error) cell volume (blue,  $\mu\text{m}^3$ ) and proportions of dividing (orange) and paired (black) cells of *Anulus australis* at Muizenberg Beach on 16 August 2019. a) Station 2 surface samples, b) station 3 surface samples, c) station 2 sediment samples, d) station 3 sediment samples

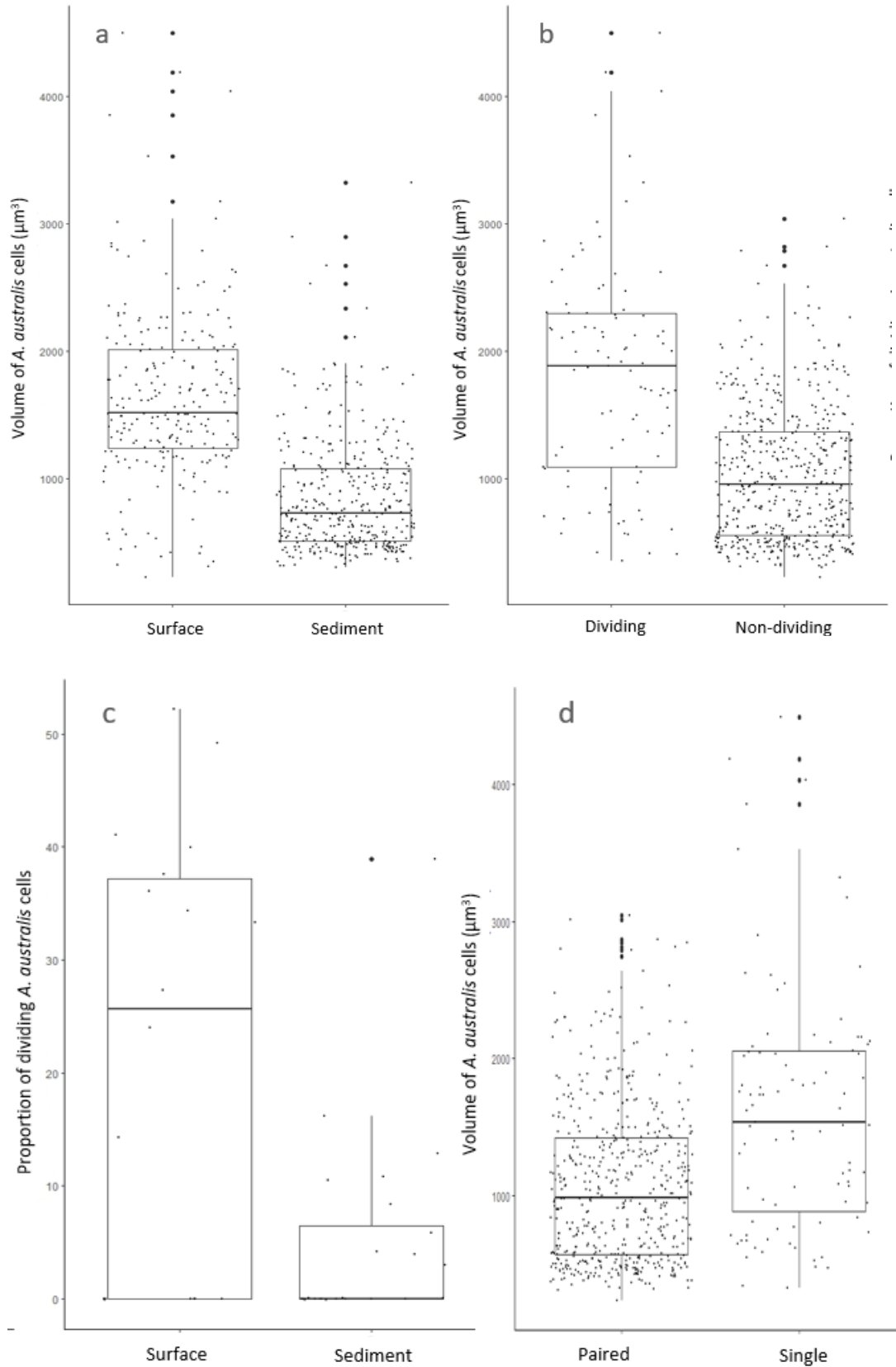


Figure 13: Boxplots showing the estimated volumes ( $\mu\text{m}^3$ ) of individual *Anulus australis* cells from stations 2 and 3 at Muizenberg Beach on 16 August 2019. a) Cells in the surface waters and sediments, b) cells that are dividing or not dividing, and c) comparisons of volume ( $\mu\text{m}^3$ ) of the surface and sediment (right) and dividing and non-dividing cells (left) of *A. australis* cells across Station 2 & 3.

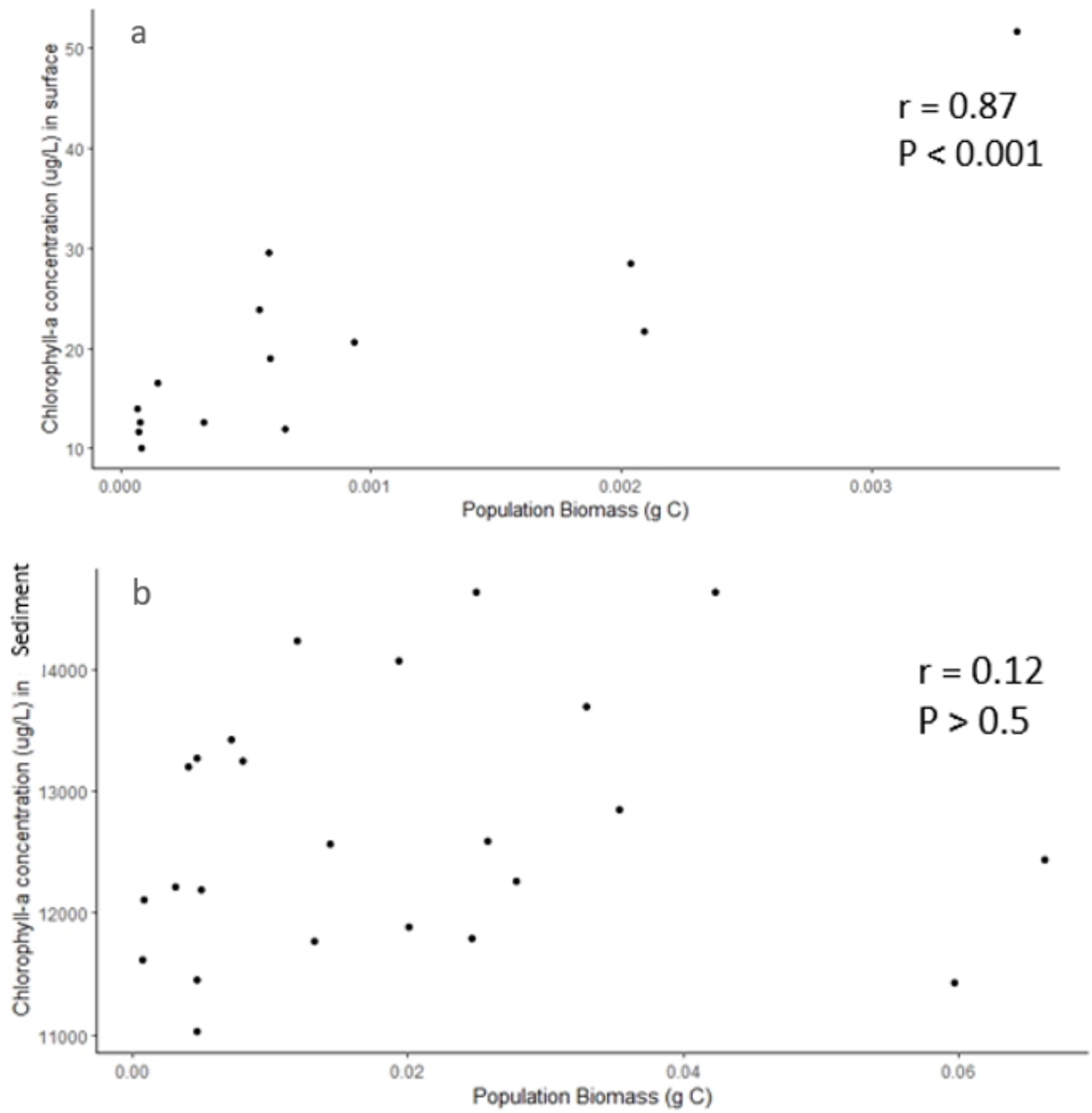


Figure 14: Relationships between chlorophyll-a I concentrations ( $\mu\text{g}\cdot\text{L}^{-1}$ ) and *Anaulus australis* biomass (g C) at Muizenberg Beach on 16 August 2019. a) surface waters, b) sediment.

## Discussion

This study found that *A. australis* exhibits a similar diel cycle at Muizenberg Beach (South-West Coast) to that previously found at Sundays River Beach (South Coast), with some key distinctions. Both the sediment and surface cell concentrations of *A. australis* showed an increase in the late morning with a decline in the afternoon, similar to results reported by previous studies in Algoa Bay, South Africa (McLachlan & Lewin, 1981; Sloff, McLachlan & Bate, 1984), and for other species of surf zone diatoms globally (Lewin & Hruby, 1973; Lewin & Rao, 1975). A key aspect of the *A. australis* Muizenberg Beach populations are the high cell concentrations found, with cell counts on a non-patch day reaching up to  $10^5$  cells.mL<sup>-1</sup>, a stark contrast to the maximum cell concentrations of 500 cells.mL<sup>-1</sup> at Sundays River Beach during a no-patch day (it may be important to note here that the conditions sampled closely preceded a patch event) and *A. australis* cell concentrations on the order of  $10^5$  within patches (Sloff, McLachlan & Bate, 1984). Although sediment cell concentrations tracked changes in the planktonic component of the populations, as found by Talbot & Bate (1989), sediment concentrations were much higher than most of the cell concentrations recorded at Sundays River Beach ( $7.5 \times 10^9$  cells per running meter in sediment). Talbot & Bate (1988c) suggested that cells lay dormant in the sediment during periods of calm conditions, often behind the breaker zone, to be resuspended upon turbulent conditions and pushed inshore by circulation patterns. They would then repopulate the surf zone water column, until conditions become calm, upon which they would once again sink back into the sediment, thus creating a mesoscale turbulent-calm-turbulent variability in the population dynamics. This reservoir of cells in the sediment was first noted at Sundays River by Talbot & Bate (1987).

There is a signal of a late morning peak in cell concentrations for both the sedimented and surface water column populations of *A. australis*. Whilst replication is needed to define a diel cycle, results are to findings from Sundays River Beach. Previous work on *A. australis* at Muizenberg Beach also found a similar peak in the late afternoon, with cell concentrations during this second peak being higher than the cell concentrations in the morning (de Vos, 2018). The sampling during both these studies was at hourly intervals, a time scale that is logistically challenging due to the physical intensity of this work, and the time it takes to analyse large quantities of these samples, and this high frequency sampling thus not been deployed in many studies. The second peak in abundance could be a phenomenon that has not yet been noticed at Sundays River Beach, but has been noted in two sampling occasions at Muizenberg. Alternatively, this could also indicate a unique feature of the *A. australis* population at Muizenberg. These peaks corresponded with changes in tide, and thus a possible explanation is that changes in tide introduced more mixing, which resuspended sedimented cells.

Wind conditions, although moderate in speeds, remained in an onshore direction throughout the day of sampling. The observed intense patch on the day after sampling would be expected after periods

of onshore winds and turbulent conditions (Talbot & Bate, 1988c; Talbot, Bate & Campbell, 1990; Odebrecht et al., 2014; Tedesco et al., 2017), although predictability of these patches is difficult (Chapter 3). The conditions on the sampling day represented pre-patch conditions, and thus surface water and sediment samples could have contained higher cell concentrations than average.

As expected, the concentration of cells at surface decreased as one moved further away from shore, beyond the surf zone. The inner surf zone had clear maxima in cell concentrations throughout the day. These are similar to results found by Talbot & Bate (1988b) at Sundays River Beach and indicate that cells are retained in the surf zone to a large extent. Afternoon declines in cell concentrations became more pronounced as one moved offshore, possibly indicating that there is a spillover of cells into the deeper stations during the peak in the morning, but that there may be little retention of cells without the presence of the surf zone circulation. Cells were also at their highest concentrations at the mid-shore Station 2, indicating that cells are retained in the surf zone.

At Muizenberg Beach the surf zone was almost entirely dominated by *A. australis*, both in the surface waters and sediment, with almost no other phytoplankton species present. Cell concentrations of other phytoplankton species increased as one moved offshore, a pattern that is directly opposite to that of *A. australis*, indicating that *A. australis* is uniquely adapted to a surf zone existence. The diel cycle present in these other species also indicated that these inshore accumulations are largely dependent on physical circulation, rather than biological factors. A key distinction in this diel cycle for other species is that, unlike *A. australis*, cell concentrations did not decline to zero in the evenings and a large proportion of the population remained present in the surface waters.

In the surface water, the significant relationship with chlorophyll-*a* concentration indicates that *A. australis* contributed a large part of the chlorophyll-*a* content within the surface waters of the surf zone. This result, as well as results by de Vos (2018,) indicated that the chlorophyll-*a* concentrations of the cells probably changed during the day, with a decrease in cellular chlorophyll-*a* content in the afternoons perhaps due to cell division. du Preez, Campbell & Bate (1990) found that although *A. australis* cells occur in high irradiance conditions, they are not suited to photosynthesize optimally in high light environments. It was proposed by du Preez, Campbell & Bate (1990) and du Preez & Campbell (1996b) that cells may use short surface suspension time, high cell densities (shading) and turbulent conditions that cause murky waters to avoid photoinhibition. Du Preez, Campbell & Bate (1990) also noted that there was no change in cell chlorophyll-*a* concentrations using laboratory experimentation from samples collected in the early morning. Du Preez & Campbell (1996b) found that *A. australis* cells have a high chlorophyll-*a* specific photosynthetic rate, and thus complete their photosynthetic requirement within the first five hours of the day. However, due to the sudden drop

in chlorophyll-*a* concentration in the afternoon without a corresponding decrease in cell concentrations (nor an increase in other cell concentrations) found by de Vos (2018), the results of this study suggest that cells sampled in the afternoon in field conditions, with peak afternoon light exposure, might experience a decrease in chlorophyll-*a* concentration. This decrease may be explained by the increase in cell concentration due to cell division, whilst each cell now contains only half the chlorophyll-*a*.

Chlorophyll-*a* concentrations in the sediment were positively correlated to other species cell concentrations, indicating that, even though *A. australis* dominates the sediment in terms of biomass (abundance), these cells may have much lower chlorophyll-*a* concentrations in the sediment. Du Preez & Bate (1992) found that *A. australis* underwent physiological changes indicative of a resting phase when left in the dark and could still regain photosynthetic abilities after being kept in darkness for 75 days. During darkness exposure, chlorophyll-*a* decreased linearly after three days. This could explain why chlorophyll-*a* concentrations are not correlated with the cell concentrations for *A. australis* in the sediment as less light exposure may decrease chlorophyll-*a* content of the cells.

Nitrate and ammonium values were relatively high, as expected for a coastal region. Mean concentrations of nitrate ( $1.41 \pm 1.13 \mu\text{mol.L}^{-1}$ ), nitrite ( $0.13 \pm 0.03 \mu\text{mol.L}^{-1}$ ) and ammonium ( $15.39 \pm 11.89 \mu\text{mol.L}^{-1}$ ) are much higher at Muizenberg Beach than recorded at Sundays River Beach, where Lewin & McLachlan (1981) recorded mean values respectively of 0.121, 0.029, and  $0.093 \mu\text{mol.L}^{-1}$  respectively over an 18-month sampling period. Lewin & McLachlan's (1981) samples were taken during patch events, but Muizenberg Beach and the False Bay area are nutrient-rich compared with the South-East Coast of South Africa, having a strong influence from coastal upwelling. Other factors, such as stormwater runoff, groundwater seepage, and sewage wastewater inputs also could account for the difference in nitrogen species concentrations, especially ammonium. Campbell & Bate (1996) also reported high nutrient concentrations at Muizenberg, attributing this to the input of polluted aquifers.

The negative relationship between *A. australis* concentrations and ammonium is an indication that *A. australis* may be preferentially taking up this nitrogen source (Appendix, Figure A7; Figure 11), with significantly higher concentrations of ammonium seen offshore, in the absence of *A. australis*. These results are similar to that of Hoffenberg (2017), where significant negative correlations were found between cell concentrations of *A. australis* and ammonium concentrations. Nitrate and nitrite both had positive relationships with *A. australis* concentrations, possibly indicating preferential uptake of ammonium. For all nitrogen compounds, an increase in concentration occurred around the time of

the second, afternoon peak in cell concentrations, possibly brought in by the high tide (Appendix, Figure A7).

Other nutrients measured included phosphate and silicate, where phosphate had a positive relationship with cell counts of *A. australis*, and silicate showed a weak negative relationship. These relationships are similar to those found by Hoffenberg (2017). It can be noted that large decreases in silicate concentrations occurred during the peaks in cell concentrations across all stations (Appendix, Figure A7), probably caused by silicate uptake by the diatoms during these periods, although further laboratory and *in situ* evidence would be required to confirm these dynamics.

Cells in the surface waters had a distinct increase in cell volume compared with those in the sediment. These results are similar to previous work on the diel cycle of cell characteristics of *A. australis* and show that cells with increased surface area and volume may be more readily suspended (Talbot & Bate, 1986, 1987a, 1988a). Dividing cells were also more dominant in the surface waters than in the sediment, similar to results found at Sundays River Beach. Dividing cells were also found to be significantly larger in volume than non-dividing cells. Previous studies have noted that, during peak cell concentrations, patches are almost exclusively made up of dividing cells (Talbot & Bate, 1988a, 1989; Talbot, Bate & Campbell, 1990), indicating that although these patches are not the result of rapid cell division, cell division may play an important role in their formation. Talbot and Bate (1986) suggested that the increase in surface area of cells during cell division phases may increase buoyancy of cells, and thus a diel cycle in cell division could be the cause of the diel pattern seen in cell concentrations. However, it is difficult to determine whether cells are floating due to this phase of cell division, or whether the division of cells is rather triggered synchronously by other factors that occur during the floatation period, e.g., increased light or tides.

Across the sediments and surface waters, the paired condition of the *A. australis* cells was more prevalent than single cells (Figure 10). There was a decrease in paired cells and an increase in single cells of *A. australis* at each sampling time before and after the peaks in cell concentrations (Appendix, Figure A5), however due to small sample size little conclusion can be drawn from this yet. It remains in question whether *A. australis* cells are paired as a phase during cell division or whether cells are joining to increase volume (surface area) to remain afloat.

Biomass of *A. australis* tracked changes in cell concentrations in both the sediment and surface water and had a strong positive correlation to the measured chlorophyll-*a* values (Figure 8). Thus, during this study *A. australis* made up the bulk of the biomass in the surface waters (Figure 14), and chlorophyll-*a* measurements could be used as a rapid measure of *A. australis* abundance, rather than time-consuming microscope counts.

In conclusion, this study provided valuable insights into the diel cycle and population dynamics of *A. australis* at Muizenberg Beach, revealing similarities and distinctions compared to findings at Sundays River Beach. The distinct late-morning peak in cell concentrations, coupled with high sediment cell counts, highlights the unique surf zone adaptation of *A. australis*. Tidal height and wind speed and direction influences cell distribution. The dominance of *A. australis* in both surface waters and sediment, along with its significant contribution to chlorophyll-*a* content, underscores its ecological importance in the surf zone. Nutrient correlations suggest *A. australis* preference for ammonium, perhaps reflecting an abundance of this nitrogen species in the surf zone possibly due to river outflow and human influence. The increase in cell volume during peak concentrations, coupled with the prevalence of dividing cells, suggests a role for cell division in patch formation. Overall, these findings enhance our understanding of *A. australis* ecological niche and contribute to the broader knowledge of diatom population dynamics in surf zones.

## Chapter 3: Time series view (2019-2021) of *Anaulus australis* patch events at Muizenberg Beach

### Abstract

In this chapter machine learning techniques are utilised to analyse photographs of brown patches in the surf zone, assumed to mainly comprise *Anaulus australis*, and to investigate seasonal signals in the occurrence of these patches and their association with environmental factors. Photographs of the Muizenberg Beach surf zone in False Bay, South Africa, were taken every 12 minutes from February 23, 2019, to May 31, 2021, resulting in a dataset of 47,020 photographs. Python libraries were used to process the images by resizing and cropping them and assigning each image a numeric score patch presence and intensity, as well as a score for sea state adapted from the Beaufort scale. Machine learning models were trained on Google Cloud Platform to predict sea state scores and patch intensity scores for the rest of the photographic data set. Environmental data, including modeled tidal heights and in situ wind speed and direction measurements were also obtained. This dataset represents the longest-running time series data on *Anaulus australis* in South Africa. A clear seasonal trend in patch frequency was observed, with an increase in patch prevalence during winter months (May, June, July, August). A maximum number of 15 days with patch events were recorded in May 2021, compared to an overall average of 5 days recorded per month. Highest frequency of patch events was recorded at 11:00 on daily timescales. While specific causes of this increase are challenging to attribute, a generalized linear model found sea state score to be significantly positively influential and tidal heights to be significantly negatively influential in the occurrence of *A. australis* patch events. However, other factors like rainfall and wave height may play roles in explaining these patterns and should be included in future studies.

## Introduction

Surf zone diatoms are found in ecosystems that are notoriously difficult to sample. The sandy beaches where they occur have turbulent often turbulent surf zones with high wind and wave action. These conditions are tiring to work in and are in some cases dangerous. This makes it difficult to conduct studies at high spatiotemporal resolutions and hence our understanding of the dynamics of surf zone diatoms at these beaches is hampered by the physical limitations of sampling. Analyzing laboratory samples using microscopy is also a time intensive process and can be especially subject to human error and biases. However, new marine observational technologies are increasing the amount of data that can be generated using simple sampling methods, like image or sensor generated data sets (Beyan & Browman, 2020; Malde et al., 2020).

Long term studies of surf zone diatoms are sparse, due to the physical challenges of in situ sampling in the surf zone and time-consuming challenges of laboratory analyses. Large-scale time series data are important in detecting changes in species composition and distributions (Campbell, 1996; Carballeira et al., 2018). This author is aware of a total of only twelve publications (Lewin, Hruby & Mackas, 1975; Lewin, 1978; Talbot & Bate, 1987a; Lewin, Schaefer & Winter, 1989; Gayoso & Muglia, 1991; Campbell & Bate, 1998; Odebrecht et al., 2003, 2010; Netto & Meneghel, 2014; Menéndez et al., 2016; Tedesco et al., 2017; Carballeira et al., 2018) that use long-term sample data sets, i.e., time series data for a period of one year or more. A few notable studies will be discussed here.

At Copalis Beach, United States of America, Lewin et al., (1975) collected bi-weekly seawater samples and environmental data for a period of two years (1971-1972) and noted the year-round presence of surf zone diatoms *Attheya armatus* (dominant in abundance) and *Asterionellopsis socialis*, regardless of environmental conditions, with slight seasonality noted. Later, Lewin (1978) and Lewin et al., (1989) expanded on this dataset (1971-1982) to include around five years of data and found that diatom populations tend to maintain seasonal cycles regardless of nitrate concentration fluctuations – with a decrease in cell concentrations in the summer months, more severely so in *Asterionellopsis socialis* populations that disappeared completely at times. Little evidence was provided for the causes of this seasonality at Copalis Beach.

Talbot & Bate (1987) conducted aerial surveys of the surf zone of Sundays River Beach, South Coast South Africa, to study the relationship of the patches to rip currents – hence exploiting the advantages of high vantage points to identify and take photographs of these events. In contrast to work at Copalis beach, Talbot, Bate & Campbell (1990) noted that *A. australis* bears no physical adaptation to temperature and hence, at Sundays River Beach, South Africa, no seasonality of patch events or cell concentrations have been reported (McLachlan & Lewin, 1981; Talbot & Bate, 1986; Talbot, Bate &

Campbell, 1990). This trend was attributed by these studies to the warm temperate climate of this region.

Gayoso & Muglia (1991) conducted monthly samples from November 1989 to March 1991 at Pehuen-Có Beach, Argentina, and also found that the surf zone diatom species present here, *Attheya armatus*, does not fluctuate in abundance with seasons.

In contrast, Odebrecht et al. (2003) recorded monthly samples from February 1994 to 2002 at Cassino Beach, Brazil, and noted a strong seasonal cycle in diatom populations, with a decrease in abundance in summer months. In this study, uncharacteristically low abundances were also noted in specific winter seasons and due to long term data, this was attributed to mud depositions (that may disrupt suspension from sediment or cause shading) from high river runoff during very rainy seasons. This data set was continued until 2007 (16 years), and it highlighted a decrease in the frequency of patch events of *A. glacialis*, marking the 1998 mud deposition as a turning point for the population (Odebrecht et al., 2010). This mud slide was the result of an El Niño event, and this data set highlights the importance of long time series to detect the effects of large-scale climate change. This study was among the first noting long term seasonal trends in surf zone diatom populations and attempted to identify causal factors like these environmental events. This study was influential in furthering understanding of what drivers of surf zone diatom populations' abundance on these longer timescales might be.

Netto & Meneghel (2014) also found a seasonal trend in accumulation events at the beaches of Laguna, South Brazil, and determined that, although not the only resource for meiofauna populations, the increase in patch events in the winter by almost six-fold in some months forms an important resource for surf zone fauna and meiofauna during times of food shortage. Netto & Meneghel (2014) and Odebrecht et al. (2014) both attributed the increase in patch events in winter seasons to an increase in cold fronts.

Lastly, Carballeira et al. (2018) monitored four estuaries on the Artabro Coast, Spain, at several beaches and sampled patch events. These data, along with a literature review of African and European *Attheya armata* diatom populations, once again revealed no seasonality of this species. Carballeira et al. (2018) proposed that the patch events associated with this species in Spain may be linked to processes that affect the sediment-water interface, i.e., turbulent conditions that suspend sand, rather than any seasonal association.

In conclusion, the reviewed studies on surf zone diatoms present a diverse range of findings, indicating that the seasonal dynamics of these organisms across different locations are influenced by various

factors. Overall, the variability in results underscores the importance of considering additional factors, such as river outflow, tides, storms, and climatic events, in understanding the complex dynamics of surf zone diatom populations.

#### Aims for Muizenberg Beach, South Africa

Globally, there appears to be some seasonal trends in the population abundance of some species where the beach ecosystem is subject to trends in turbulent weather conditions. Whilst the diel cycle of these diatoms is a characteristic feature and is well studied at several sites, the seasonality of these diatoms and their associated patch events are less well understood due to the lack of long-term, high-resolution data.

The variability of these results in determining trends in surf zone diatom abundance across seasonal timescales leads to the question of whether patterns are likely to occur in South Africa. Although some evidence indicating some seasonality has been produced at Sundays River Beach, studies of long-term, high-resolution data are difficult to conduct and replicate. In addition, the South African coastline is vast, with large variations in environmental conditions and habitats. In particular, the surf zone at Muizenberg Beach, South Africa has had no long term or even mesoscale sampling activity conducted to date.

Machine learning offers a unique solution to the challenge of analysing large data sets and is quickly growing in its use as a tool for data-driven learning in marine science. Machine learning is a type of artificial intelligence where computational models can learn to predict outcomes without being explicitly programmed or instructed. This study aims to use machine learning methods to analyse a large set of photographs of the surf zone, to determine whether there is a seasonal signal in the presence of patch events and whether these events are associated with wind and/or measures of turbulence in the surf zone.

## Methods

### Photographic data – Model input data set up

Muizenberg Beach is situated at the bottom of a section of the Table Mountain National Park, and thus from the vantage point of the mountain side, there is a clear view of the Muizenberg surf zone. Photographs were taken of the stretch of Muizenberg Beach every 12 minutes from 23 February 2019 to 31 May 2021, using a Nikon D300 SLR (single lens reflex) camera mounted on a tripod (50 cm) with a Tokina AF 20–35 mm lens and a polarising filter. Nighttime photographs were excluded and thus, in total, 47020 photographs were captured and analysed in this data set.

Photographs were taken at this 12-minute interval to capture high resolution movement and changes in the surf zones, since it has been noted that *A. australis* patches can appear and disappear over a period of two hours (de Vos, 2018). This interval best allowed for the capture of any patch events.

Python (CV 2 and Panda Libraries) were used to resize images to half the number of pixels (decrease resolution and thus size), as well as crop some of the buildings and sky out of the images (500 pixels from the top and bottom, and 50 pixels from the left) (Figure 15).

The presence and absence of patches were visually assessed, and patches were scored for intensity on a three-point scale from zero to two. A score of zero was allocated to images where no patch was present, a score of one where patches were present but not very intense, and a score of two where there were dark brown patches (Figure 16). 21000 photographs were scored for patch intensity; this was done to achieve an event number of 2000 in order to train the machine learning model. 2380 photographs were visually assessed to assign a sea state score according to the Beaufort Scale (Fry, 1967) (Figure 17). This assessment was done on the ocean behind the breaker zone and in the same pixel quadrant as far as possible.

Image quality was also visually assessed and for images where glare, weather or low light conditions prevented an assessment of the image, the image was assigned a patch intensity score of negative one. This data was also inputted into the model to assess image quality and images that were assigned a value of negative one were excluded from the analysis.



Figure 15: Original input images (a) resized to crop out buildings and sky and reduce resolution (b).



Figure 16: Examples of images classified as a score of 1 (a) indicating presence of a mild patch, and a score of 2 (b) indicating an intense patch.



Figure 17: Examples of photographs classified according to the Beaufort scale with a score of 1 (a), 2 (b), 3 (c) and 4 (d).

## Photographic data – Model training

A data frame was created with the patch intensity score, image quality assessment, sea state score and time and date of the photograph. This data frame was formatted to fit the structure required for Google Cloud Project AutoML Vision and uploaded to Google Cloud Storage (GCS). The model was trained on Google Cloud Platform (GCP) using a subset of the training data for 120 node hours. The model validates the scores by predicting the values on another subset of the labelled data, called the validation set. The score of these images is then compared with the “true” labels in the input data and assessed for precision and recall.

Feedback from the algorithm delivered a 90.03% precision rate (i.e., how good the model is at scoring the result correctly), and an 87.61% recall rate (i.e. of the number of images given a particular score, the proportion that were correctly scored). Each image was also labeled with a confidence threshold, and images that were scored with less than 0.5 confidence were excluded from the data model.

Google Cloud AutoML leverages transfer learning, a method that uses pre-trained machine learning models and adapts them quickly to new training data, using proprietary deep-learning models already trained by Google Cloud. This provides greater accuracy for any given dataset than would training a model from scratch.

A custom regression algorithm (TPOTClassifier) was run on a subset of the data to ground truth the results given by the more powerful processing algorithms of GCP AutoML Vision. In this model the images were resized to be eight times smaller. This model creates an array that includes a value for each pixel of each image. This classifier then suggests a “pipeline” or model to implement, in order to assign predicted scores based on the input training data. Because the GCP AutoML Vision allowed for faster and better processing, these data were selected to be used, but the custom model confirmed that the AutoML Vision model was, in fact, the best model.

## Environmental data

Tidal heights on hourly timescales were interpolated from data supplied by the South African Navy for the study period from 23 February 2019 to 31 May 2021. These tidal height data were extrapolated to match the time for each photograph. For the study period, in situ wind speed and direction data for hourly timescales were also obtained from Cape Town International Airport through the support of the South African Weather Service. This wind station was nearest to the study site and was thought to be the best obtainable estimate of wind conditions available. The average daily windspeed and direction were calculated, and the number of hours in the onshore (South-South East) direction were recorded.

## Analysis

After training, the model was used to predict value scores from negative one to two for all images in the dataset, indicating poor quality image (-1), no patch (0), mild patch (1) and intense patch (2) presence. This data set was used to visualise the cumulative frequency of patch events over time of day and time of year.

Similarly, with that of the Beaufort scale the model output assigned a sea state score value to each photograph (Figure 17).

Images where the model failed to assign a value or where the confidence of the predicted score was below the 95% confidence score were excluded from the analysis. Any images that were assigned a negative one indicating poor quality or visibility, and any days where less than 10 photographs were captured for the day were excluded from the analysis.

To standardise the data across different numbers of sample photographs taken for analysis periods of months and days, the number of patch events per month or day was multiplied by the average number of sample photographs to increase the magnitude of the frequency data and divided by the number of sample photographs over the represented time period.

For example, for the cumulative number of patches per month:

*no. of patch events*

$$= \frac{\text{Sum of months patch events} \times \text{average no. of photographs per month for the full study period}}{\text{sum of sample photographs for the month}}$$

T-tests were conducted to establish relationships between environmental variables and the frequency of patch events. In addition, a general linear model was fit to the data to determine influential variables for *A. australis* patch frequencies, and model validation plots were inspected (Appendix, Figure A 8). The model was conducted using a stepwise approach to select models of lowest AIC values in R version 2023.12.0.369 (Posit team, 2023).

## Results

There is a seasonal trend in the frequency of patch events over the course of a year (Figure 18), with a notable increase in the presence of patch events during autumn and winter months (May to August). With the overlay of the average tidal height on each month, there is an association of the seasonal low tidal heights with the increased patch event frequency in the winter, as well as an association of reduced frequency of patch events during seasonal high tidal heights (Figure 18). Since tidal height data from patch days were used, the curve of the line is not a smooth sinusoidal curve. A two-sample t-test indicated a significant difference in the mean tidal height (m) for days with patch presence (scored with 1) (mean = 0.98, SD = 0.068) was significantly different compared to days where patches are absent (scored with 0) (mean = 1.00, SD = 0.089) ( $t = 2.26$ ,  $df = 280.86$ ,  $p < 0.05$ ), whilst a Spearman's ranked correlation test reveals there is a significant relationship between the average daily tidal heights and patch presence-absence (Spearman's ranked means,  $r = -0.11$ ,  $n = 766$ ,  $p < 0.05$ ).

From Figure 19 there is a visual pattern where a higher sea state score equates to less frequent patch events. However, increased patch frequency during winter months is preceded by an increase in sea state score. A two-sample t-test indicated that an average sea state score is slightly lower for periods with high patch presence (mean = 1.51, SD = 0.82) than periods with absence of patch events (mean = 1.74, SD = 0.67) (T-test,  $t = -3.13$ ,  $df = 198.51$ ,  $p < 0.01$ ).

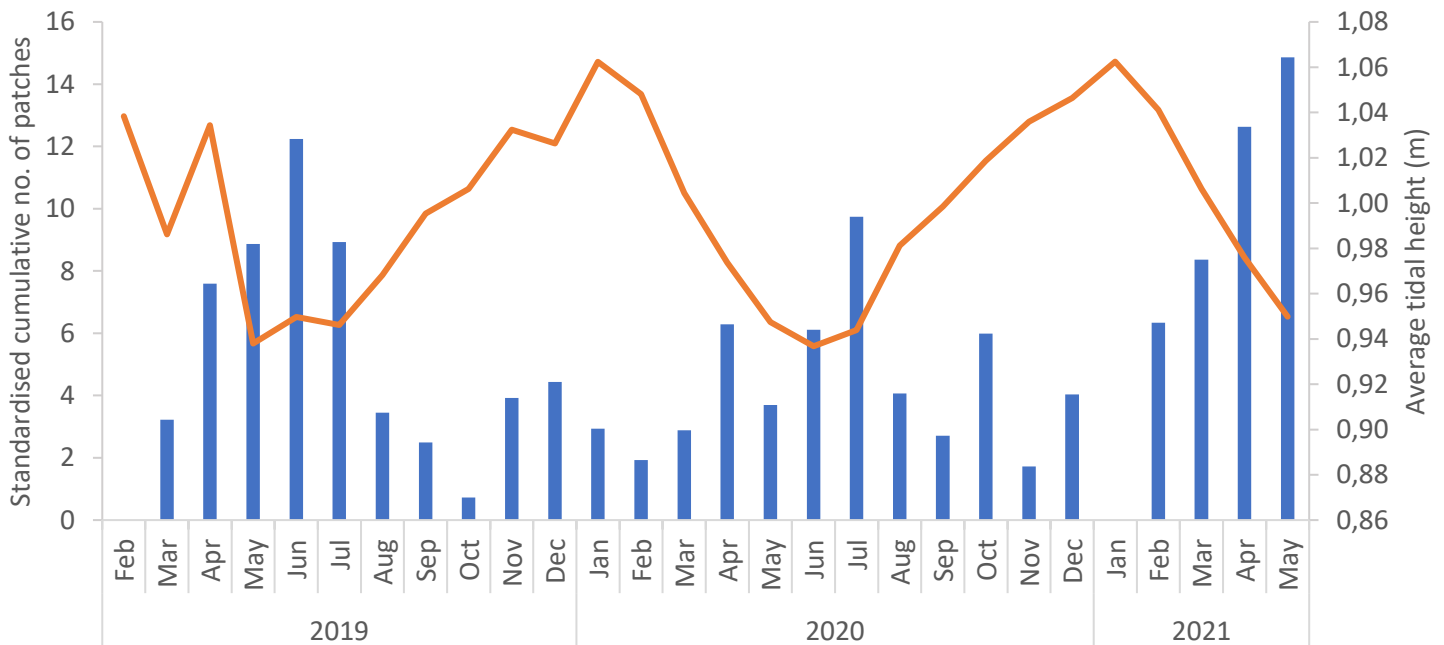


Figure 18: The standardised summed number of days where patches were observed over the study period, with tidal heights in metres overlaid on the secondary y-axis (orange line).

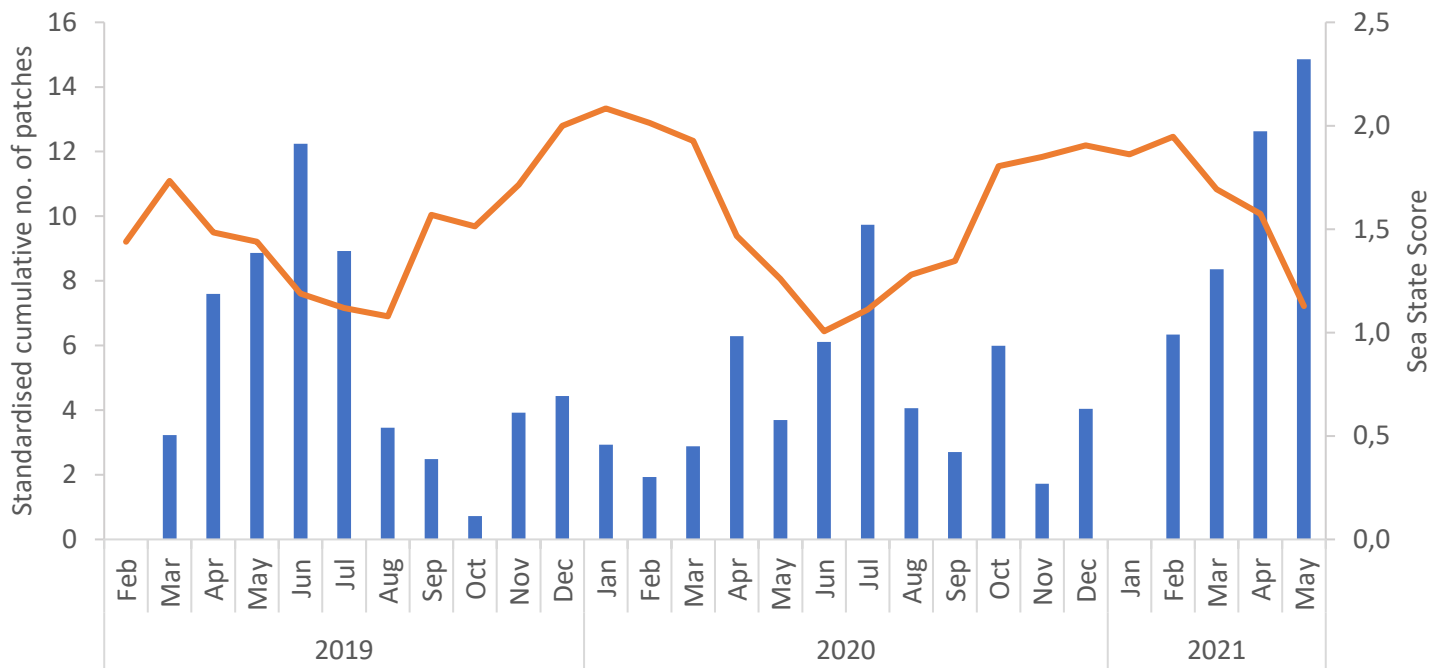


Figure 20: The standardised summed number of days where patches were observed over the study period, with the average monthly sea state score overlaid on the secondary y-axis (orange line).

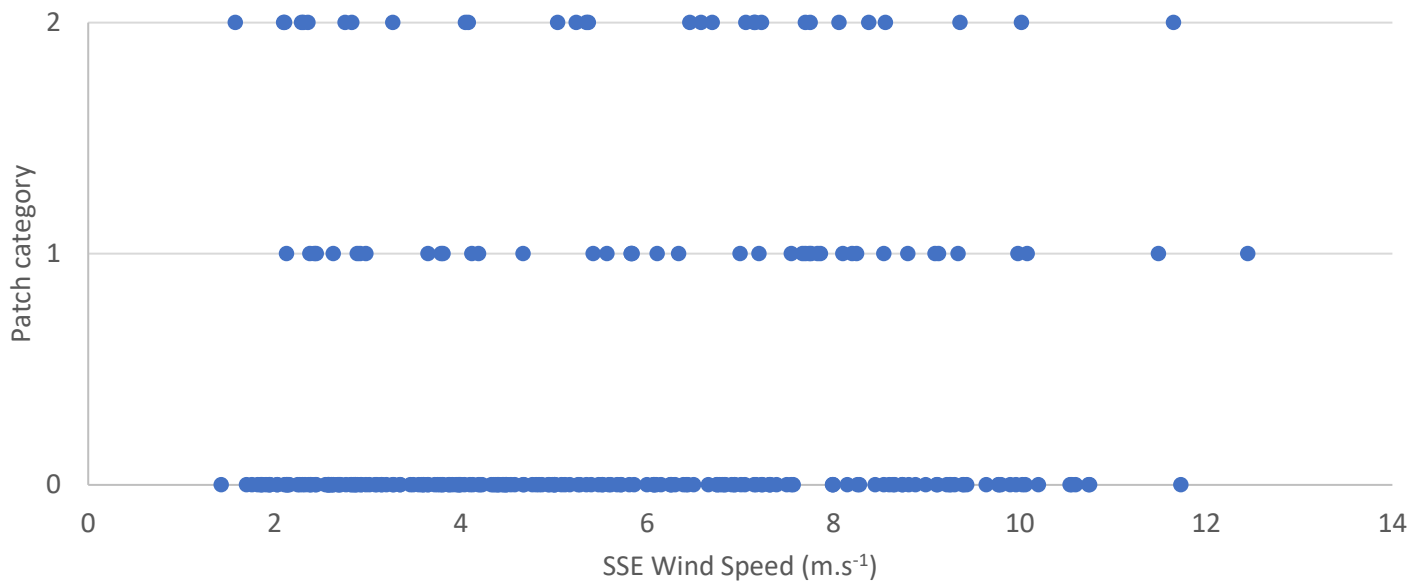


Figure 19 :Patch events (1 = mild patch, 2 = intense patch, 0 = no patch) recorded for wind speeds where the wind direction is onshore direction (South-East, or South-South-East) for more than 2 hours

When plotting the wind speed against patch intensity score (0 being no patch, 1 being mild patch and 2 being intense patches) for days where the wind direction is primarily in an onshore direction (South-East, or South-South-East) for more than 2 hours, no significant trend is noted (Figure 20). Average daily wind speed (Spearman's ranked means,  $r = 0.04$ ,  $n = 766$ ,  $p > 0.05$ ) yielded no significant relationship with the daily presence or absence of *A. australis* patch events when using a Spearman's test, whilst a weak negative relationship is found with the average daily wind direction (Spearman's ranked means,  $r = -0.16$ ,  $df = 764$ ,  $p < 0.001$ ) as well as a weak positive relationship with the number of hours of wind direction in a South-South-Easterly direction (Spearman's ranked means,  $r = 0.10$ ,  $df = 764$ ,  $p < 0.01$ ) yielded no significant relationship with the daily presence or absence of *A. australis* patch events.

Using the Welch two sample t-test, a significant difference in mean wind direction was found between days where patches are present (mean =  $202.33^\circ$  from North (SSW),  $SD = 50.24$ ) and absent (mean =  $184.03^\circ$  from North (S),  $SD = 51.65$ ) (T-test,  $t = 3.97$ ,  $df = 229.59$ ,  $p < 0.0001$ ). Similarly, the mean number of hours of wind recorded in a South-South-Easterly direction (onshore) is higher for days where patches are present (mean = 10.50 hours,  $SD = 9.27$ ) versus absent (mean = 7.91 hours,  $SD = 7.52$ ) (T-test,  $t = -3.16$ ,  $df = 197.58$ ,  $p < 0.01$ ). No such difference was found for the mean wind speeds on days where patches are present versus absent (T-test,  $t = 0.33$ ,  $df = 200.39$ ,  $p > 0.05$ ).

When the frequency of patches is plotted against the time of day, the distribution of the curve leans toward a peak at 12:00 for mild and intense patch events (Figure 21).

When all variables are considered, tidal heights have significant negative influence on the presence of patch events, whilst sea state score has a significant positive influence (Table 2).

Table 2: Generalised linear model results table for *A. australis* presence-absence as response variable and tidal height (m), wind speed ( $m.s^{-1}$ ), wind direction (degrees from North), sea state score, and no. of hours of wind in an SSE direction as explanatory variables.

	Coefficient Estimate	Std. Error	t-value	P-values
Intercept	0.66	0.17	3.81	0.0001
Tidal Height (m)	-0.46	0.0091	-2.70	0.007
Wind Speed	-0.017	0.0091	-1.84	0.06
Sea State Score	0.073	0.027	2.71	0.007
Wind direction	0.0004	0.0004	-1.13	0.3
No. of hours in an SSE direction	0.0045	0.0027	1.66	0.1

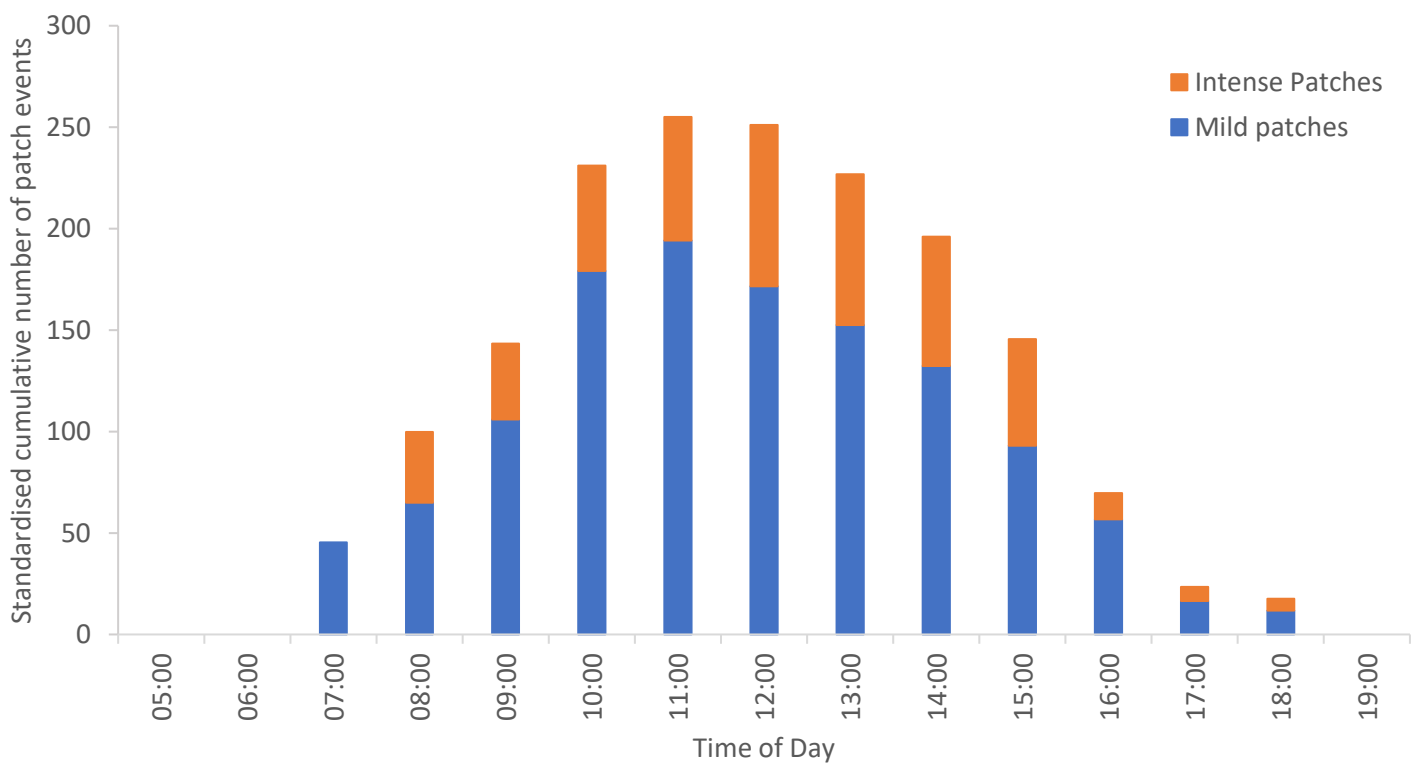


Figure 21: Number of patches recorded standardised against the number of photographs taken and plotted against the hour of the day over the study period, with blue indicating the portion of mild patches and orange for intense patches.

## Discussion

This data set marks the longest running time series dataset on *Anaulus australis* patches at Muizenberg, South Africa to date, with very few high-resolution, long term, time series data sets recorded on surf zone diatoms globally.

Over the study period from February 2019 to May 2021 a clear seasonal trend can be noted (Figure 18), with increased patch prevalence during winter months. Very few other studies noted seasonal trends, and no such seasonality has been noted for *Anaulus australis* in South Africa before (McLachlan & Lewin, 1981; Talbot, Bate & Campbell, 1990). It is, however, difficult to attribute causes for this increase using this data set, but the result is consistent with studies linking the prevalence of patches to storms and turbulence.

Talbot & Bate (1988d) noted that longer periods of low energy surf conditions resulted in lower cell concentrations, whilst periods of high wave energy were thought to resuspend cells, thus resulting in the increased cell concentrations. Du Preez & Bate (1992) also noted patch events linked to turbulent conditions. Du Preez, Campbell & Bate, (1990) and du Preez & Campbell (1996) proposed that, during turbulent conditions, cells are exposed to a more optimal zone of increased light availability, whilst the sporadic shading effect of bubbles, increased cell densities and suspended sand and particles protect cells from photoinhibition at surface light levels. Talbot & Bate (1989), found a rather striking link of the frequency of patch events to wave heights (Figure 18). Talbot & Bate (1987a) and Lewin & Hruby (1973) also found patches to occur during low or receding tides, however this pattern was noted on daily or weekly timescales (Figure 18). In these instances, tides may influence population density by concentrating cells in shallower water or exposing cells to increased light availability.

The sea state score modelled did not yield a significant pattern alongside the frequency of patch events (Figure 19). Overall, sea state score was difficult to predict using the current model and seems to be selecting for a variable that tracks changes in tidal height. This may be because the visual assessment of sea state score may not be a good proxy of turbulence, or that water turbulence may not be a significantly influential variable but rather a confounding effect of another factor, e.g. tidal range, seasonal weather patterns or human impacts. A larger training data set may yield more accurate results in future.

A seasonal effect is seen in the frequency of patches at Muizenberg Beach, and no effect of onshore wind is clearly distinguished (Figure 20). Talbot & Bate (1988d) found no seasonality in the appearance of *A. australis* patches at Sundays River Beach, with no direct effect of wind on *A. australis*, although strong offshore winds may remove cell patches. Du Preez, Campbell & Bate, (1990) and Sloff, McLachlan & Bate (1984) found patches occur in the presence of rip currents, and during onshore

wind conditions at Sundays River Beach, and although some evidence in this study indicates that wind direction and the length of time of onshore winds has some relationship to the prevalence of patches. It should be noted that wind speed and direction and sea state score variables were not influential when included in the generalised linear model, whilst tidal heights were. These results are in line with previous studies suggesting that wind may have more of an indirect effect on the occurrence of patches.

Talbot & Bate (1988d, 1989) also note that during their study of a storm cycle at Sundays River Beach, *A. australis* population increased within the surf zone corresponded with wave height, whilst Odebrecht et al. (2003) linked seasonality to rainfall. Tidal heights together with sea state score were used to explore possible relationships and were found to be influential in the frequency of *A. australis* patches at Muizenberg beach. These long-term data and any rainfall or wave height data variables should be included in future studies to further define patterns of seasonality in patch events. Rainfall, river, and storm water outflows are thought to increase nutrient loading into surf zones and could thus be a significant nutrient input for diatom populations globally (Bate & McLachlan, 1987; Odebrecht et al., 2003).

The peak of the number of cell patches during the day (Figure 19) corresponds to timing noted by de Vos (2018) and is also shown in Chapter 2, where peaks in cell concentrations were noted during the late morning, even when no patches were visible. These data could, however, be skewed due to the number of viable photographs for analysis, as early morning and late afternoon photographs have a higher frequency of bad and failed images due to lighting and glare at those times.

In recent years, the application of machine learning technology has contributed to marine science in enhancing our understanding of complex ecological systems, and now specifically to the study of surf zone diatoms like *Anaulus australis*. Using this technology for image analysis and classification is particularly useful for surf zone ecosystems since image data sets are easily generated. In addition, the use of these methods for analysis removes inaccuracies and biases present in manual analysis, and overall allows for the analysis of far larger data sets. Combined with other oceanographic data sources these instruments can be applied to help understand seasonal changes and the influence of human activity over time.

## Chapter 4: Conclusion

Sandy beach ecosystems are key in supporting diversity of marine life and have great cultural and socio-economic value (Schlacher et al., 2014). For some time, these ecosystems were regarded as desert like, barren with little life. However, in recent years, studies have shown that much life in the form of benthic species and micro-organisms are supported by primary production from phytoplankton and nutrient inputs from foreign systems (kelp and terrestrial vegetation) (McLachlan & Defeo, 2018). This study contributes to this understanding of the role of sandy beach ecosystems, in furthering our knowledge of key primary producers: surf zone diatoms, with a particular focus on *Anaulus australis*.

Although *A. australis* has received more focus than most surf zone diatom species in the literature in the past, most studies originate from a single study site, Sundays River Beach (South Coast) in Algoa Bay, South Africa (Odebrecht et al., 2014). This study tests some basic knowledge created for this species at the Sundays River Beach site, in a new study site at Muizenberg Beach (South-West Coast), False Bay, South Africa.

It is clear from the study of the diel cycle of *Anaulus australis* at Muizenberg Beach that a diel cycle is present in the population, as with many other studies of surf zone diatoms (Lewin & Schaefer, 1983; Talbot & Bate, 1988a; Talbot, Bate & Campbell, 1990), although cell concentrations were very high. McLachlan & Lewin (1981) reported that mean patch cell concentrations of *A. australis* is  $1.94 \times 10^3$  cells.mL<sup>-1</sup> with a recorded range of  $5 \times 10^3$  to  $1 \times 10^6$  cells.mL<sup>-1</sup>, whilst this study recorded samples on the order of  $10^9$  cells.mL<sup>-1</sup>. This could be due to the more eutrophic environment present at Muizenberg Beach compared to Sundays River Beach (McLachlan & Lewin, 1981). In addition, whilst this sediment population did not mirror surface cell concentrations as in some previous studies, sediment *A. australis* populations at Muizenberg Beach remained orders of magnitude higher than sediment *A. australis* populations recorded previously. This suggests a large, mostly static population of diatoms in the sediment, lending evidence to the hypothesis that these may in fact be a more benthic species (Carballeira et al., 2018).

Key findings from this study also include a two-year, high resolution time series of presence-absence data of *A. australis* patches at Muizenberg Beach. To date, it is the longest running, highest resolution data set of patch occurrences of surf zone diatoms globally. Very few studies globally have reported any seasonality of patch events, and this study contributes to shedding light on seasonal or annual patterns of surf zone diatoms that are otherwise very difficult to study. The results generated from this data clearly indicate a predictable variability in the frequency of patches in the Muizenberg system, whereby patch events increase in frequency in winter months.

This data set was generated using machine learning techniques that have proven effective in reducing labour and human error and biases in the classification of images for presence and absence of *A. australis* patches. The use of machine learning techniques that are emerging globally are being applied increasingly in the field of marine science.

This study also aimed to link some of the environmental factors to the population dynamics of *A. australis*. Predicted tidal heights were found to be influential in determining cell concentrations on a diel time scale, as well as on seasonal timescales. Wind direction, sea state score and nutrients are also implicated to varying degrees in determining cell concentrations or patch presence of *A. australis* on diel and seasonal timescales. Whilst future studies would need to determine causal links to draw definitive conclusions, one could hypothesize that on a seasonal timescale this may be linked to the increased turbulence in winter allowing cells in the benthos to be suspended, as well as increased rainfall and wind, which in turn increases river runoff and stormwater outflow loading of the surf zone with excess nutrients.

This author would recommend that future studies utilise data sets like the photographic dataset generated here as it is relatively easy and inexpensive to generate and allows one to isolate instances of patch events and link them to in situ measurements of wind regime, nutrient concentrations, wave and tidal heights. It should also be investigated that the effect of environmental variables is generally not immediately impactful, and a degree of offset should be applied to account for any lag in the influence of these variables on patch presence. Perhaps, considering the high correlation between chlorophyll-*a* concentrations and *A. australis* cell counts found in this study and by Hoffenberg (2017), one could use the chlorophyll-*a* concentrations as a proxy for *A. australis* concentrations, thereby decreasing labour and time of processing microscopy samples significantly through a relatively inexpensive proxy for in situ samples to ground truth photographic data sets.

Research on surf zone diatoms is crucial for understanding coastal ecosystems, as they serve as primary producers, forming the foundation of coastal food webs (McLachlan & Defeo, 2018). These microscopic algae play a key role in nutrient cycling, absorbing, and storing nutrients and are believed to absorb excess nutrients, acting as a buffer for nutrient loading caused by human activities in coastal ecosystems (Bate & McLachlan, 1987; du Preez & Campbell, 1996b). As coastal environments face increasing threats from climate change and anthropogenic influences, understanding the role and responses of surf zone diatoms is essential for effective ecosystem management and conservation.

## References

- Bate, G.C. & McLachlan, A. 1987. Surf zone discoloration by phytoplankton: The consequence of pollution? *Marine Pollution Bulletin*. 18(2):65–67. DOI: 10.1016/0025-326X(87)90568-6.
- Cahoon, L.B., Bugica, K., Wooster, M.K. & Dickens, A.K. 2017. Factors affecting surf zone phytoplankton production in Southeastern North Carolina, USA. *Estuarine, Coastal and Shelf Science*. 196:269–275. DOI: 10.1016/j.ecss.2017.07.012.
- Campbell, E.E. 1996. The global distribution of surf diatom accumulations. *Revista Chilena de Historia Natural*. 69(July):495–501.
- Campbell, E.E. & Bate, G.C. 1987. Factors influencing the magnitude of phytoplankton primary production in a high-energy surf zone. *Estuarine, Coastal and Shelf Science*. 24:741–750.
- Campbell, E.E. & Bate, G.C. 1988. The estimation of annual primary production in a high energy surf-zone. *Botanica Marina*. 31(4):337–344. DOI: 10.1515/botm.1988.31.4.337.
- Campbell, E.E., Bate, G.C. and Rust, I.C., 1990. *The Flora of the Sandy Beaches of Southern Africa*. Institute for Coastal Research, UPE.
- Campbell, E.E. and Bate, G.C., 1991. The flora of the sandy beaches of southern Africa. III. The South Coast Microflora. *Institute for Coastal Research Report*, (26), p.129.
- Campbell, E.E. & Bate, G.C. 1996. Groundwater as a possible controller of surf diatom biomass. *Revista Chilena de Historia Natural*. 69:503–510.
- Campbell, E.E. & Bate, G.C. 1997. Coastal features associated with diatom discoloration of surf-zones. *Botanica Marina*. 40(3):179–185. DOI: 10.1515/botm.1997.40.1-6.179.
- Campbell, E.E. & Bate, G.C. 1998. Tide-induced pulsing of nutrient discharge from an unconfined aquifer into an *Anaulus australis*-dominated surf-zone. *Water SA*. 24(4):365–370.
- Campbell, E.E., du Preez, D.R. & Bate, G.C. 1988. Photosynthetic rates and photoinhibition of surf diatoms in fluctuating light. *Botanica Marina* 31(5): 411–416.  
<http://www.degruyter.com/view/j/botm.1988.31.issue-5/botm.1988.31.5.411/botm.1988.31.5.411.xml>.
- Carballeira, R., Leira, M., López-Rodríguez, M.C. & Otero, X.L. 2018. *Attheya armata* along the European Atlantic Coast – The turn of the screw on the causes of “surf diatom”. *Estuarine, Coastal and Shelf Science*. 204:114–129. DOI: 10.1016/j.ecss.2018.02.033.
- da Silva Maria, L., de Oliveira da Rocha Franco, A., Odebrecht, C., Giroldo, D. & Abreu, P.C. 2016. Carbohydrates produced in batch cultures of the surf zone diatom *Asterionellopsis glacialis* sensu lato: Influence in vertical migration of the microalga and in bacterial abundance. *Journal of Experimental Marine Biology and Ecology*. 474:126–132. DOI: 10.1016/j.jembe.2015.10.009.
- de Vos, C., 2018. Dynamics of the surf-zone diatom *Anaulus australis* at Muizenberg Beach. Honours project. University of Cape Town (unpublished).
- du Preez, D.P. 2017. Phylogeny and phylogeography of dominant South African surf diatoms. MSc Thesis, Nelson Mandela University.

- du Preez, D.R. & Bate, G.C. 1992. Dark Survival of The Surf Diatom *Anaulus Australis* Drebes et Schulz. *Botanica Marina*. 35(4):315–320. DOI: 10.1515/botm.1992.35.4.315.
- du Preez, D.R. & Campbell, E.E. 1996a. Cell coatings of surf diatoms. *Revista Chilena de Historia Natural*. 69:539–544.
- du Preez, D.R. & Campbell, E.E. 1996b. The photophysiology of surf diatoms-a review. *Revista Chilena De Historia Natural*. 69(4):545–551.
- du Preez, D.R., Campbell, E.E. & Bate, G.C. 1990. Photoinhibition of Photosynthesis in the Surf Diatom, *Anaulus australis* Drebes et Schulz. *Botanica Marina*. 33(6):539–544. DOI: 10.1515/botm.1990.33.6.539.
- Drebes, G. & Schulz, D. 1989. *Anaulus australis* sp. nov. (Centrales, Bacillariophyceae), a New Marine Surf Zone Diatom, Previously Assigned to *A. birostratus* (Grunow) Grunow. *Botanica Marina*. 32(1):53–64. DOI: 10.1515/botm.1989.32.1.53.
- Gayoso, A.M. & Muglia, V.H. 1991. Blooms of the surf-zone diatom *Gonioceros armatus* (bacillariophyceae) on the South Atlantic Coast (argentina). *Diatom Research*. 6(2):247–253. DOI: 10.1080/0269249X.1991.9705170.
- Grindley, J.R. & Taylor, F.J.R. 1970. Factors affecting plankton blooms in false bay. *Transactions of the Royal Society of South Africa*. 39(2):201–210. DOI: 10.1080/00359197009519113.
- Groenewald, Grea. (2020). R Manual, Numerical Skills and Stats Module. University of Cape Town. Cape Town (Internal publication)
- Hoffenberg, A., 2017. Dynamics of the surf-zone diatom *Anaulus australis* at Muizenberg Beach. Honours project. University of Cape Town (unpublished).
- Kahn, A. E. & Cahoon, L. B. (2012) Phytoplankton Productivity and Photophysiology in the Surf Zone of Sandy Beaches in North Carolina, USA. *Estuaries and coasts*. [Online] 35 (6), 1393–1400.
- Kruger, I. and Wilson, E.G., 1984. Morphology and affiliation of the centric diatom *Anaulus birostratus* (Grunow) Grunow from South Africa. *South African Journal of Marine Science*, 2(1), pp.163-194.
- Lewin, J. 1978. Blooms of surf-zone diatoms along the coast of the Olympic Peninsula, Washington. IX. Factors controlling the seasonal cycle of nitrate in the surf at Copalis Beach (1971 through 1975). *Estuarine and Coastal Marine Science*. 7(2):173–183. DOI: 10.1016/0302-3524(78)90073-7.
- Lewin, J. & Hruby, T. 1973. Blooms of surf-zone diatoms along the coast of the Olympic Peninsula, Washington. II A diel periodicity in buoyancy shown by the surf-zone diatom species, *Chaetoceros armatum* T. West. *Estuarine and Coastal Marine Science*. 1:101–105.
- Lewin, J. & Mackas, D. 1972. Blooms of surf-zone diatoms along the coast of the Olympic Peninsula, Washington. I. Physiological investigations of *Chaetoceros armatum* and *Asterionella socialis* in laboratory cultures. *Marine Biology*. 16:171–181.
- Lewin, J. & Norris, R.E. 1970. Surf-zone diatoms of the coasts of Washington and New Zealand (*Chaetoceros armatum* T. West and *Asterionella* spp.). *Phycologia*. 9(2):143–149. DOI: 10.2216/i0031-8884-9-2-143.1.

- Lewin, J. & Rao, V.N.R. 1975. Blooms of surf-zone diatoms along the coast of the Olympic Peninsula, Washington. VI. Daily periodicity phenomena associated with *Chaetoceros armatum* in its natural habitat. *Journal of Phycology*. 11:330–338.
- Lewin, J. & Schaefer, C.T. 1983. The Role of Phytoplankton in Surf Ecosystems. *Sandy Beaches as Ecosystems*. 381–389. DOI: 10.1007/978-94-017-2938-3\_26.
- Lewin, J., Hruby, T. & Mackas, D. 1975. Blooms of surf-zone diatoms along the coast of the Olympic Peninsula, Washington: V. Environmental conditions associated with the blooms (1971 and 1972). *Estuarine and Coastal Marine Science*. 3(2):229–236. DOI: 10.1016/0302-3524(75)90024-9.
- Lewin, J., Schaefer, C.T. and Winter, D.F., 1989. Surf-zone ecology and dynamics. In *Elsevier Oceanography Series* (Vol. 47, pp. 567-594). Elsevier.
- McGregor, S. & Strydom, N.A. 2020. Feeding ecology and microplastic ingestion in *Chelon richardsonii* (Mugilidae) associated with surf diatom *Anaulus australis* accumulations in a warm temperate South African surf zone. *Marine Pollution Bulletin*. 158(July):111430. DOI: 10.1016/j.marpolbul.2020.111430.
- McLachlan, A. & Defeo, O. 2018. Beach and Surf-Zone Flora. *The Ecology of Sandy Shores*. 63–73. DOI: 10.1016/b978-0-12-809467-9.00004-7.
- McLachlan, A. & Lewin, J. 1981. Observations on Surf Phytoplankton Blooms Along the Coasts of South Africa. *Botanica Marina*. 24:553–557.
- Menéndez, M.C., Fernández Severini, M.D., Buzzi, N.S., Piccolo, M.C. & Perillo, G.M.E. 2016. Assessment of surf zone environmental variables in a Southwestern Atlantic sandy beach (Monte Hermoso, Argentina). *Environmental Monitoring and Assessment*. 188(8). DOI: 10.1007/s10661-016-5495-9.
- Netto, S.A. & Meneghel, A. 2014. Pulse of marine subsidies: the role of surf diatom *Asterionellopsis glacialis* accumulations in structuring the meiofauna of sandy beaches. *Marine Biodiversity*. 44(3):445–457. DOI: 10.1007/s12526-014-0253-0.
- Odebrecht, C., Abreu, P.C., Fugita, C.C. and Bergesch, M., 2003. The impact of mud deposition on the long-term variability of the surf-zone diatom *Asterionellopsis glacialis* (Castracane) Round at Cassino beach, Brazil. *Journal of Coastal Research*, pp.486-491.
- Odebrecht, C., Bergesch, M., Rörig, L.R. & Abreu, P.C. 2010. Phytoplankton interannual variability at Cassino Beach, Southern Brazil (1992-2007), with emphasis on the Surf Zone Diatom *Asterionellopsis glacialis*. *Estuaries and Coasts*. 33(2):570–583. DOI: 10.1007/s12237-009-9176-6.
- Odebrecht, C., du Preez, D.R., Abreu, P.C. & Campbell, E.E. 2014. Surf zone diatoms: A review of the drivers, patterns and role in sandy beaches food chains. *Estuarine, Coastal and Shelf Science*. 150(PA):24–35. DOI: 10.1016/j.ecss.2013.07.011.
- Posit team (2023). RStudio: Integrated Development Environment for R. Posit Software, PBC, Boston, MA. URL <http://www.posit.co/>.
- Schlacher, T.A., Jones, A.R., Dugan, J.E., Weston, M.A., Harris, L., Schoeman, D.S., Hubbard, D.M., Scapini, F., et al. 2014. Open-coast sandy beaches and coastal dunes. In *Coastal Conservation*. Cambridge University Press. 37–94. DOI: 10.1017/cbo9781139137089.004.

- Sloff, D.S., McLachlan, A. & Bate, G.C. 1984. Spatial Distribution and Diel Periodicity of *Anaulus birostratus* Grunow in the Surf Zone of a Sandy Beach in Algoa Bay, South Africa. *Botanica Marina*. 27(10):461–466. DOI: 10.1515/botm.1984.27.10.461.
- South African Navy. 2019. *South African Tide Tables*. Annual publication, HO-2
- Sun, J. & Liu, D. 2003. Geometric models for calculating cell biovolume and surface area for phytoplankton. *Journal of Plankton Research*. 25(11):1331–1346. DOI: 10.1093/plankt/fbg096.
- Talbot, M. & Bate, G. 1986. Diel periodicities in cell characteristics of the surfzone diatom *Anaulus birostratus*: their role in the dynamics of cell patches. *Marine Ecology Progress Series*. 32(1):81–89. DOI: 10.3354/meps032081.
- Talbot, M. & Bate, G. 1988a. The use of false buoyancies by the surf diatom *Anaulus birostratus* in the formation and decay of cell patches. *Estuarine, Coastal and Shelf Science*. 26:155–167.
- Talbot, M. & Bate, G. 1988b. Distribution Patterns of the Surf Diatom *Anaulus birostratus* in an Exposed Surfzone. *Estuarine, Coastal and Shelf Science*. 26:137–153.
- Talbot, M.M.B. & Bate, G.C. 1987a. The spatial dynamics of surf diatom patches in a medium energy, cusped beach. *Botanica Marina*. 30(6):459–466. DOI: 10.1515/botm.1987.30.6.459.
- Talbot, M.M.B. & Bate, G.C. 1987b. Rip current characteristics and their role in the exchange of water and surf diatoms between the surf zone and nearshore. *Estuarine, Coastal and Shelf Science*. 25(6):707–720. DOI: 10.1016/0272-7714(87)90017-5.
- Talbot, M.M.B. & Bate, G.C. 1988c. The relative quantities of live and detrital organic matter in a beach-surf ecosystem. *Journal of Experimental Marine Biology and Ecology*. 121(3):255–264. DOI: 10.1016/0022-0981(88)90092-5.
- Talbot, M.M.B. & Bate, G.C. 1988d. The response of surf diatom populations to environmental conditions. Changes in the Extent of the Planktonic Fraction and Surface Patch Activity. *Botanica Marina*. 31(2):109–118. DOI: 10.1515/botm.1988.31.2.109.
- Talbot, M.M.B. & Bate, G.C. 1989. Beach morphodynamics and surf-zone diatom populations. *Journal of Experimental Marine Biology and Ecology*. 129(3):231–241. DOI: 10.1016/0022-0981(89)90105-6.
- Talbot, M.M.B., Bate, G.C. & Campbell, E.E. 1990. A review of the ecology of surf-zone diatoms, with special reference to *Anaulus australis*. *Oceanography and Marine Biology: An Annual Review*. 28:155–175.
- Tedesco, E.C., Ribeiro, S.M.M.S., Pompeu, M., Gaeta, S.A. & Cavalcante, K.P. 2017. Low-latitude accumulation of the surf-zone diatoms *Anaulus australis* (Drebes & Schulz) and *Asterionellopsis glacialis* (Castracane) round species complex in the Eastern Coast of Brazil. *Brazilian Journal of Oceanography*. 65(2):324–331. DOI: 10.1590/S1679-87592017137806502.
- Utermöhl, H., 1958. Zur vervollkommnung der quantitativen phytoplankton-methodik: Mit 1 Tabelle und 15 abbildungen im Text und auf 1 Tafel. *Internationale Vereinigung für theoretische und angewandte Limnologie: Mitteilungen*, 9(1), pp.1-38.
- Winter, D.F., 1983. A theoretical model of surf zone circulation and diatom growth. In *Sandy Beaches as Ecosystems: Based on the Proceedings of the First International Symposium on Sandy Beaches*,

*held in Port Elizabeth, South Africa, 17–21 January 1983* (pp. 157-167). Dordrecht: Springer Netherlands.

## Appendix

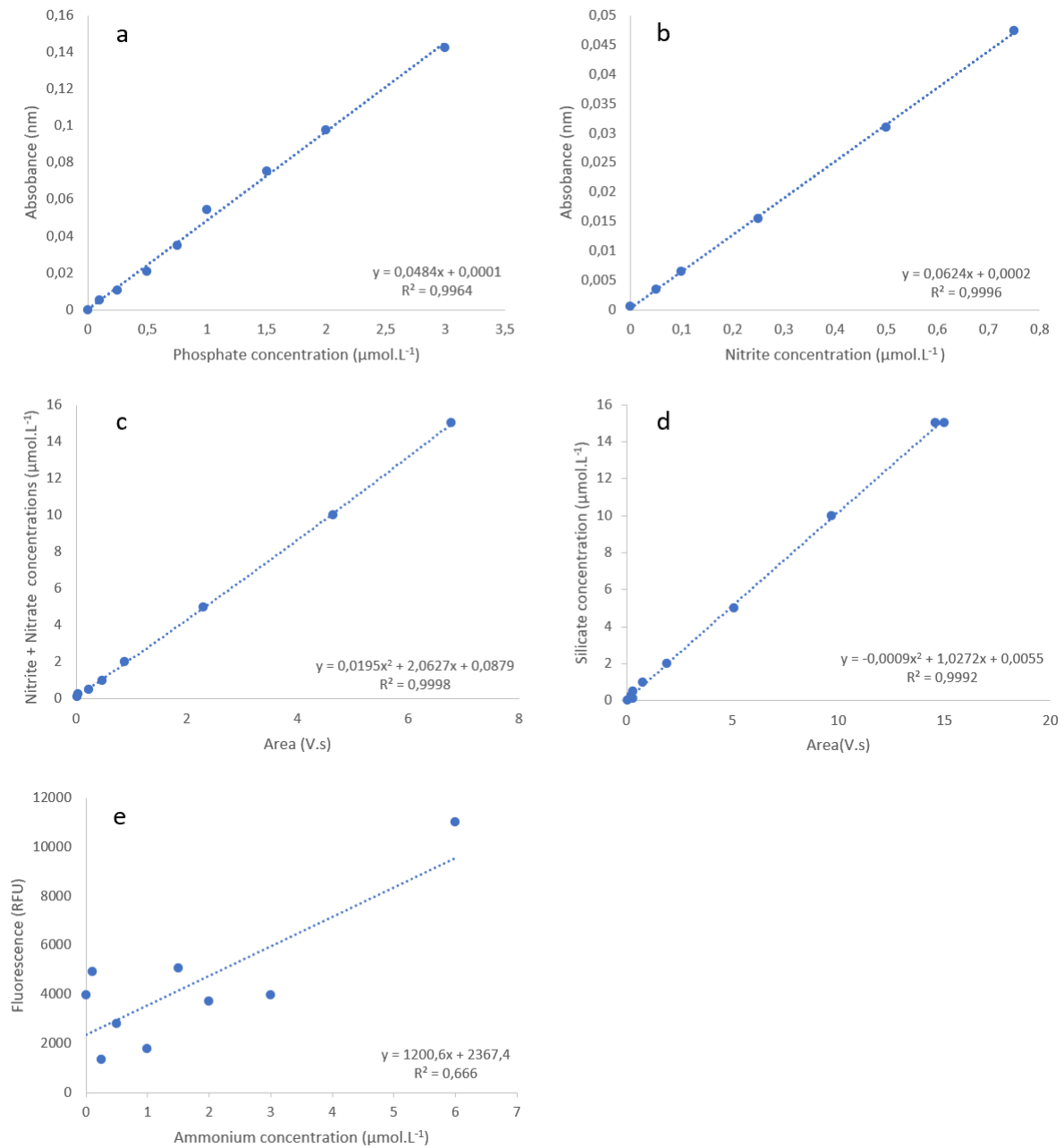


Figure A 1: Standard curves used to determine nutrient concentrations for a) phosphate, b) nitrite, c) nitrate + nitrite, d) silicate and e) ammonium.

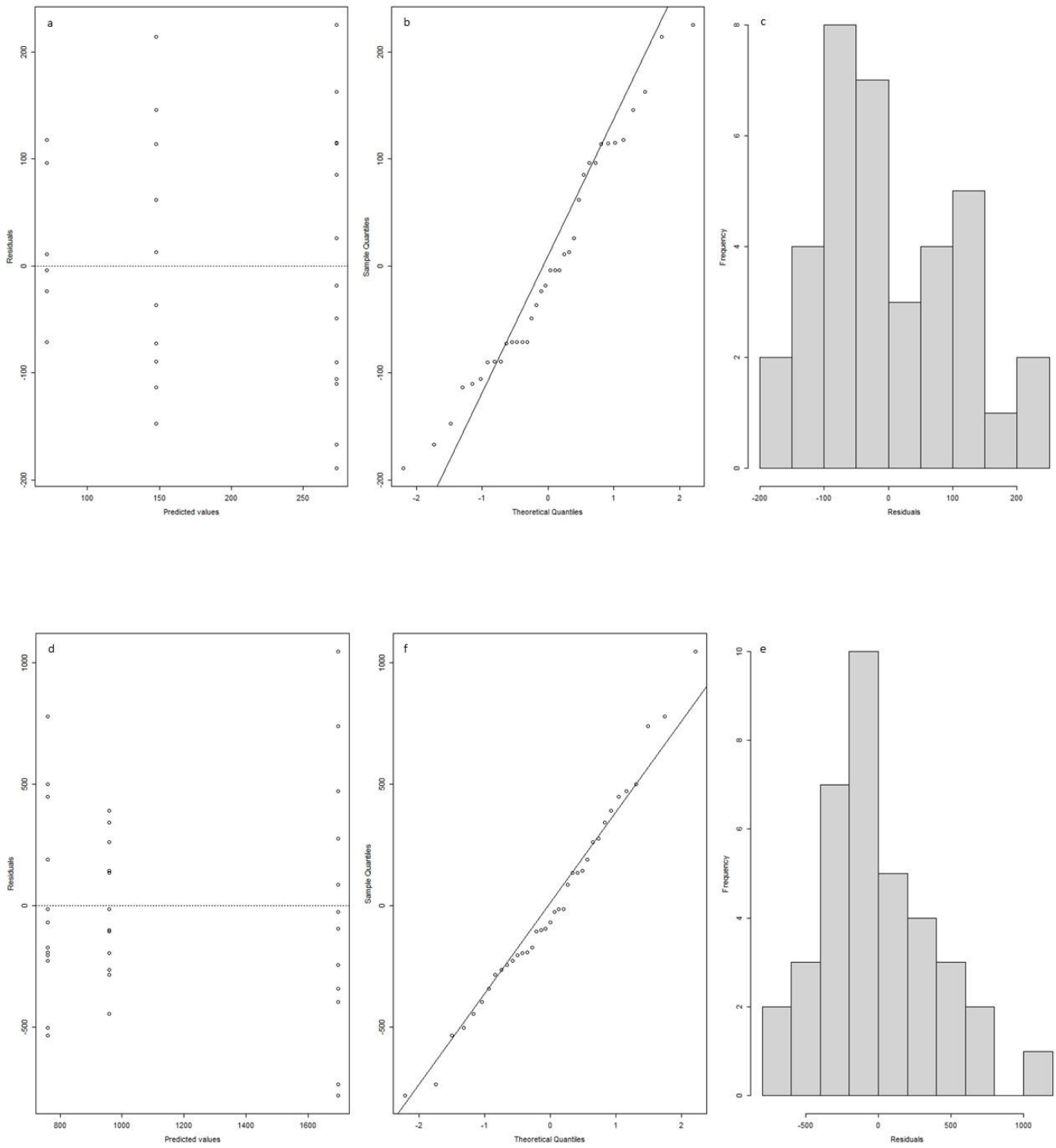


Figure A 2: Model validation plots ANOVA and Post-hoc Tukey test for comparison between stations for surface *A. australis* cell concentrations (square root transformed data)

Table A 1: Table A1: Results of the ANOVA and Tukey tests comparing *A. australis* cell concentrations between stations in the surface and sediment.

<b>ANOVA</b>		<b>Df</b>	<b>Sum sq.</b>	<b>Mean sq.</b>	<b>F-value</b>	<b>P-value</b>
Surface	Stations (as a factor)	2	260560	130280	10.63	0.000273
	Residuals	33	404353	12253		
Sediment	Stations (as a factor)	2	5871548	2935774	16.54	9.6e-06
	Residuals	34	6033365	177452		

<b>Tukey</b>		<b>diff in Mean</b>	<b>lower CI</b>	<b>upper CI</b>	<b>P-value</b>
Surface	2-3	76.17	-37.21	189.55	0.24
	1-3	201.85	93.11	310.58	<0.001
	1-2	125.68	14.40	236.95	0.024
Sediment	1-3	197.6	-215.61	610.85	0.478
	2-3	935.89	514.48	1357.30	<0.001
	2-1	738.27	325.04	1151.50	<0.001

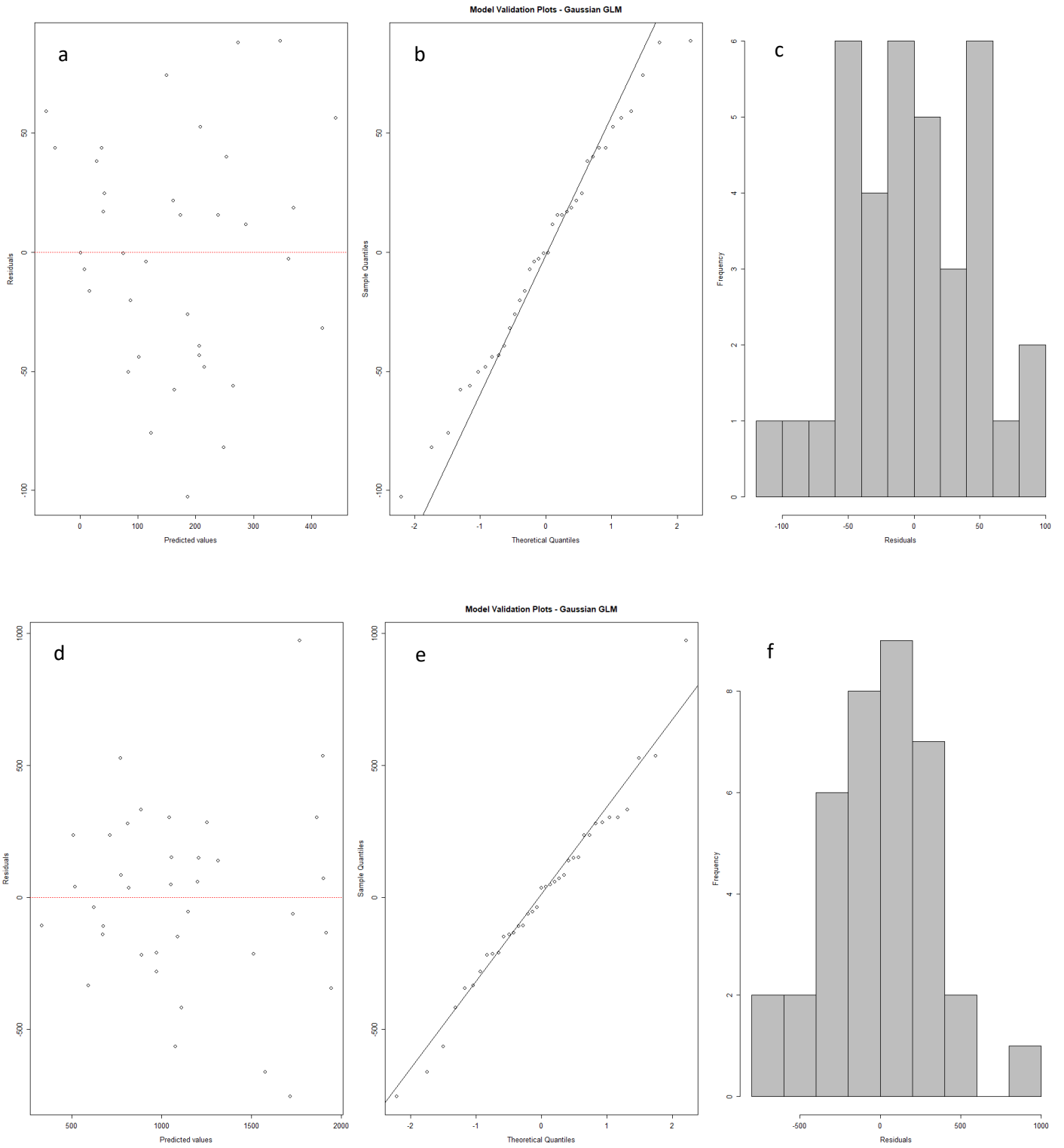


Figure A 3: Residual plots with *A. australis* cell concentrations as a response variable in the surface water (a, b, c) and the sediment (d, e, f)

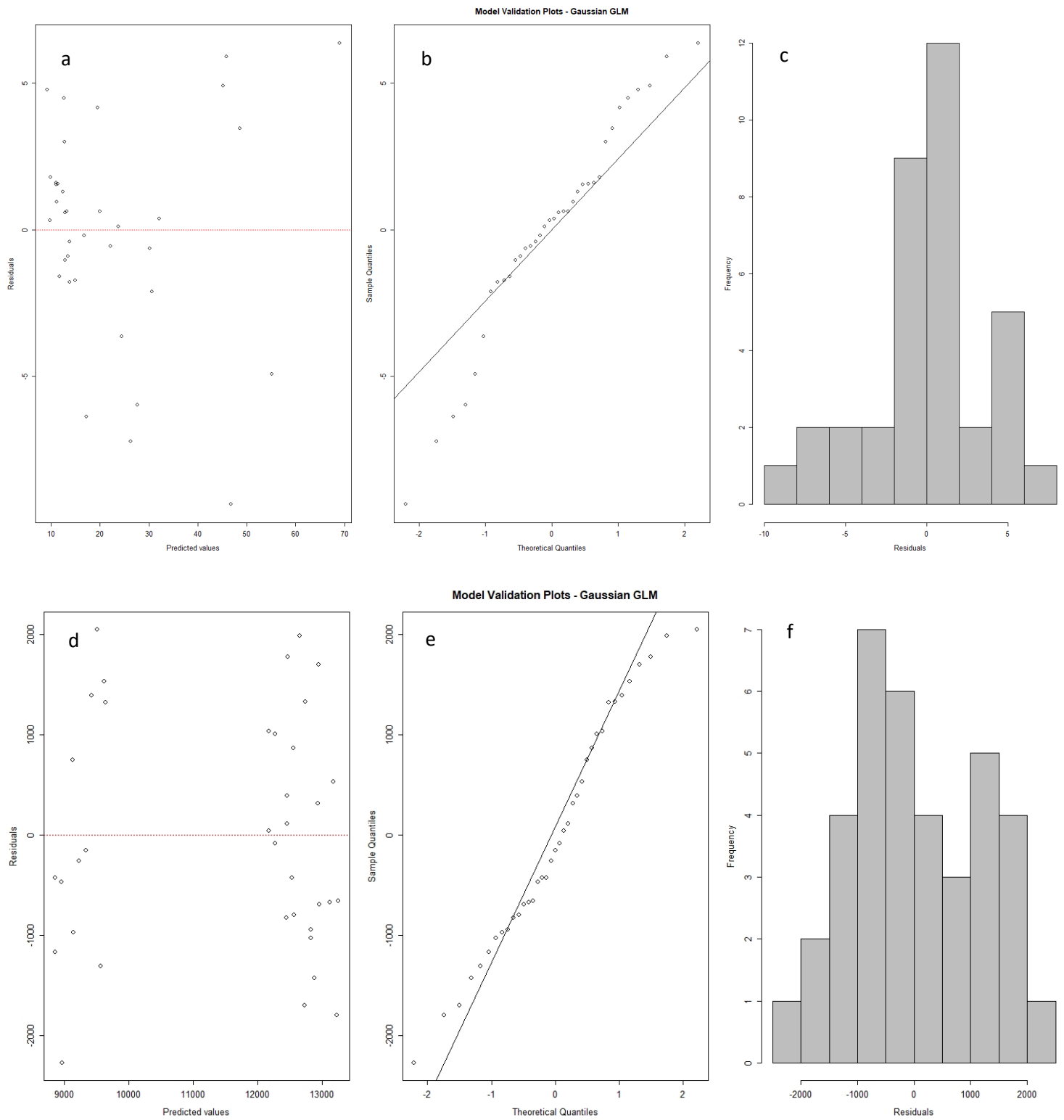


Figure A 4: Residual plots with Chlorophyll-a concentrations as a response variable in the surface water (a, b, c) and the sediment (d, e, f)

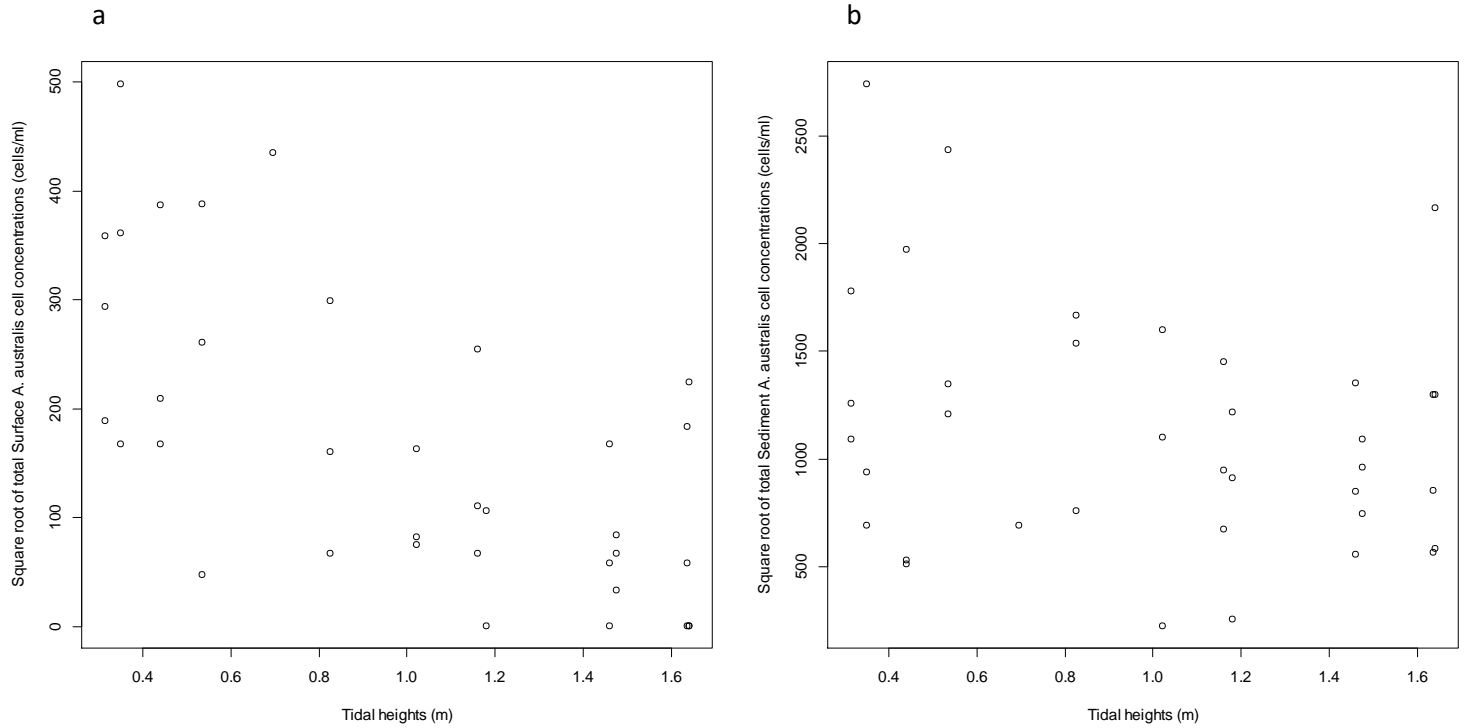


Figure A 6: Scatterplot of total cell concentrations of *A. australis* (cell/m) at the surface (a) and sediment (b) against tidal heights (m).

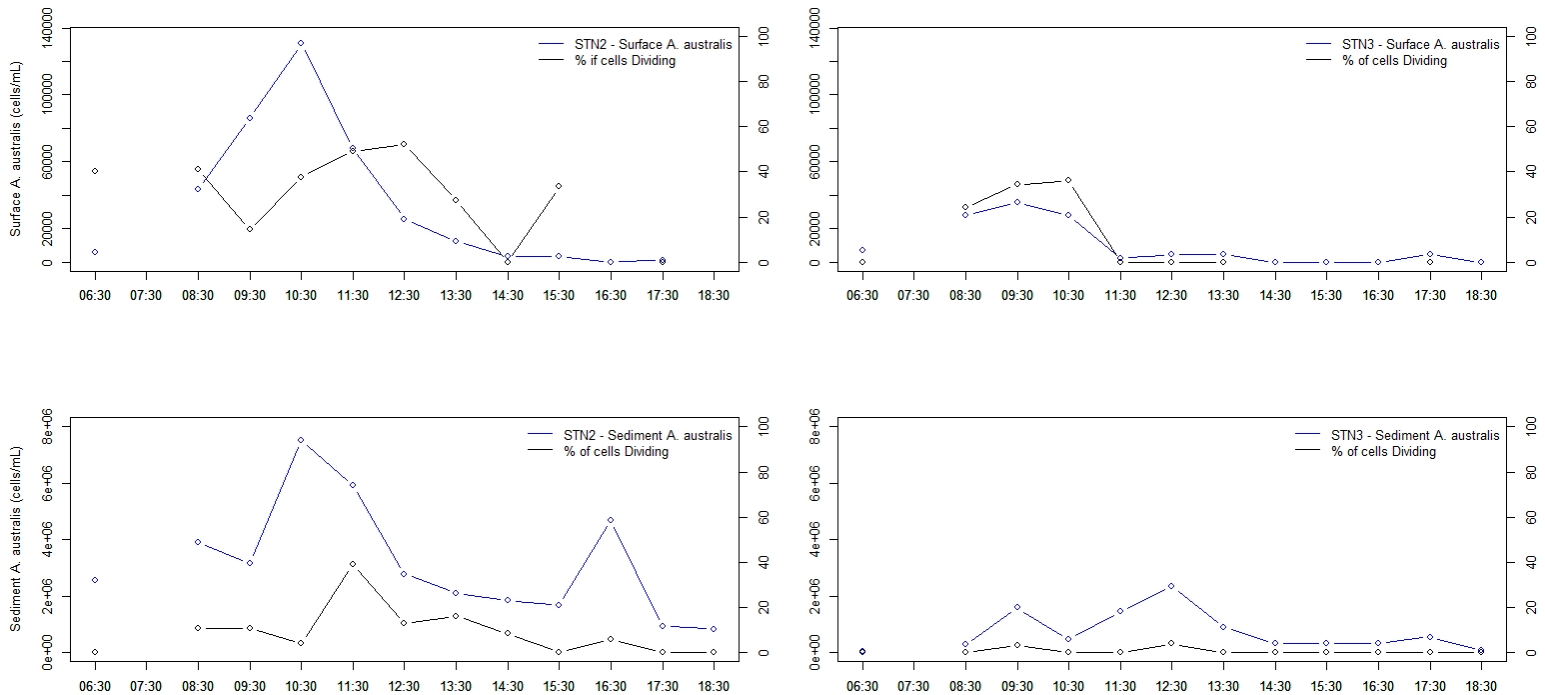
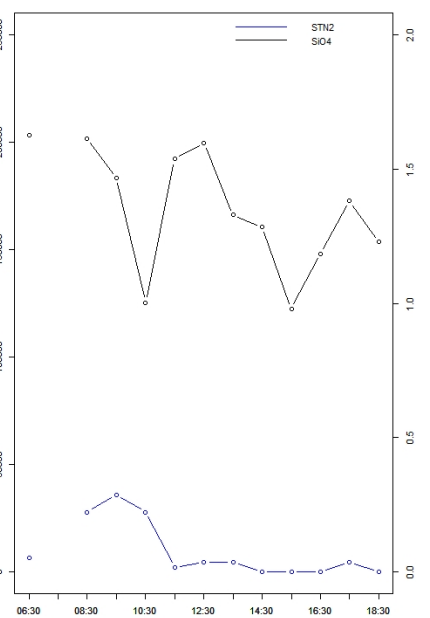
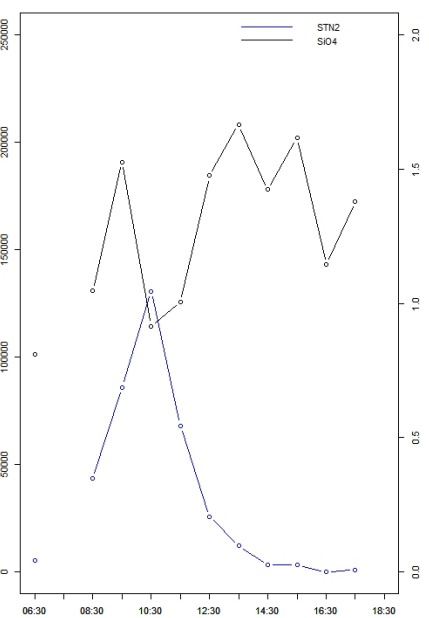
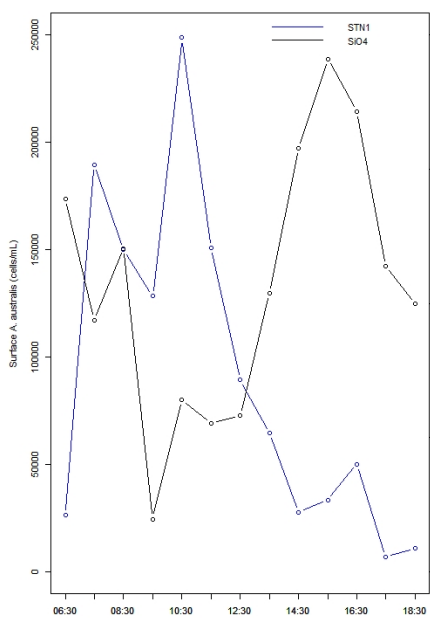
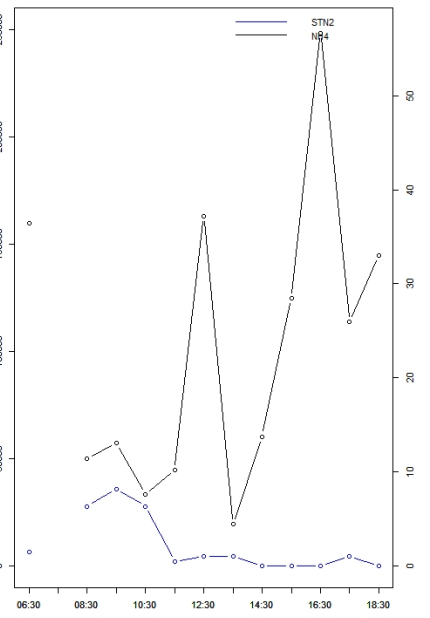
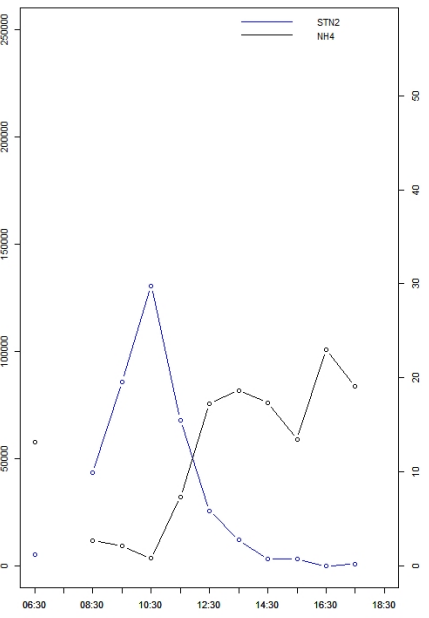
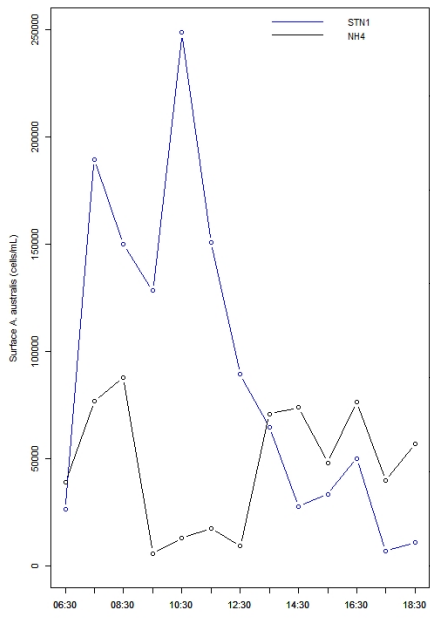
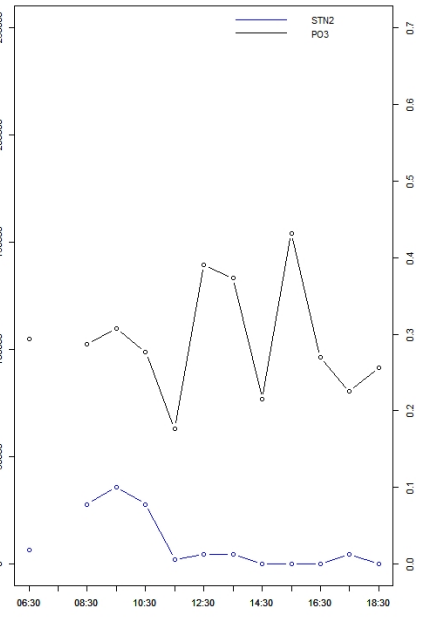
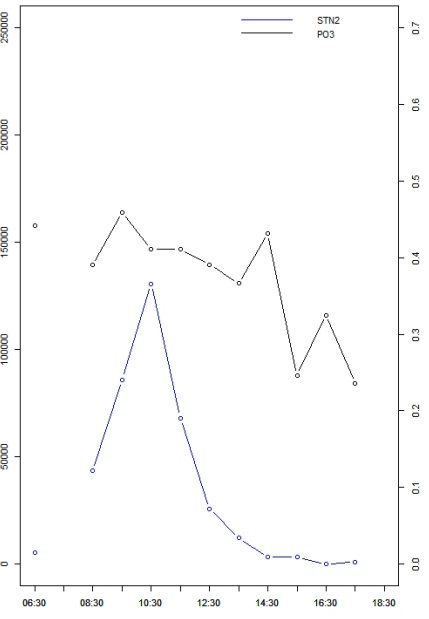
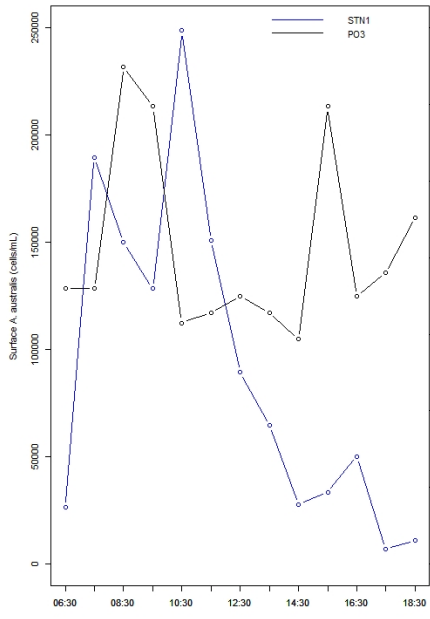


Figure A 5: Proportion of dividing cells (black, %), alongside total cell concentrations of *A. australis* (blue, cells.mL<sup>-1</sup>) plotted over time of day for Station 2 & 3



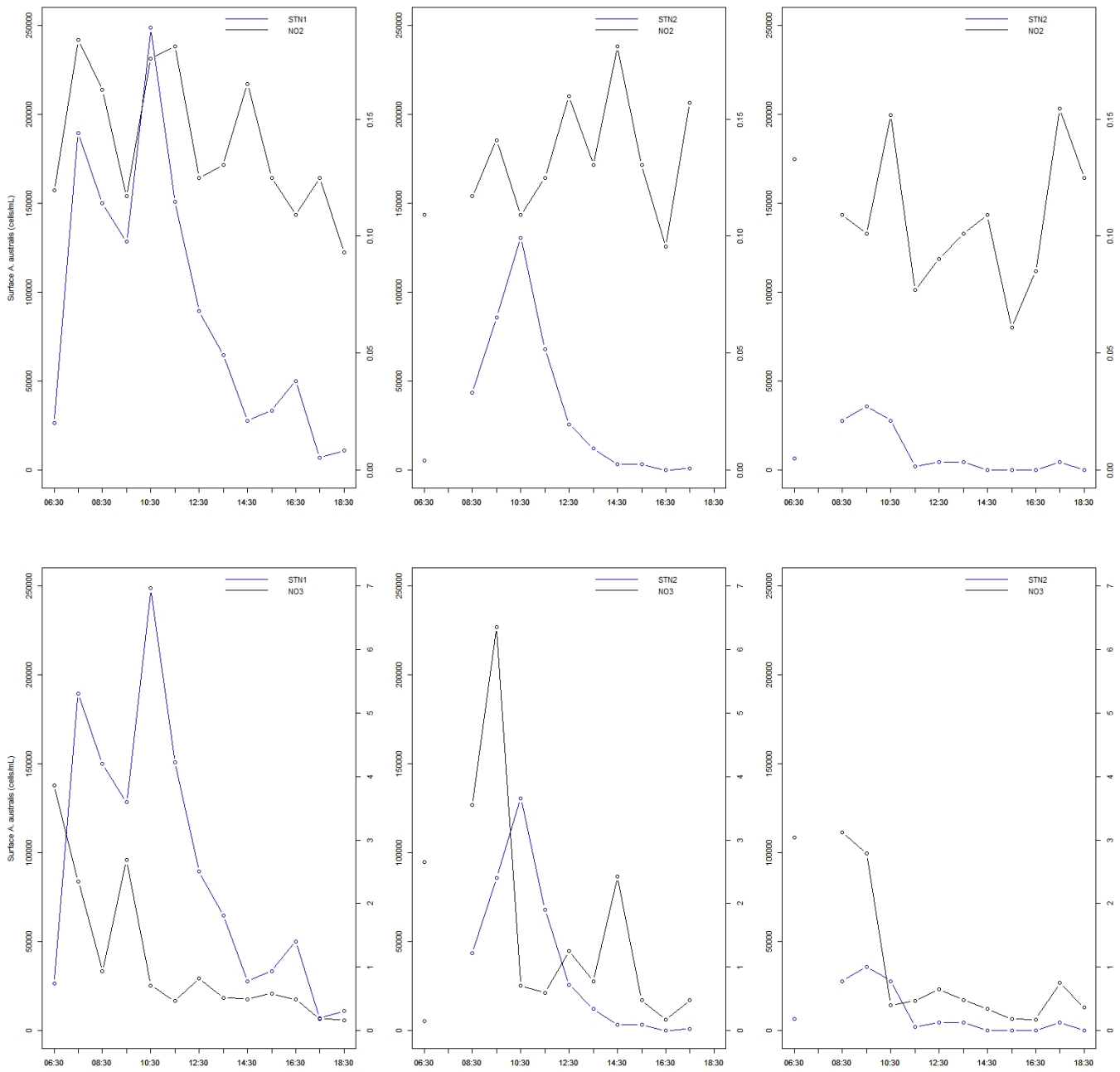


Figure A 7: Nutrient concentrations ( $\mu\text{g.L}^{-1}$ ) of nitrite ( $\text{NO}_2$ ), nitrate ( $\text{NO}_3$ ), silicate ( $\text{SiO}_4$ ), phosphate ( $\text{PO}_3$ ) and ammonium ( $\text{NH}_4$ ) for each station, plotted alongside cell concentrations of *A. australis* ( $\text{cells.mL}^{-1}$ ) in hourly timescales.

Table A 2: Descriptive statistics for nutrients including Mean (mean), standard deviation (St. Dev), variance (Var) and sample size (n) of for surface water samples of nutrient concentrations at three stations (Station 1-3) for all time points sampled.

	Nutrient	Mean	St. dev	Variance	Sample size
Station 1	Nitrite	0.14	0.03	$9.08 \times 10^{-4}$	13
	Nitrate	1.10	1.13	$1.28 \times 10^0$	13
	Phosphate	0.41	0.12	$1.48 \times 10^{-2}$	13
	Ammonium	10.81	6.60	$4.36 \times 10^{+1}$	13
	Silicate	1.07	0.50	$2.48 \times 10^{-1}$	13
Station 2	Nitrite	0.13	0.03	$6.55 \times 10^{-4}$	11
	Nitrate	1.77	1.87	$3.50 \times 10^0$	11
	Phosphate	0.37	0.08	$5.66 \times 10^{-3}$	11
	Ammonium	12.28	7.78	$6.05 \times 10^{+1}$	11
	Silicate	1.27	0.30	$8.93 \times 10^{-2}$	11
Station 3	Nitrite	0.11	0.03	$8.28 \times 10^{-4}$	12
	Nitrate	1.06	1.17	$1.37 \times 10^0$	12
	Phosphate	0.29	0.07	$5.62 \times 10^{-3}$	12
	Ammonium	23.19	15.71	$2.47 \times 10^{+2}$	12
	Silicate	1.35	0.23	$5.09 \times 10^{-2}$	12

Table A 3: Descriptive statistics for nutrients including Mean (mean), standard deviation (St. Dev), variance (Var) and sample size (n) of for surface water samples of nutrient concentrations of the combined samples across all three stations.

	Nutrient	Mean	St. dev	Variance	Sample size
All Stations	Nitrite	0.13	0.03	$9.47 \times 10^{-4}$	36
	Nitrate	1.41	1.13	$1.97 \times 10^0$	36
	Phosphate	0.36	0.11	$1.11 \times 10^{-2}$	36
	Ammonium	15.38	11.89	$1.41 \times 10^{+2}$	36
	Silicate	1.22	0.38	$1.42 \times 10^{-1}$	36

Table A 4: Mean (mean), standard deviation (St. Dev), variance (Var) and sample size (n) of for surface and sediment (depth) samples of *A. australis* at three stations (Station) for all time points sampled.

Depth	Station	Mean	St. dev	Variance	sample size
Surface	Station 1	90621.15	76516.23	$5.85 \times 10^{+9}$	13
Surface	Station 2	34536.46	43339.82	$1.88 \times 10^{+9}$	11
Surface	Station 3	9497.42	13026.13	$1.70 \times 10^{+8}$	12
Sediment	Station 1	977625.70	494662.19	$2.45 \times 10^{+11}$	13
Sediment	Station 2	3160465.08	2032274.41	$4.13 \times 10^{+12}$	12
Sediment	Station 3	726030.42	716033.58	$5.13 \times 10^{+11}$	12

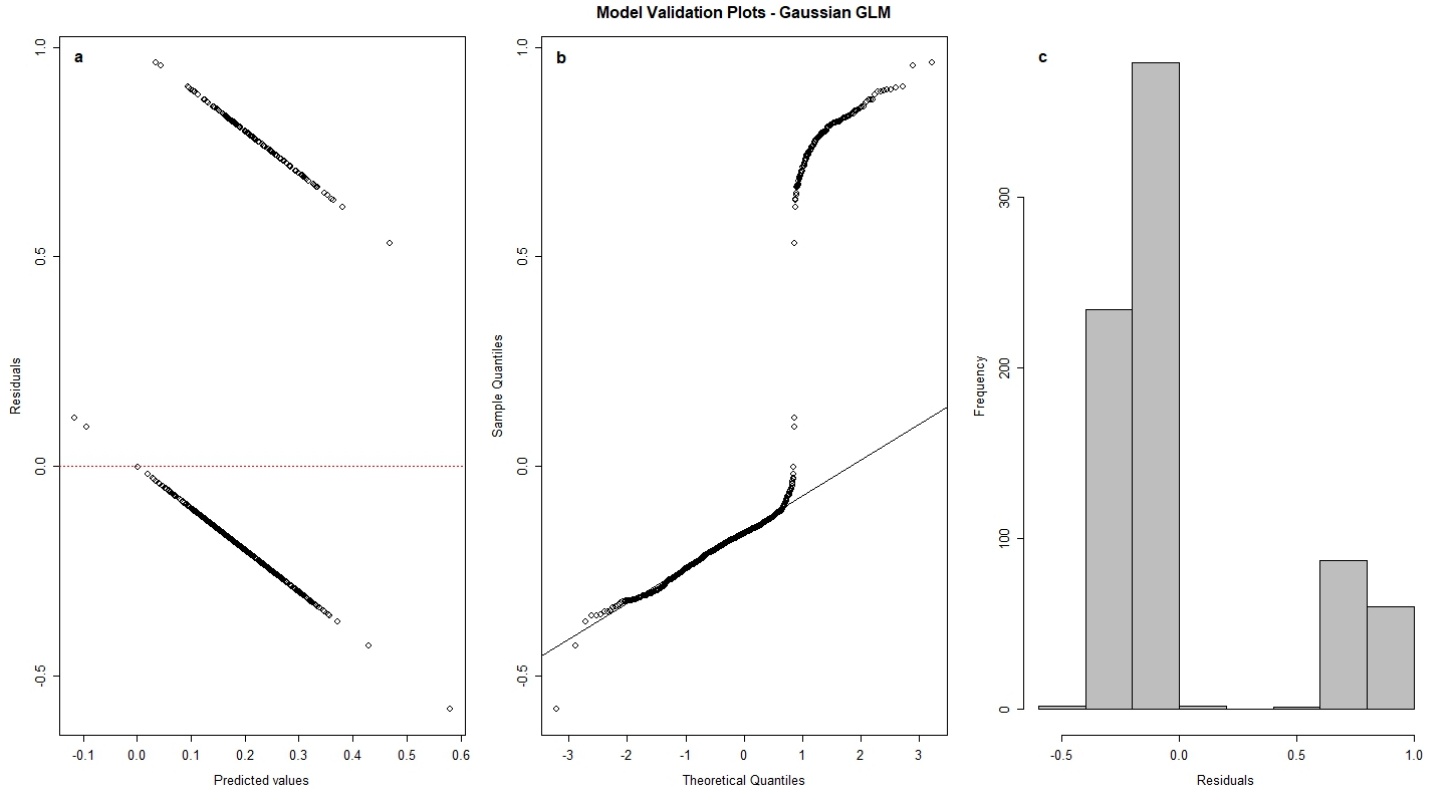


Figure A 8: Generalised linear model validation plots with patch presence-absence as a response variable